STRUCTURE-FUNCTION RELATIONSHIP STUDIES IN THE DISULFIDE-BOND REDUCTASE DSBD AND A *C*-TYPE APOCYTOCHROME

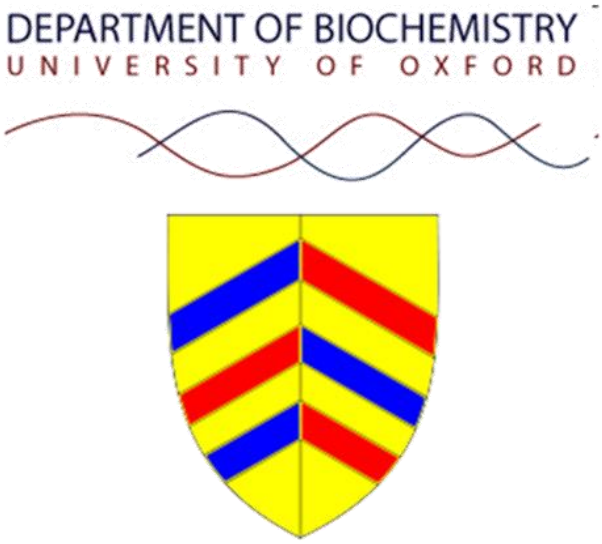

PARASKEVI KRITSILIGKOU

MSC BY RESEARCH IN BIOCHEMISTRY

MERTON COLLEGE

DEPARTMENT OF BIOCHEMISTRY, UNIVERSITY OF OXFORD

TRINITY TERM 2011

STRUCTURE-FUNCTION RELATIONSHIP STUDIES IN THE DISULFIDE-BOND REDUCTASE DSBD AND A *C*-TYPE APOCYTOCHROME

Paraskevi Kritsiligkou - MSc by research in Biochemistry
Merton College, Biochemistry Department,
University of Oxford

The efficient covalent attachment of heme to *c*-type apocytochromes in the periplasm of Gram-negative bacteria requires the provision of reductant. Heme attachment is facilitated by a system of eight proteins, the Cytochrome *c* maturation (Ccm) system. The disulfide bond oxidoreductase DsbD, a member of the Disulfide bond formation system (Dsb), transfers reductant to the Ccm system via interaction with one of its proteins, CcmG. This study is focused on two key proteins of these systems, the periplasmic disulfide bond oxidoreductase DsbD and a *c*-type apocytochrome, apocytochrome *c*-b_{562}. A new method was established to assess the function of DsbD by linking it to the levels of *c*-type cytochrome maturation. This method was used to evaluate the activity of a range of DsbD variants. In addition, analysis of the biophysical properties of apocytochrome *c*-b_{562} was carried out using NMR spectroscopy. For this analysis, backbone assignments were completed for both oxidation states of the protein. Finally, studies aimed to determine the biophysical properties of the residues of the CXXCH heme binding motif were performed.

SOME OF THE WORK PRESENTED IN THIS THESIS HAS BEEN PUBLISHED:

Mavridou D. A., **Kritsiligkou P.**, Saridakis E., Goddard A. D., Stevens J. M., Ferguson S. J., Redfield C. (2011). "Oxidation state-dependent protein-protein interactions in disulfide cascades." *J Biol Chem* **286**(28): 24943-24956.

Acknowledgements

Reading for an MSc by research in Oxford has been one of the greatest experiences in my life. I believe that during the past two years I was exposed to high quality research and I have been lucky to be able to do exciting experiments. I would like to thank all the people who contributed to this.

Firstly, I would like to thank Prof. Stuart J. Ferguson for accepting me on this course and for giving me the opportunity to work in his lab, for his guidance and for always having faith in me.

I would also like to thank Prof. Christina Redfield for her supervision through the past two years. I really appriciate all her efford and patience when teaching me about NMR spectroscopy and for all her help and understanding.

I am also thankful to Dr Julie M. Stevens for helpful insights and usefull discussions and all the support she has given me over the past two years (also for her understanding and kindness and all those exciting winter mornings).

Also, I would like to thank James and Alan for always being helpful with comments such as "Did you find that cysteine pK_a value yet?" or "This is the plasmid you should use for cloning!", respectively. Louise for helping me with Analysis and Lorena for helping me with the NMR machines.

Προφανώς, ένα πολύ μεγάλο, τεράστιο, ευχαριστώ πάει σε σένα, Ντεσποίνα Μάβριντου. Το ξέρεις πως δεν υπάρχουν αρκετά λόγια να περιγράψω το πόσο ευγνώμων είμαι για τη βοήθειά σου όλα αυτά τα χρόνια και για την απεριόριστη συμβολή σου σε αυτό το thesis. Είναι σαν δεύτερο δικό σου. Σε ευχαριστώ επίσης που καταφέρνεις να είσαι εξαίσια σουπερβαιζορ και άριστη φίλη ταυτόχρονα.

Το μεγαλύτερο ευχαριστώ πάει στους γονείς μου και την οικογένεια μου, γιατί χωρίς την βοήθειά τους δεν θα έγραφα αυτά αυτή τη στιγμή. Σας ευχαριστώ που παρόλες τις δυσκολίες

επιλέξατε να με στηρίξετε σε κάθε μου βήμα και που πιστεύετε σε μένα. Και σας ευχαριστώ για όλη την αγάπη σας.

Abbreviations

A	Ampere
Ccm	Cytochrome *c* maturation
cDsbD	C-terminal domain of DsbD
CXXC motif	Cysteine-X-X-Cysteine motif
CXXCH motif	Cysteine-X-X-Cysteine-Histidine motif
Da	Dalton
DNA	deoxyribonucleic acid
DsbD-His_6	wild-type full-length DsbD bearing a C-terminal His_6-tag
DsbD-Strep	wild-type full-length DsbD bearing a C-terminal Strep-tag II
Dsb system	Disulfide bond system
DTT	dithiothreitol
g	gram
IPTG	isopropyl β-D-thiogalactopyranoside
H	hour
HMQC	Heteronuclear Single Quantum Coherence
HSQC	Heteronuclear Single Quantum Coherence
k	kilo
l	liter
LB	Luria-Bertani
µ	micro
m	milli
M	molar; mega
n	nano
nDsbD	N-terminal domain of DsbD
NMR	Nuclear Magnetic Resonance
NOE	nuclear Overhauser effect
NOESY	Nuclear Overhauser Effect SpectroscopY
OD	optical density
Pa	Pascal
PCR	polymerase chain reaction
PDB	protein data bank
pK_a	$-\log_{10}$ of the acid dissociation constant

ppm	parts per million
rpm	revolutions per minute
s	second
SDS-PAGE	sodium dodecyl sulphate polyacrylamide gel electrophoresis
Sec	secretion
TMBZ	3,3',5,5'-tetramethylbenzidine
tmDsbD	membrane-embedded domain of DsbD
TOCSY	TOtal COrrelation Spectroscopy
TrxA or Trx	thioredoxin
V	Volt

Table of Contents

CHAPTER 1

Introduction

1.1 Heme molecules in proteins

Heme is one of the most common iron-containing molecules in nature. It is a lipophilic moiety that chelates iron and when free in solution it is rapidly oxidised to hemin. In addition, heme is toxic for cells because of its peroxidase activity and it tends to polymerise at neutral pH (Van den Berg et al. 1988). To avoid such effects, heme is always found in association with proteins *in vivo*. These proteins are either heme carriers or proteins that need heme as a prosthetic group for their function.

1.1.1 Heme *b*

Heme *b* is the most abundant form of heme that can be found in association with polypeptide chains. Proteins that contain heme *b* include myoglobins and hemoglobins, as well as members of the peroxidase family. Usually heme *b* is associated with the polypeptide chain through coordination of the iron with a specific residue, most often a histidine. Heme *b* can undergo modifications and alterations, for example additions of long chains to its 2-vinyl group, forming different types of heme, such as heme *o* (Mogi et al. 1994).

1.1.2 Heme *c*

Heme *c* derives from heme *b* after modification. The difference is that the vinyl groups of heme *c* are covalently bound to one or two cysteine residues of the polypeptide chain via thioether bonds (Barker and Ferguson 1999). Proteins that contain heme *c* are called *c*-type cytochromes (See section 1.2). It is clear that this modification of the heme cannot occur without the heme-free form of the protein and a post-translational modification system (Cytochrome *c* maturation (Ccm) system) that keeps both the heme and the apocytochrome in the correct state and facilitates the provision and attachment of the heme (Figure 1.1).

1.2 *c*-type cytochromes

1.2.1 Functions of *c*-type cytochromes

c-type cytochromes can be found in all kingdoms of life (Bertini et al. 2007). The fact that they have heme covalently bound provides a wide range of different functionalities for these proteins. Primarily, they function as electron carriers in fundamental energy transduction processes. They interact with other enzymes or other cytochromes in the transfer of electrons from a primary donor to a terminal acceptor, as part of respiration or photosynthesis. *c*-type cytochromes can also be responsible for the biosynthesis of cofactors, such as tryptophan tryptophylquinones, or lipidic signaling molecules, and they can bind gases such as carbon monoxide (Sanders et al. 2010). The *c*-type cytochrome molecules located in the intermembrane space of mitochondria in some eukaryotes also have a distinct and essential role in triggering programmed cell death (apoptosis) upon release to the cytosol (Caroppi et al. 2009).

1.2.2 Structure of *c*-type cytochromes

c-type cytochromes have diverse structures. Most of them are highly helical proteins, but number of heme molecules attached to the polypeptide can vary significantly. Unlike *c*-type cytochromes in eukaryotes, such as cytochrome *c* with only one heme, many bacterial *c*-type cytochromes are multiheme proteins. The variation is wide; most proteins have around four of five heme molecules attached but there are some described such as one protein from *Geobacter sulfurreducens* that incorporates 27 heme groups (Mowat and Chapman 2005). Even in proteins with the same number of heme molecules, their molecular weight could differ.

Almost all *c*-type cytochromes have in common a characteristic CXXCH heme binding motif. The two cysteine residues are covalently bound to vinyl groups of the heme and the

histidine residue acts as an axial ligand to the heme iron. The N-terminal cysteine of the CXXCH motif binds to the vinyl-2 group of the heme, whereas the C-terminal cysteine of the motif binds to the vinyl-4 group (Barker and Ferguson 1999).

There are *c*-type cytochromes that do not have this CXXCH heme binding motif. Variation can be identified in the number of the "XX" residues between the cysteine residues, such as the CXXXXCH motif in *Desulfovibrio sp.* cytochrome c_3 (Aragao et al. 2003; Herbaud et al. 2000), or the $CX_{15}CH$ motif of *Wolinella succinogenes* MccA (Hartshorne et al. 2007). In addition, in cytochromes *c* from euglenozoa the heme binding motif is F/AXXCH (Fulop et al. 2009). In bacterial NrfA nitrate reductase, one of the five heme binding motifs of the protein is CXXCK (Einsle et al. 1999), having lysine instead of histidine as the axial ligand.

1.2.3 *c*-type cytochromes in *Escherichia coli*

c-type cytochomes in *Escherichia coli* are not produced during aerobic growth conditions. Under different anaerobic growth conditions up to six *c*-type cytochromes can be expressed (Iobbi-Nivol et al. 1994). They vary in size, structure and number of heme molecules covalently attached; all of them though are multiheme proteins. For example NrfB is a 20.7 kDa protein that binds 4 hemes, TorC is a 43.6 kDa protein that binds 4 hemes and NapB is a 16.2 kDa protein that binds 2 hemes.

1.2.4 Apocytochromes *c* in *E. coli*

Although *c*-type apocytochromes *in E.coli* are produced in the cytoplasm the holoproteins in this organism are periplasmic or membrane anchored proteins with their globular heme-containing domain facing the periplasm. Heme attachment also occurs in the periplasm. Apocytochromes have a signal peptide that leads to their transport to the periplasm through the Sec protein translocation system. They are delivered across the inner membrane with the N-terminus first and in an unfolded state. It has been suggested that, when in the periplasm,

the cysteine residues of the CXXCH motif are oxidised to form a disulfide bond (see section 1.4.1).

Most *c*-type apocytochromes are insoluble and unstable proteins. Consequently, their characterisation has been challenging. Engineered *c*-type cytochromes based on *b*-type cytochromes have been shown to be more stable in the apo form making them a useful tool for further studies (Barker et al. 1995).

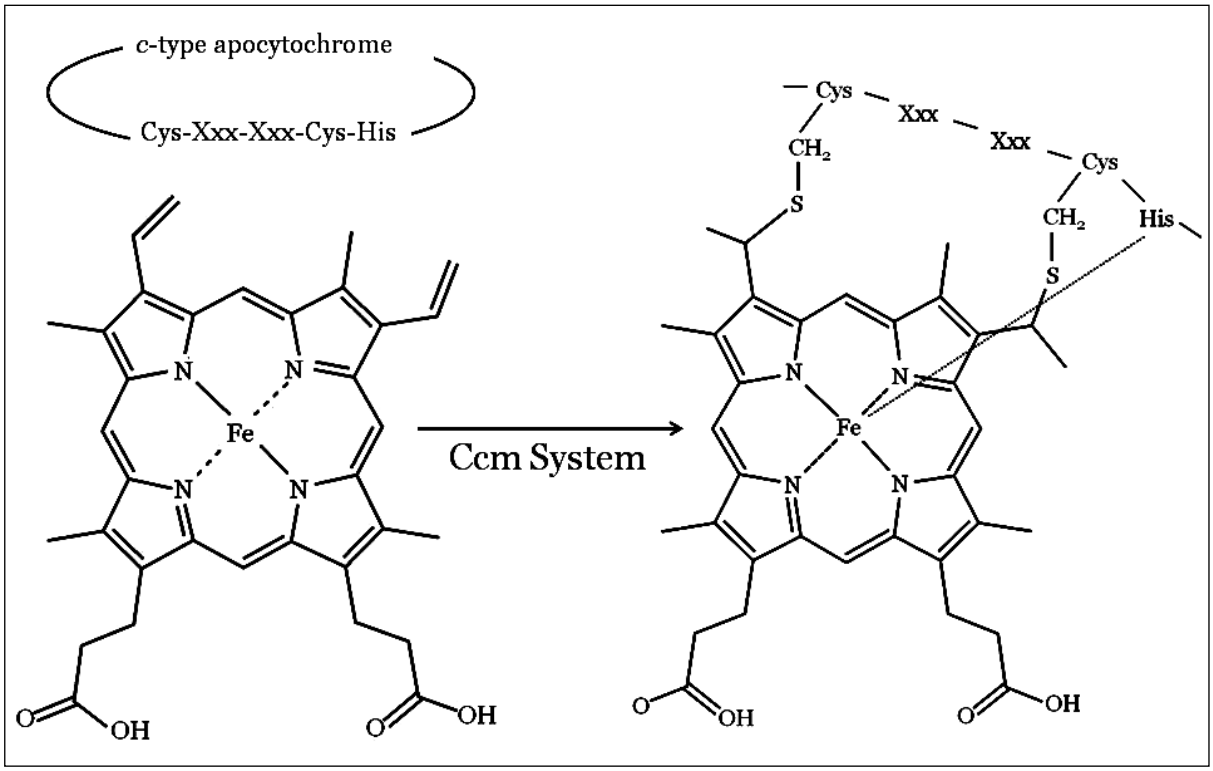

Figure 1. 1: Attachment of heme *b* to a *c*-type apocytochrome through the help of the Ccm system results in heme *c* and *c*-type apocytochromes.

1.3 Biogenesis of *c*-type cytochromes in *E. coli*

For the post translational modification in *c*-type cytochromes, there is a requirement for a system of proteins that facilitate this process called, the Cytochrome *c* maturation (Ccm) system. In *E. coli*, it consists of eight different proteins, CcmA-H (Figure 1.2). These proteins have different functions, very few of them are known. The genes expressing these proteins

are located in the *ccm* operon; in other bacteria that is not always the case (Thony-Meyer 1997).

The proteins of the Ccm system can be crudely separated into two categories; the proteins that have been linked to the handling of the heme and the proteins that are important for keeping the apocytochrome in its reduced form (without a disulfide bond between the cysteine residues of the CXXCH motif) (Kranz et al. 2009).

1.3.1 Heme handling and attachment: CcmABCDEF

CcmA is a 23 kDa soluble protein that is located in the cytoplasm, but is associated to the inner membrane (Goldman et al. 1997). It has an ATP binding site and is proposed to function as a dimer for ATP hydrolysis as part of an ATP binding cassette (ABC) protein. Other components of ABC proteins are usually membrane-spanning proteins and periplasmic-binding proteins that bind on a transmembrane protein and are associated with a transport function. In the Ccm system of *E .coli*, the CcmA dimer is has been shown to interact with CcmB . However, the stoichiometry of the ABC proteins is not known. It has been a matter of controversy if the dimer of CcmA interacts with two molecules of CcmB proteins, or a CcmB and a CcmC molecule (Feissner et al. 2006; Goldman et al. 1997). Also, it had been thought that these ABC proteins needed for the transport of heme to the periplasm; however, even after deletion of the appropriate *ccm* genes, heme is still transported (Cook and Poole 2000; Schulz et al. 1999; Stevens et al. 2004). As understood to date, the role of these ABC proteins is in energy coupling to other components of the Ccm system by ATP hydrolysis, this energy is necessary for the function of other proteins on the pathway (Christensen et al. 2007).

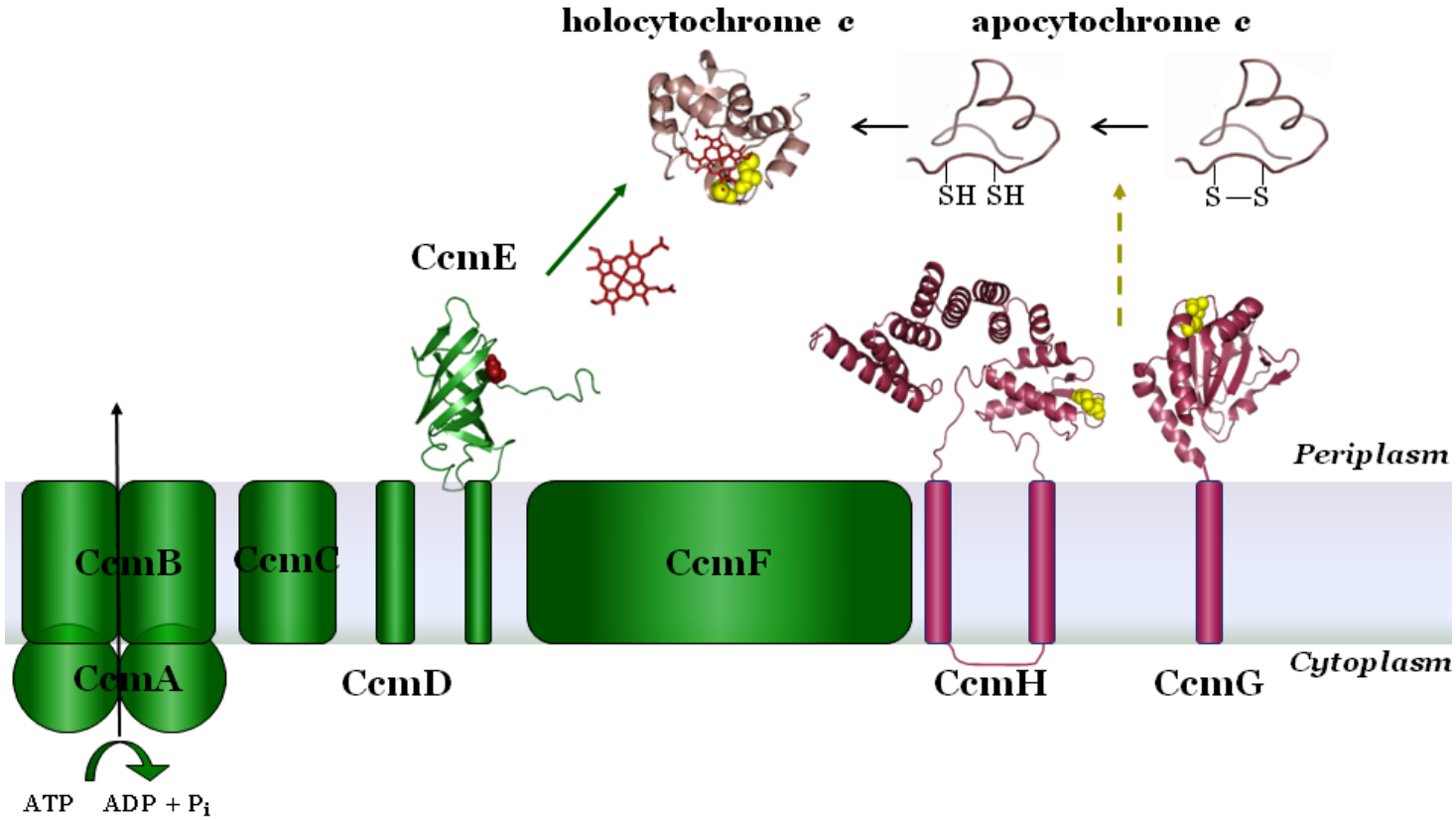

Figure 1. 2: The cytochrome *c* maturation (Ccm) system in *E.coli*. The system consists of eight proteins CcmA-H. CcmA-F (shown in green) are thought to be responsible for handling of the heme. CcmG-H (in red) are responsible to maintain the the cysteine residues of the CXXCH heme binding motif of the *c*-type apocytochrome in their thiol form, for the heme to be covalently attached. The structures shown are from the following pDB entries : CcmE (1J6Q) (Arnesano et al. 2002) , N-CcmH (2HL7) (Di Matteo et al. 2007), for C-CcmH the structure used is of its analogue NrfG (2E2E) (Han et al. 2008), CcmG (2B1K) (Ouyang et al. 2006), cytochrome *c* (155C) (Timkovich and Dickerson 1976).

CcmB is a 24 kDa integral membrane protein (Goldman et al. 1997). Nothing is known about the structure of this protein but it has been shown through bioinformatic structure predictions that it has 6 transmembrane helices. The loops between the transmembrane helices tend to be longer on the cytoplasmic side of the membrane, probably for interaction with CcmA. It has also been shown that CcmB interacts with CcmC (Feissner et al. 2006) .

CcmC is a 28 kDa membrane protein, also with 6 predicted transmembrane helices. It has been proven that CcmC interacts with proteins CcmD and CcmE (Ahuja and Thony-Meyer 2005). It forms a tight heme containing complex CcmC:heme:CcmE (Richard-Fogal and Kranz 2010). CcmD is a 7 kDa membrane protein and CcmE is an 18 kDa membrane anchored protein with a large periplasmic domain. CcmE has the ability to bind heme covalently via a histidine residue (His130) (Lee et al. 2005) .

As understood to date, heme is transported to the periplasm through an unidentified route. When in the periplasm, it interacts with a specific area (the WWD domain) in one of the periplasmic loops of CcmC (Richard-Fogal and Kranz 2010). This domain is flanked by 2 histidine residues located in other periplasmic loops that have been shown to contribute to heme coordination, acting as axial ligands. Heme can then be transferred on to CcmE and it is proposed that the 2-vinyl group of the heme forms a covalent bond with His130 (Lee et al. 2005). A lot of studies have focused on this histidine residue of CcmE, because of the unusual chemistry of the covalent bond with heme (Daltrop et al. 2002; Harvat et al. 2009). In addition, a natural variant of the Ccm system has been identified in which the heme-binding residue of CcmE is a cysteine (Goddard et al. 2010).

When CcmE has heme covalently bound, it is believed to dissociate from the complex with CcmC and to interact with CcmF and the *c*-type apocytochrome (Richard-Fogal and Kranz 2010). There are two essential prerequisites for the resolution of the CcmC:heme:CcmE complex. Firstly the provision of energy from ATP hydrolysis involving CcmA and secondly,

the presence of CcmD. Little is known about CcmD, but even though it is a very small protein it has been suggested that it is the "glue" of the Ccm system. When CcmD is not present, CcmE does not get released from its complex with CcmC and maturation of *c*-type cytochromes is abolished (Richard-Fogal et al. 2008).

CcmF is a 70 kDa protein with more than 11 predicted transmembrane helices and is proposed to be the "heart" of the Ccm system. It has been shown to interact with both CcmE (Ahuja and Thony-Meyer 2003) and CcmH (Ren et al. 2002). In recent studies, heme bound to CcmF was detected and the proposed explanation was that by binding to CcmF, the heme that is already bound to CcmE can be maintained in the reduced, ferrous state for transfer to the *c*-type apocytochrome (Richard-Fogal et al. 2009). CcmE has long been proposed to be the protein that actually attaches the heme moiety to the *c*-type apocytochrome.

1.3.2 Reduction of the apocytochrome: CcmGH

As mentioned previously, *c*-type apocytochromes are transported to the periplasm through the Sec system in an unfolded state, with their N-terminus first (Thony-Meyer and Kunzler 1997). In the oxidising environment of the periplasm, there is evidence that the cysteines of the CXXCH heme binding motif are oxidised by the periplasmic oxidase DsbA (see section 1.4.1). Hence a disulfide bond can be formed and this event prevents attachment of the heme (Daltrop et al. 2002). Reduction of the disulfide bond therefore, has to occur before heme attachment.

It has been suggested that the proteins CcmG and CcmH transfer the necessary reducing power to the apocytochrome. However, it is not currently known if CcmG or CcmH is the direct reductant provider. Interaction with *c*-type apocytochromes has been reported for both proteins.

CcmG (also named DsbE) is a 21 kDa membrane ancored protein with a periplasmic thioredoxin-like fold. It has been shown that CcmG is reduced by DsbD (see section 1.4.4) however it is not clear what receives reductant from CcmG; it could either be the apocytochrome or the N-terminal domain of CcmH. Loss of CcmG abolishes *c*-type cytochrome formation, which is not reversed even with addition of exogenous reductant (Reid et al. 2001). Surprisingly however, in experiments where one or both cysteines of CcmG were replaced by serines, there were low levels of *c*-type cytochrome maturation that were enhanced with addition of exogenous reductant (Fabianek et al. 1998). This could suggest a different role for CcmG that is not only dependent on its cysteines but is essential for *c*-type cytochrome maturation.

CcmH is a 39 kDa protein. It has two membrane anchored periplasmic domains connected by a loop in the cytoplasm. This fusion protein in *E. coli* seems to be an exception, because in most proteobacteria CcmH can be found as two proteins that are expressed separately and named CcmH and CcmI. The N-terminal domain of CcmH (CcmH in other organisms) has a three-helix-bundle folds with a conserved pair of cysteines in a characteristic CXXC motif (see section 1.4) and it is thought that it can function as a thiol-disulfide oxidoreductase (Di Matteo et al. 2007). The C-terminal domain of CcmH (CcmI in other organisms) is highly helical and contains two TPR (tetratricopeptide repeat) motifs. Structural information about C-CcmH is extrapolated from protein NrfG, an analogue of C-CcmH, for which the structure has been determined (Han et al. 2008).

The exact route of reductant that leads to the cysteins in the CXXCH heme-binding motif to be in a thiol form remains unknown, because the exact functions of CcmG and CcmH are not well characterised. It is known however, that the reductant is provided to the Ccm system by the protein DsbD.

1.4 The disulfide bond formation system in *E. coli*

Disulfide bonds in proteins usually contribute to the stabilisation of a folded protein conformation. There are more than 300 proteins in Gram-negative bacteria, located outside the cytoplasm, that need disulfide bonds for their correct folding and consequently function. The disulfide bridges that need to be introduced occur between pairs of specific cysteine residues.

It was long thought that disulfide bonds form spontaneously *in vivo*, even though formation of disulfide bonds *in vitro* is a very slow process (Bardwell et al. 1991). The necessity of a system of proteins that can catalyse the formation of disulfide bonds is now recognised (reviewed in (Kadokura and Beckwith 2010)). The Disulfide bond formation system (Dsb system) is responsible for formation and isomerisation of disulfide bonds. In *E. coli* this system comprises of five different proteins, DsbA-G, most of which have a CXXC motif in their active site; this motif is quite common thiol-disulfide exchange reactions.

Thiol-disulfide oxidoreductases usually have a thioredoxin-like fold with a CXXC motif and it is believed that in such folds, the N-terminal cysteine of the CXXC is the residue that defines the reactivity of the protein. For these proteins, it is proposed that the catalytic mechanism involves a nucleophilic attack by the thiolate anion (S^-) form of a cysteine residue of one protein on the disulfide bond of the partner protein (Figure 1.3).

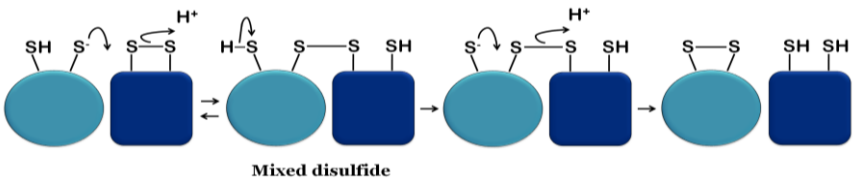

Figure 1. 3: Schematic representation of a thiol-disulfide exchange reactions. A thiolate anion, originating from the deprotonation of a free thiol, displaces one sulfur of the disulfide bond in the oxidised species. That results in the formation of a transient mixed-disulfide intermediate. In the second exchange reaction, the remaining thiolate anion attacks the mixed-disulfide bond and resolves it.

1.4.1 DsbA

DsbA is a 23 kDa monomeric periplasmic protein with a modified thioredoxin fold; it has a 65 residue-long helical domain between the N-terminal βαβ motif and the C-terminal ββα of thioredoxin. The CXXC motif is located in the α helix of the N-terminal domain. The protein functions as an oxidase, inserting disulfide bonds into substrate proteins as they arrive in the periplasm. It is active when it is in its oxidised form - with the cysteines of the CXXC motif connected via a disulfide bond (Bardwell et al. 1991)

One of the deprotonated cysteine residues of the substrate attacks the sulfur atom of the N-terminal cysteine of DsbA (Cys30) leading to the formation of a disulfide-bonded intermediate between DsbA and the substrate. The remaining cysteines of the substrate CXXC motif are deprotonated and attack the sulfur atom of the substrate cysteine bound to DsbA. A disulfide bond is then formed between the cysteine residues of the substrate and DsbA is released in its inactive, reduced form (Bardwell et al. 1991). Cys30 has been identified to have a unique feature: a very low pK_a value for a non-catalytic cysteine. Normally a cysteine residue in a random coil has a pK_a value would be 8.5-9. C30 has a pK_a value of about 3.3. Thus, at normal biological pH the cysteine is always in the reactive thiolate anion state (Guddat et al. 1998; Nelson and Creighton 1994), which makes DsbA a very powerful oxidase.

In addition, it has been suggested that the properties of the CXXC motif of DsbA are not the only feature that results in its function. A cis-proline residue, located in a loop in close proximity in space but not in sequence to the CXXC motif, contributes to the stability of the protein, substrate recognition and probably substrate release (Charbonnier et al. 1999).

DsbA is considered to be the most oxidising of all oxidases in thiol-disulfide cascades. It can generate disulfide bonds very easily, however it does it in a non-specific manner. It is

possible that unnecessary disulfide bonds are introduced, like in *c*-type apocytochromes or for proteins with more than 2 cysteine residue disulfide bonds are introduced wrongly.

1.4.2. DsbB

When DsbA gets released from the mixed-disulfide intermediate with its substrate, the cysteines of the CXXC motif are in the thiol form. For the protein to be active again, a disulfide bond should be re-introduced. For this "recycling" of DsbA, another protein is needed, DsbB (Bardwell et al. 1993).

DsbB is a 20 kDa inner membrane protein with four transmembrane helices and four conserved cysteine residues located in the first and second periplasmic loop. DsbB restores the disulfide bond of DsbA by using the oxidising power of the electron-transport chain. Electrons from DsbA, through DsbB, are transferred to quinones. Under aerobic growth conditions ubiquinone is the electron acceptor, and that then becomes reoxidised by terminal oxidases passing electrons to O_2. Under anaerobic growth conditions menaquinone is the electron acceptor, which becomes reoxidised by an anaerobic electron-transport system and the electrons are transferred to an electron acceptor other than oxygen (Bader et al. 1999). Thus, DsbB is functional in different growth conditions.

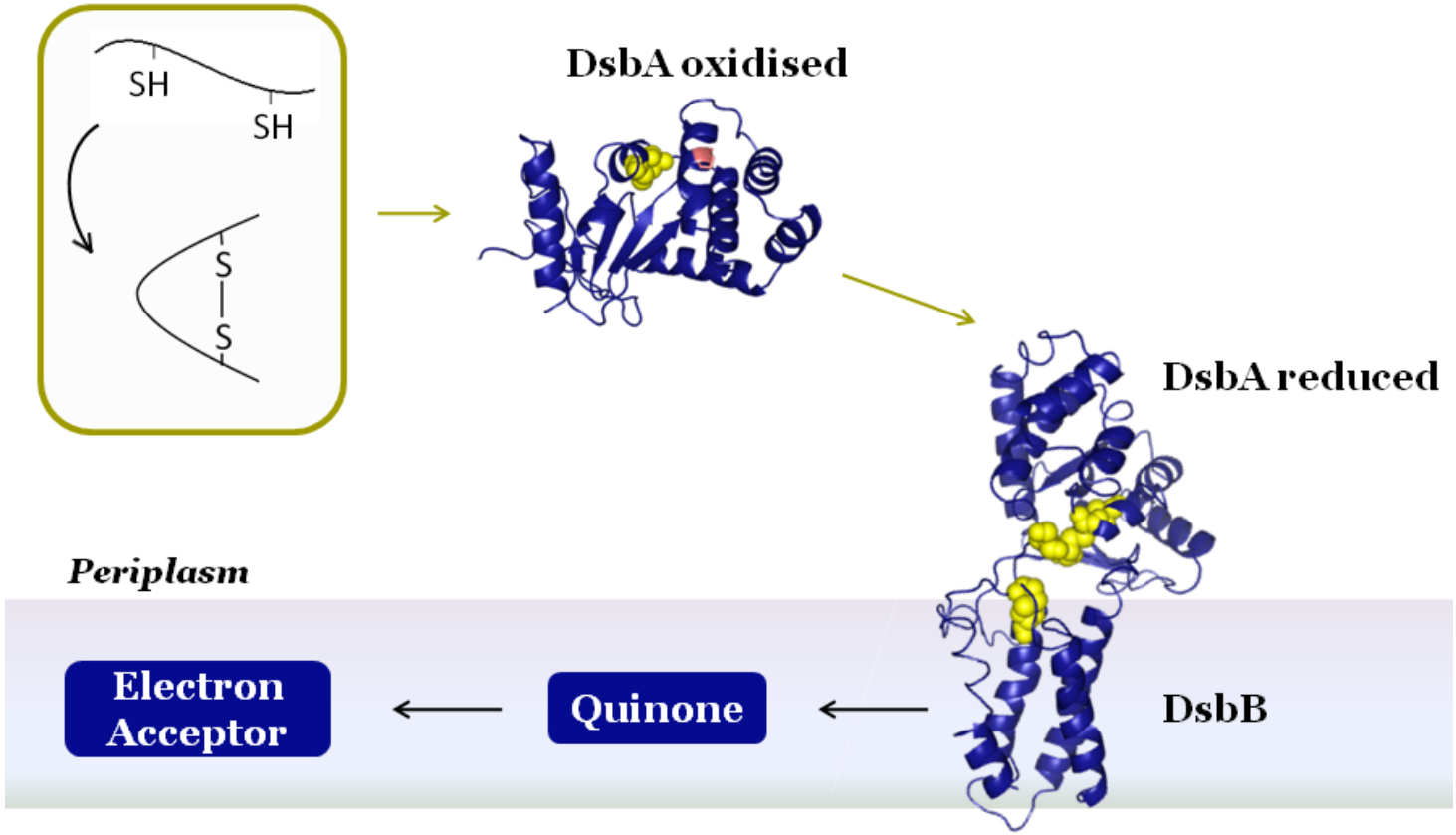

Figure 1. 4: Oxidative protein folding in the periplasm of gram negative bacteria. DsbA (1FVK) (Guddat et al. 1997) in its active, oxidised form inserts disulfide bonds to substrates. After this reaction the protein becomes reduced. For the recycling of DsbA, DsbB a transmembrane protein is needed. DsbA and DsbB form a complex (2ZUP) (Inaba et al. 2009). DsbA becomes oxidised and DsbB transfers electrons to a quinone and then to a final electron acceptor. The cysteine residues are depicted by yellow spheres. The cis-proline residue that contributes to the stability of DsbA is coloured in pink. The yellow arrows represent transfer of electrons.

The four cysteine residues of DsbB are organised in two pairs. Cys41 and Cys44 form a CXXC motif whereas the other pair is located in positions 104 and 130. There are two models proposed for the function of DsbB. Both are accepted and consistent with the existing structures and are in agreement with the assumption that Cys30 of DsbA in its thiolate anion form attacks Cys104 of the Cys104-Cys130 bond. That results in formation of an intermediate disulfide bonded complex between Cys30 of DsbA and Cys104 of DsbB. After that there are two scenarios. One model suggests that Cys130 immediately attacks Cys41, that is in a disulfide bond with Cys44, forming a Cys41-Cys130 disulfide bond (Kadokura and Beckwith 2002). After formation of the interloop disulfide bond, the reduced Cys44 thiolate forms a charge–transfer complex with ubiquinone, avoiding this way release of DsbA in a prior step, because Cys130 is "locked" in the disulfide bond with Cys41 (Inaba et al. 2006). In the alternative model, electron transfer to quinone proceeds through sequential exchange reactions and then reduction of quinone. In this model release of DsbA occurs before the interloop electron transfer (Inaba et al. 2006). The interaction between DsbB and quinone is not fully understood and further studies are needed to elucidate the mechanism.

1.4.3. DsbC and DsbG

Proteins containing cysteine residues are prone to unwanted modifications in the oxidising periplasmic space. As mentioned previously, DsbA is considered to be a very good oxidant, forming disulfide bonds rapidly and non-specifically. This ability of DsbA can lead to formation of the wrong disulfide bonds and subsequent misfolding and aggregation, if the substrate protein has more than two cysteine residues. Alternatively, single-cysteine containing proteins can get irreversibly sulfenated. Two proteins exist in the periplasm to correct wrongly-formed disulfide bonds and to reverse oxidation of single cysteine residues, DsbC and DsbG, respectively.

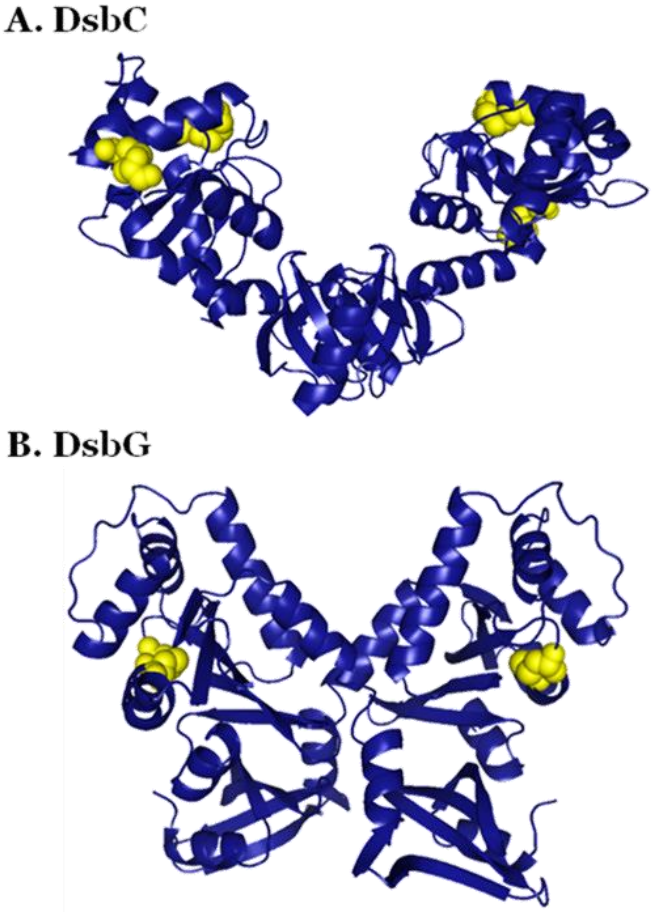

Figure 1. 5: A. The structure of the DsbC homodimer (1EEJ) (McCarthy et al. 2000) B. Structure of the DsbG homodimer (1V57) (Heras et al. 2004). The cysteine residues are represented in yellow spheres.

DsbC is a 46 kDa homodimeric protein located in the periplasm. Each (23 kDa) monomer has an N-terminal thioredoxin domain with a conserved CXXC motif (C98-C101) and a C-terminal helical domain which is responsible for the dimerisation (Missiakas et al. 1994). The dimer has a V-shaped structure, where the cysteines of the monomer face the inside of the V-shape and are found in the reduced state *in vivo* (McCarthy et al. 2000).

There are two models proposed for the function of DsbC (Kadokura et al. 2003; Rietsch et al. 1997); in the first DsbC is an isomerase, in the second it functions as a reductase. In both cases, the reaction starts when Cys98 of DsbC attacks the incorrect disulfide bond of the substrate, resulting in a mixed-disulfide intermediate. If DsbC functions as an isomerase, the mixed disulfide could be attacked by another cysteine of the substrate, allowing a different

disulfide bond to form in the substrate and DsbC would then be realased from the complex. If DsbC functions as a reductase, the mixed disulfide could be attacked by Cys101 of DsbC, generating an oxidised DsbC and a reduced substrate, which can then be reoxidised by DsbA. DsbC has been also reported to have a chaperone activity, which allows the protein to bind unfolded substrates.

DsbG is an analogue of DsbC, having both chaperone and isomerase activity as shown *in vitro*. It has a slightly larger monomer (26 kDa) and a 24% aminoacid sequence identity to DsbC. The cleft of the V-shaped structure in DsbG is almost twice the size of DsbC and there are several acidic residues forming a negatively charged surface that doesn't exist in DsbC, suggesting possibly different substrates for DsbG, possibly larger and with less hydrophobic surfaces than those of DsbC (Heras et al. 2004). Recently (Depuydt et al. 2009), substrates of DsbG were identified. DsbG preferentially interacts with three periplasmic proteins in the family of L,D-transpeptidases, that have a single cysteine residue that is essential for their function. This cysteine residue can become oxidised to a sulfenic acid, and DsbC and DsbG can protect it from sulfenylation. It appears that DsbG is more proficient in this task than DsbC.

1.4.4 DsbD

DsbC and DsbG but also other proteins in the bacterial periplasm need to be maintained in their reduced form in order to be functional (Rietsch et al. 1997). The necessary reductive power is provided by DsbD (Missiakas et al. 1995). DsbD and its analogue from Gram-positive bacteria CcdA are the only proteins known that are able to transfer reductive power from the cytoplasm, across the inner membrane and into the periplasmic space.

DsbD is a 59 kDa protein with three distinct domains. An N-terminal domain with an immunoglobin-like structure (nDsbD), a core membrane domain with eight transmembrane

segments (tmDsbD) and a C-terminal domain with a thioredoxin-like fold (cDsbD). In each domain there is a conserved pair of cysteine residues essential for the function of the protein, Cys103-Cys109 in nDsbD, Cys163-Cys285 in tmDsbD and Cys461-Cys464 in cDsbD (Stewart et al. 1999).

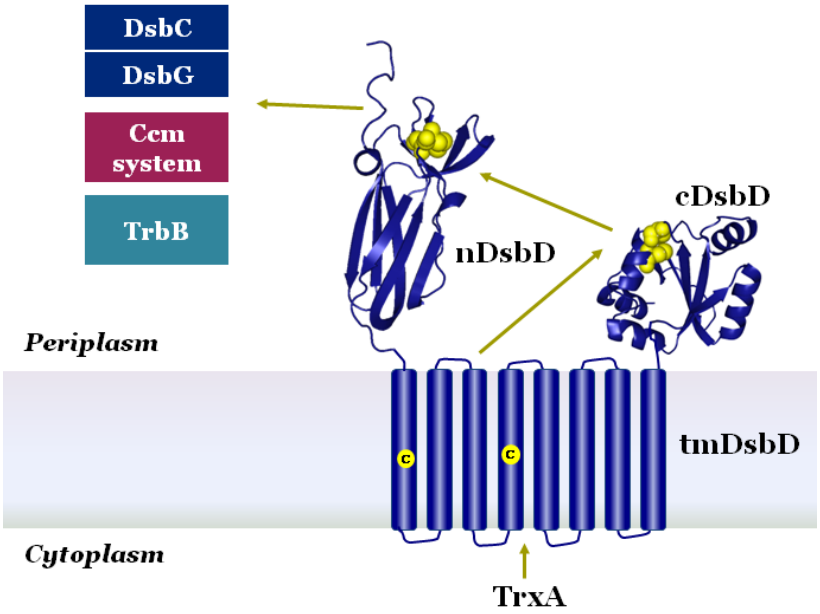

Figure 1.6: DsbD transfers reducing power from the cytoplasm to the periplasm. It has three distinct domains. An N-terminal domain (nDsbD) with an immunoglobin like fold (1L6P) (Goulding et al. 2002), a tm domain (tmDsbD) with eight transmembrane helices and a C-terminal domain (cDsbD) with a thioredoxin-like structure (2FWH) (Stirnimann et al. 2006). In each domain there is a pair of cysteine residues (in yellow), all of which are conserved and essential for the function of the protein. The reductant is transferred when cytoplasmic thioredoxin reduces the disulfide bond of the cysteines in tmDsbD. Then the disulfide bond in cDsbD gets reduced and sequentially the disulfide bond in nDsbD gets reduced. The reductive power is then transferred to the partners of nDsbD DsbC , DsbG, CcmG and TrbB

The proposed mechanism for electron transfer to the periplasm starts with reduction of the disulfide bond of Cys163-Cys285 in the transmembrane domain by cytoplasmic thioredoxin TrxA, after interaction of the two proteins in the cytoplasmic side of the inner membrane. It is believed that the transmembrane domain has an hourglass-like structure and can switch conformations; it be found “open” either on the cytoplasmic or the periplasmic side of the membrane. After reduction of the disulfide bond, the structure of tmDsbD is believed to alter and this rearrangement allows the reduced cysteines to interact with the cysteines of the

CXXC motif of cDsbD (Cys461-Cys464) on the periplasmic side of the membrane. Reduced cDsbD can then interact with nDsbD and the disulfide between cysteines Cys103-Cys109 gets reduced. Then, the reduced cysteines in nDsbD can interact with oxidised partners of nDsbD that need to be reduced in order to be active (Haebel et al. 2002; Rozhkova and Glockshuber 2007).

As mentioned previously, reductive power from DsbD is transferred to DsbC and DsbG, as well as CcmG of the Ccm system. Recently, another partner of DsbD has been identified, a structurally distinct isomerase, TrbB (Hemmis et al. 2011). TrbB is expressed from conjugative plasmid F and needs the presence of DsbD to remain reduced.

1.5 Aims of the work described in this thesis

The Ccm system of post-translational covalent heme-attachment is dependent on the Dsb system in the bacterial periplasm. The work presented in this thesis aims to elucidate mechanistic aspects and structure-function relationships in two key proteins of these pathways, DsbD and a *c*-type apocytochrome.

Chapter 3 is focusing on functional studies of DsbD. DsbD is a unique protein with interesting biochemical properties. Studies on the role of specific amino acid residues for the activity of the protein *in vivo* require a new method. This led to the development of a novel protocol with which we have the ability to monitor the functionality of DsbD by linking it with the levels of mature *c*-type cytochrome produced. In this chapter the description of the method and the assessment of DsbD variants are presented. Variants on DsbD that were examined had been identified in biophysical studies to affect the properties of DsbD. In the second part, variants of tmDsbD that have not been characterised previously were assessed using this method.

Chapter 4 aims to understand the biophysical properties of the residues of the heme binding CXXCH motif in *c*-type apocytochromes using NMR spectroscopy. The properties of this motif can give insight on the interaction of the *c*-type apocytochrome with proteins of the Ccm system and can reveal why the CXXCH motif was selected for heme binding. In the first part of this chapter, it is verified that an engineered *c*-type apocytochrome is the ideal *c*-type apocytochrome for NMR studies and is described how backbone assignments of the apoprotein were conducted. Complete backbone assignments are necessary for any further protein-protein interaction study by NMR spectroscopy. The second part of this chapter focuses on pH dependent NMR experiments that generate information about the pK_a values of residues of the C-terminus of the protein including the CXXCH motif.

CHAPTER 2

Materials and methods

2.1 Bacterial Strains and Plasmids

The bacterial strains used in this study are described in Table 2.1. The plasmids used in this study are presented in Table 2.2.

Dh5a cells were used for molecular biology. JCB387 cells were used for expression of cytochrome *c*-type b_{562}. MC1000 (parental) and MC1000 DsbD deletion strains were used for *in vivo* anaerobic growths.

Table 2.1: Bacterial strains used in this study

Strain	Genotype	Source/Reference
Dh5α	F$^-$ *end*A1 *gln*V44 *thi-1 rec*A1 *rel*A1 *gyr*A96 *deo*R *nup*G Φ80 *lac*ZΔM15 Δ(*lacZYA-argF*)U169, *hsd*R17(r_K^- m_K^+), λ–	Stratagene
JCB387	*E. coli* RV Δ*nirB*	(Hussain et al. 1994)
MC1000	*ara*D139, Δ(*ara, leu*)7697, Δ*lac*X74, *gal*U, *gal*K, *str*A	(Casadaban and Cohen 1980)
MC1000ΔDsbD	*ara*D139, Δ(*ara, leu*)7697, Δ*lac*X74, Δ*dsbD, gal*U, *gal*K, *str*A	(Stewart et al. 1999)

Table 2.2: Plasmids used in this study

Plasmid	Vector	Expressed Protein(s)	Source/Reference
pDsbd1	pTTQ18	*E. coli* DsbD (residues G1-P546), SA (spacer), C-terminal Strep-tag II	(Mavridou et al. 2009)
pDsbd3	pTTQ18	*E. coli* C464A-DsbD (residues G1-P546) C-terminal His6-tag	(Mavridou et al. 2009)
pDsbd7	pTTQ18	*E. coli* Q488A-DsbD (residues G1-P546), SA (spacer), C-terminal Strep-tag II	This work
pDsbd8	pTTQ18	*E. coli* D455N-DsbD (residues G1-P546), SA (spacer), C-terminal Strep-tag II	This work
pDsbd9	pTTQ18	*E. coli* D455N/E468Q-DsbD (residues G1-P546), SA (spacer), C-terminal Strep-tag II	This work
pDsbd10	pTTQ18	*E. coli* Q488K-DsbD (residues G1-P546), SA (spacer), C-terminal Strep-tag II	This work
pDsbd11	pTTQ18	*E. coli* V462A-DsbD (residues G1-P546), SA (spacer), C-terminal Strep-tag II	This work
pDsbd1d	pTTQ18	*E. coli* P249A-DsbD (residues G1-P546), SA (spacer), C-terminal Strep-tag II	Lab stock
pDsbd1f	pTTQ18	*E. coli* P333A-DsbD (residues G1-P546), SA (spacer), C-terminal Strep-tag II	Lab stock
pDsbd1g	pTTQ18	*E. coli* P284A-DsbD (residues G1-	Lab stock

		P546), SA (spacer), C-terminal Strep-tag II	
pDsbd1j	pTTQ18	*E. coli* G266A-DsbD (residues G1-P546), SA (spacer), C-terminal Strep-tag II	Lab stock
pDsbd1k	pTTQ18	*E. coli* G206A-DsbD (residues G1-P546), SA (spacer), C-terminal Strep-tag II	Lab stock
pDsbd1m	pTTQ18	*E. coli* G213A-DsbD (residues G1-P546), SA (spacer), C-terminal Strep-tag II	Lab stock
pDsbd1n	pTTQ18	*E. coli* G155A-DsbD (residues G1-P546), SA (spacer), C-terminal Strep-tag II	Lab stock
pRZ001	pEG278	*Paracoccus denitrificans* cytochrome cd_1	(Mavridou et al. 2011)
pEC86	pACYC184	*E. coli* Cytochrome *c* maturation operon	(Arslan et al. 1998)
pb562CXXCH	pCE820	*E. coli* cytochrome b_{562} carrying R98C/Y101C mutation	(Barker et al. 1995)

2.2 Genetic Techniques

2.2.1 Competent Cells

For competent cell production a preculture of each strain in SOB medium was incubated at 37 ºC with shaking at 200 rpm overnight (Table 2.3). 2 ml of this culture were transferred to of 200 ml SOB medium and grown at 37 ºC with shaking at 200 rpm until an OD_{550} value of 0.45. Then, cells were incubated on ice for 30 min and subsequently centrifuged at 2500 xg for 15 min at 4 ºC. The pellets were resuspended in 66 ml of RF1 solution (Table 2.4) and were incubated on ice for 60 min. Then, they were centrifuged at 2500 xg for 15 min at 4 ºC and resuspended in 16 ml of RF2 solution (Table 2.5). Finally they were incubated on ice for 15 min, aliquoted (220 μl aliquots) and were frozen in a dry ice / methanol bath.

Table 2.3: SOB medium

Component	**g/l solution**
Peptone	20
Yeast Extract	5
NaCl	0.584

KCl	0.184
$MgCl_2$	2.032
$MgSO_4$	2.44

Table 2.4 RF1 solution (the pH was adjusted at 5.8 using 0.2M acetic acid)

Component	**g/l solution**
RbCl	12
$MnCl_2.4H_2O$	9.9
K Acetate	2.945
$CaCl_2.2H_20$	1.5
Glycerol	150

Table 2.5: RF2 solution (the pH was adjusted at 6.8 with NaOH)

Component	**g/l solution**
MOPS	2.09
RbCl	1.2
$CaCl_2.2H_20$	11
Glycerol	150

2.2.2 Transformation of competent cells with plasmid DNA

100 μl competent cells were thawed on ice and incubated with plasmid DNA for 30 min on ice. After heat shock at 42 ^oC for 30 s, cells were left on ice for 2 min. 800 μl of LB (10 g/l peptone, 5 g/l yeast extract and 10 g/l NaCl) were then added and the cells incubated at 37 ^oC, with shaking at 200 rpm for 1 h. For plasmids encoding the gene for resistance to gentamycin, the cells were left to recover for 1.5 h. Cells were centrifuged at 3000 xg for 2 min, the majority of the supernatant LB was decanted and the cells were resuspended in 100 μl of the residual LB medium. The suspension was then plated on solid LB agar medium (LB medium with 1.5 % w/v agar - see section 2.3.1) and incubated overnight at 37 ^oC.

2.2.3 Purification of plasmid DNA and PCR products

Purification of plasmid DNA was performed using QIAprep Spin Miniprep Kit (Qiagen), according to the manufacturer's instructions. Purification of PCR products was carried out using the QIAquick PCR Purification Kit or the QIAquick Gel Extraction Kit (Qiagen).

2.2.4 Agarose gel electrophoresis

For electrophoresis of DNA samples, agarose gels consisting of TAE buffer (40 mM Tris-acetate pH 8.0, 1 mM EDTA), 1 % agarose and 0.2 μg/ml ethidium bromide were used. The DNA samples were loaded with 6x gel loading dye (10 mM EDTA, 50 % v/v glycerol, 0.5 % bromophenol blue). Electrophoresis was performed in TAE buffer, at a constant current of 70 mA. Hyperladder I (Bioline) was used as a DNA standard.

2.2.5 DNA sequencing

All the plasmids that were produced during this work were sequenced to confirm that the DNA sequence of the insert encodes the protein of interest. Plasmid DNA sequencing was performed by GeneService (Oxford).

2.2.6 Site-directed mutagenesis

Mutations were introduced to plasmids pDsbd1 and pDsbd8 using the QuikChange site-directed mutagenesis method (Stratagene), as described in the manufacturer's instruction manual. The primers for each mutation are presented in the table below (Table 2.6) and were kindly provided by Dr. D.A.I. Mavridou. The PCR reactions were carried out using KOD DNA polymerase (Novagen) following the product guidelines.

Table 2.6: Oligonucleotides used for site-directed mutagenesis

Template	Primers	Sequence (5'-3')	Plasmid
pDsbd1	Q488A - fw Q488A - rev	GACACGGTCTTACTTGCGGCCAACGTCACGGCC GGCCGTGACGTTGGCCGCAAGTAAGACCGTGTC	pDsbd7
pDsbd1	D455N - fw	CCGGTGATGTTAAATCTTTATGCCGACTG	pDsbd8

	D455N - rev	CAGTCGGCATAAAGATTTAACATCACCGG	
pDsbd8	E468Q - fw E468Q - rev	GCCTGTAAAGAGTTTCAGAAATACACCTTCAGC GCTGAAGGTGTATTTCTGAAACTCTTTACAGGC	pDsbd9
pDsbd1	Q488K - fw Q488K - rev	GACACGGTCTTACTTAAGGCCAACGTCACGGCC GGCCGTGACGTTGGCCTTAAGTAAGACCGTGTC	pDsbd10
pDsbd1	V462A - fw V462A - rev	CTTTATGCCGACTGGTGCGCCGCCTGTAAAGAGTTTG CAAACTCTTTACAGGCGGCGCACCAGTCGGCATAAAG	pDsbd11

2.3 Bacterial Growth Conditions

2.3.1 Growth Media

Aerobic cultures of *E. coli* were grown in LB medium (10 g/l peptone, 5 g/l yeast extract and 10 g/l NaCl). Bacterial growth on solid media was performed on plates with LB and 1.5 % w/v agar.

For production of proteins labelled with ^{13}C at the C^{β} of their cysteine residues, cells were grown in 2xTY rich medium broth (16 g/l peptone, 10 g/l yeast extract and 5 g/l NaCl) where [3-^{13}C]-L-cysteine (Cambridge Isotopes) (40 μg/ml per liter of culture) was added.

For production of uniformly ^{15}N-labelled proteins, M9 minimal medium was used. This consists of 100 ml/l of 10x M9 salts solution (60 g/l Na_2HPO_4 , 30 g/l KH_2PO_4 , 10 g/l NH_4Cl and 5 g/l NaCl), 1 mM $MgSO_4$, 0.1 mM $CaCl_2$, 1 mM thiamine.HCl, 10 ml/l of 20 % w/v glucose and 887 ml/l ultrapure water. The ^{15}N label was provided by substituting NH_4Cl with $^{15}NH_4Cl$ (Goss Scientific) in the 10 x M9 salts solution.

Anaerobic growths were performed using the following liquid medium: 2.5 g/l OXOID half-strength Nutrient Broth, 4.5 g/l KH_2PO_4, 10.5 g/l K_2HPO_4, 1 g/l $(NH_4)_2 SO_4$, 0.5 g/l sodium citrate, 0.1 g/l $MgSO_4 \cdot 7H_2O$, 10 mM sodium selenate, 10 mM ammonium molybdate, 10 mM KNO_3, 1 ml/l sulfur free salts (400mM $MgCl_2$, 50 mM $MnCl_2$, 25 mM $FeCl_3$, 5 mM $CaCl_2$), 40mM fumaric acid solution (pH: 7.0), 0.4% w/v glycerol and 1 mg /l thiamine.

Antibiotic selection was performed using 100mg/ml ampicillin, 34mg/ml chloramphenicol, 20mg/ml for gentamycin and 100mg/ml for carbenicillin, where needed.

2.3.2 Growth conditions

2.3.2.1 Aerobic Growths

All aerobic bacterial small scale cultures in LB were grown at 37 ^{o}C with shaking at 200 rpm overnight unless stated elsewhere.

2.3.2.2 Growths in rich medium for expression of apocytochrome *c*-b_{562}

For the expression of apocytochrome *c*-b_{562} in rich media, for production of unlabelled or 3-^{13}C L-cysteine-labelled protein, 2xTY medium was used. JCB387 cells transformed with pb562CXXCH (Amp^{R}) and pEC86 (Cam^{R}), grown on solid medium and inoculated directly into 500 ml of 2xTY in 2 l flasks. Protein induction was accomplished by addition of 1 mM IPTG from the start of the growth. Cultures were grown at 37 ^{o}C, with shaking at 200 rpm overnight.

2.3.2.3 Growths in M9 for expression of ^{15}N labelled apocytochrome b_{562}CXXCH

For the expression of uniformly ^{15}N-labelled apocytochrome b_{562}CXXCH, JCB387 cells were transformed with pb562CXXCH. 5, 30 ml precultures in 250ml flasks were set up per 5 l growth and grown at 30^{o}C with shaking at 200 rpm overnight. Cultures were centrifuged at 3000 rpm for 15 min at 4 ^{o}C and cells were then resuspended in 10 ml of Mg medium (see section 2.3.1 1 ml of this suspension was added to each 2 l flask containing 500 ml of M9 media. Cells were grown at 37 ^{o}C with shaking at 200 rpm. When they reached OD_{600} values above 0.8, 1 mM IPTG was added for induction of protein expression and the cell cultures were incubated overnight at with shaking at 37 ^{o}C 200 rpm.

2.3.2.4 Anaerobic growths for determining the activity of DsbD and variants

Anaerobic growths were used to assess the function of full-length DsbD *in vivo*. MC1000 DsbD deletion strain was complemented with plasmids that encode wild-type DsbD and variants (see Table 2.2). The strain was also transformed with plasmid pRZ001 expressing *Paracoccus denitrificans* cytochrome cd_1, the *c*-type cytochrome chosen to assess the activity of DsbD. MC1000 parental strain complemented with plasmid pRZ001 was used as a positive control.

Cells were grown anaerobically (see section 2.3.1) to allow the expression of the endogenous Ccm system, in 1 l bottles at 37 ^{o}C for 24h without shaking from overnight starter cultures also grown at 37 ^{o}C. For induction of protein expression the autoinduction method was chosen and accomplished by adding 20ml/l 10% w/v lactose monohydrate dissolved in H_2O. Ampicillin and gentamycin were used to select for the pDsbd plasmids and the pRZ001 plasmid, respectively.

2.4 Protein purification

2.4.1 Bacterial Fractionation

Periplasmic fractions for all cultures were prepared as described in (Allen et al. 2003). Cells were harvested by centrifugation at 5600 xg for 10 min at 4 ^{o}C and resuspended in 5 ml/l of culture 10 mM Tris-HCl pH 7.3, 150 mM NaCl. Cells were then centrifuged at 5600 xg for 15 min at 4 ^{o}C. The supernatant was removed and pellets were resuspended in 5 ml per liter of culture SET buffer. 30 mg of lysozyme per liter of culture was added to each cell suspension and a mild osmotic shock was obtained by adding 5ml ice cold water per liter of culture, followed by incubation at 37 ^{o}C for 30 min. The cells were centrifuged at 9000 xg for 30 min. The supernatant contained the periplasmic fraction and was retained.

2.4.2 Purification of apocytochrome *c*-b_{562}

2.4.2.1 Anion-exchange chromatography

For the purification of the apoform (heme-free form) of cytochrome *c*-b_{562} anion-exchange chromatography was performed at room temperature. 80 ml of DEAE Sepharose (GE Healthcare) were packed in a fast flow column using a peristaltic pump. The resin was washed with 5 CV (Column Volume) of ethanol, primed with 10-20 ml 2M NaCl (in case of new resin), and equilibrated with 2 CV of H_2O pH 8. A 10x dilution of the periplasmic extracts in H_2O pH 8 was loaded on the column at a flow rate of 10 ml/min. The column was washed with 2-3 CV H_2O pH 8. The protein was eluted with a 0-0.5 M NaCl gradient and 7 ml fractions were collected until the coloured (red) holocytochrome *c*-b_{562} started to elute. Each fraction was analyzed on SDS-PAGE (see section 2.5.1); gels were Coomassie blue stained (2.5.2.1) and heme stained (2.5.2.2). Gel filtration was subsequently used to remove a higher molecular height (50 kDa) contaminant coeluting with apocytochrome *c*-b_{562}.

2.4.2.2 Gel filtration

Fractions that contained cytochrome *c*-b_{562} were combined, freeze dried, dissolved in 4 ml 200mM NaCl pH 8 and centrifuged at 9000 xg for 4 min. A Superdex 75 (26/60) 124 ml bed prepacked column was used and run at room temperature with maximum pressure of 0.5 MPa. The column was run using an ÄKTAdesign system. It was equilibrated with 400 ml filtered 200 mM NaCl pH 8.0 at a flow rate of 2.5 ml/min. The protein solution was loaded and the column was run at a flow rate of 2 ml/min, collecting 1ml fractions. Protein elution was monitored by measuring the absorption at 280 nm. Selected fractions were analyzed by SDS-PAGE (see section 2.5.1). The fractions that were verified to contain apocytochrome *c*-b_{562} in a very pure form were freeze dried and redissolved in 4ml H_2O (or D_2O in case of the 3-^{13}C L-cysteine-labeled sample). The protein solution was transferred to a 3K 15ml

concentrating device (Millipore) and washed with 3 x 15 ml H_2O (or D_2O) by centrifugation at 2500 xg, by concentrating and rediluting in H_2O (or D_2O).

2.5 Protein Characterisation

2.5.1 Sodium dodecyl sulphate polyacrylamide gel electrophoresis (SDS-PAGE)

SDS-PAGE analysis was perfomed on 10% NuPAGE gels (Invitrogen) using 20x MES NuPAGE running buffer according to the manufacturer's instructions, at a constant voltage of 200V for 33min. Prestained protein marker SeeBlue Plus 2 (Invitrogen) was used. Protein samples were mixed with 3x SDS sample buffer (New England Biolabs). Disrupted whole cell extracts were mixed with 4x SDS loading buffer (12 g glycerol, 2 ml H_2O, 10 ml 10 % w/v SDS stock solution, 1 ml 1M Tris-HCl pH 7.5, 6 mg bromophenol blue). Protein samples were denatured at 95 ^oC for 2 min, whereas cell extracts were denatured for 5 min at 42 ^oC.

2.5.2 Stainings of SDS-PAGE gels

2.5.2.1 Coomassie blue stain

Coomassie blue stain was used to stain for protein and was performed with SimplyBlue SafeStain (Invitrogen) according to the manufacturer's instructions

2.5.2.2 Heme stain

Staining for covalently bound heme was done according to the method of Goodhew (Goodhew et al. 1986). The gel was equilibrated on a rocking platform in 70 ml 250 mM sodium acetate (pH 5.0) for 30 min. 33 mg of 3,3',5,5'-tetramethylbenzidine (TMBZ, Sigma-Aldrich) were dissolved in 30 ml methanol and added to the gel. The gel was left to equilibrate on the rocking platform for 10 min. 500 µl of 30 % H_2O_2 solution were added and

left to equilibrate for 10 min. The solution was then removed and replaced my ultrapure H_2O. After 10 min images of gels were recorded on a gel documentation system (GelDoc 2000, Biorad).

2.5.3 Western blotting

Proteins were detected immunologically by western blotting. Periplasmic or whole cellular extracts were analysed on SDS-PAGE (see section 2.5.1). The acrylamide gel was then transferred onto a nitrocellulose membrane using a semidry transfer process. The gel, the blotting papers and the nitrocellulose membrane (Hybond-C Extra, Amersham Biosciences) were equilibrated in transfer buffer (39 mM glycine, 48 mM Tris-HCl pH 7.3, 0.0375 % w/v SDS and 20 % v/v methanol). Transfer was carried out on a Trans-blot SD Semi Dry Transfer Cell (Bio-Rad) for 1 h at 100 mA and constant voltage of 20 V. The nitrocellulose membrane was blocked overnight at room temperature in TBS buffer (50 mM Tris-HCl pH 7.3, 150 mM NaCl, 0.1 v/v Tween-20) supplemented with 5 % w/v skimmed milk powder. The membrane was then incubated with the primary antibody diluted in the same buffer. After incubation, the membrane was washed for 3 x 5 min with TBS buffer (without added milk). The secondary antibody was diluted in TBS supplemented with 5 % w/v skimmed milk powder and incubated with the nitrocellulose membrane for 1h at room temperature. The membrane was then washed for 3 x 5 min with TBS buffer (without added milk). The secondary antibodies were conjugated to alkaline phosphate, thus staining was carried out using a SIGMA FAST alkaline phosphatase substrate tablet (SIGMA) diluted in 10 ml ultrapure H_2O Development was stopped by rinsing the membrane with ultrapure water and images of gels were recorded on a gel documentation system (GelDoc 2000, Biorad).

2.5.4 Determination of protein concentration

Determination of the protein concentration of all protein solutions of apocytochrome *c*-b_{562} was carried out using the BCA Protein Assay kit-Reducing Agent Compatible (Pierce) following the manufacturer's instructions.

2.6 *in vivo* studies

A method was established to assess the function of full-length DsbD in vivo by linking it to the maturation of a *c*-type cytochrome. *Paracoccus denitrificans* cytochrome cd_1 was the cytochrome of choice. All growths were carried out anaerobially as described in section 2.3.2.4. Each experiment was repeated six times to eliminate the variations in cytochrome *c* expression. Bacterial fractionation to isolate the periplasmic fraction was performed as described in section 2.4.1. Cytochrome cd_1 expression levels were quantified using SDS-PAGE analysis (section 2.5.1), heme staining (section 2.5.2.2) and densitometry (using the software GeneSnap) on samples normalised for wet cell pellet weight. Normalisation for wet cell pellet weight occurs following harvesting of each bacterial culture. The weights of each pellet are recorded. For normalisation, 2 μl of the periplasmic extract are loaded for the largest pellet. For smaller pellets the loadings were calculated in a reverse analogical manner. For growths where large amounts of cytochrome cd_1 were produced 1:10 dilutions of the periplasmic extracts were used to obtain reliable densitometry results.

To ensure that the results are representative for the loadings and that there is no signal saturation, different loadings of a specific periplasmic extract are presented in Appendix Supplemental Figure SF1. It is clear that loadings between 1.5-2 μl that were used for the analysis are not saturated and ideal for the purpose of this method. The correlation between heme staining and absorbance has been previously reported for cytochromes in (Goddard et al. 2010). The figure is included in Appendix, SF2.

To confirm that the expression of full-length DsbD variants was equivalent to the wild-type protein 1 ml of cell extract from each growth was centrifuged at 3000 xg for 5 min at room temperature and the cell pellet was lysed using 200 ml of BugBuster MasterMix (Merck) and agitating gently for 20 min at room temperature. Total cell extracts, normalised for wet cell pellet weight, were analysed using SDS-PAGE (see section 2.5.1) and Western blotting (see section 2.5.3). cDsbD goat antiserum raised against the cDsbD sequence of *E. coli* DsbD (1:1000 dilution) and donkey anti-sheep alkaline phosphatase conjugated antibody (1:6000 dilution were used as primary and secondary antibodies, respectively.

To confirm that the periplamic extraction process is reliable, normalised periplasmic extract from each growth were analysed by SDS-PAGE (see section 2.5.1) and Western blotting (see section 2.5.3). DsbA rabbit antiserum raised against the DsbA sequence of *E. coli* DsbA (1:1000 dilution) and goat anti-rabbit alkaline phosphatase conjugated antibody (1:6000 dilution) were used as primary and secondary antibody, respectively.

2.7 NMR spectroscopy

2.7.1 NMR spectrometers

All the NMR experiments described in this thesis have been performed on home-built NMR spectrometers in the Department of Biochemistry. Three spectrometers were used that operate at proton frequencies of approximately 500, 600 and 750 MHz. The magnets were supplied by Oxford Instruments Company. The spectrometers were equipped with home-built triple-resonance pulsed-field gradient probeheads and were controlled with GE/OMEGA software. All experiments were carried out at 293K.

2.7.2 Sample Preparation

The protein concentration in most of the samples was approximately 1 mM and the sample volumes were 600 μl when standard NMR tubes (Wilmad) were used and 280 μl for Shigemi NMR micro-tubes (Shigemi Inc). Uniformly ^{15}N-labelled samples were prepared in 95 % H_2O/5 % D_2O and [3-^{13}C]-cysteine-labelled samples were prepared in 99.9 % D_2O. All experiments, excluding pH titrations, were carried out at pH 5.2. Apocytochrome *c*-b_{562} is in its oxidised state (with a disulfide bond between the two cysteine residues) after purification; thus, for the reduction of the disulfide bond 10 mM DTT was added to the sample.

2.7.3 NMR experiments

Samples were placed in the NMR spectrometers and left to equilibrate to the desired temperature. Following this, the spectrometer was locked and the shims were optimised. Subsequently the probe was tuned and the pulse(s) calibrated. For the minimisation of the residual water peak, the transmitter offset was placed at the centre of the spectrum and set to the frequency of the water resonance. The parameters of all the experiments that were performed in this study are presented in Table 2.8.

2.7.3.1 pH titrations

1D ^{1}H experiments, ^{1}H-^{15}N -HSQC, ^{1}H-^{15}N HMQC and ^{1}H-^{13}C HSQC experiments were collected for a wide range of pHs. The pH of the sample was measured before it was transferred in the NMR tube and after the collection of the spectra. The average of those two values was used for fitting of data. In Table 2.7 the pH values that data were collected at for each experiment are presented. The values are average of the pH value prior and after the spectra collection. If the pH measurement following the spectra collection was 0.1 units different from the measurement prior to the collection of the spectra, data generated were discarded and the experiment was repeated measuring new values before and after.

Table 2. 7: pH values at which spectra were collected for each type of experiment

	Experiment Type						
pH values	**^{1}H-^{13}C HSQC Ox *c*-b_{562}**	**^{1}H-^{13}C HSQC Red *c*-b_{562}**	**^{1}H-^{15}N HSQC Ox *c*-b_{562}**	**^{1}H-^{15}N HSQC Red *c*-b_{562}**	**^{1}H-^{15}N HMQC Ox *c*-b_{562}**	**^{1}H-^{15}N HMQC Red *c*-b_{562}**	**Denatured ^{1}H-^{13}C HSQC Red *c*-b_{562}**
	4.75	2.93	4.53	4.16	4.33	3.68	5.34
	5.23	3.32	5.18	4.60	4.67	4.28	6.51
	7.17	3.79	5.52	5.16	5.28	4.77	7.22
	8.34	4.23	6.13	5.52	5.72	5.18	7.42
		4.59	6.51	6.17	5.91	5.65	7.62
		5.22	7.04	6.61	6.14	6.02	8.26
		5.58	7.54	6.81	6.32	6.41	8.48
		6.01	8.1	7.04	6.67		8.78
		6.49	8.56	7.26			9.04
		7.08	9.01	7.54			9.42
		8.14	9.34	7.91			9.70
		8.76		8.41			10.04
		9.77		8.84			10.31
							11.67

Table 2. 8: Parameters for the NMR experiments performed in this study

Experiment	**Direct ^{1}H**			**Indirect ^{1}H**		**^{15}N**		**^{13}C**		**rd**	**mixtime**	**SF(MHz)**
	scans	**sw**	**points**	**#**	**sw**	**#**	**sw**	**#**	**sw**			
1D	64	5617.98	4096	-	-	-	-	-	-	1s	-	500
^{1}H-^{15}N-HSQC	8	5617.98	1024	-	-	128	1381.21	-	-	1s	-	500
^{15}N edited NOESY-HSQC	8	5617.98	512	128	5617.98	32	1381.21	-	-	1s	150ms	500
^{15}N edited TOCSY-HSQC	8	5617.98	512	128	5617.98	32	1381.21	-	-	1s		500
HSQC-NOESY-HSQC	8	5617.98	512	50	1381.21	32	1381.21	-	-	1s	150ms	500
^{1}H-^{15}N-HMQC	16 - 64	5617.98	1024	-	-	128	8333.33	-	-	1s	-	500
1D (D_2O)	64	8000.0	4096	-	-	-	-	-	-	1.4s	-	750
^{1}H-^{13}C-HSQC	8 - 32	8000.0	1024	-	-	-	-	44	4065.04	1.4s	-	750
Denatured												
^{1}H-^{15}N-HSQC	8	6006.01	1024	-	-	128	1213.59	-	-	1.2s	-	600
^{15}N edited NOESY-HSQC	8	6006.01	512	100	5208.33	30	1213.59	-	-	1s	200ms	600
^{15}N edited TOCSY-HSQC	8	6006.01	512	100	5208.33	30	1213.59	-	-	0.9s	46ms	600
^{1}H-^{13}C-HSQC	16	8403.36	1024	-	-	-	-	44	4065.04	1.4s	-	750

2.7.4 Data processing

2.7.4.1 Spectral analysis software

Data were analysed using two software programs: NMRPipe (Delaglio et al. 1995) and CCPN Analysis (Vranken et al. 2005).

2.7.4.2 Chemical Shift Changes

Chemical shift differences between the two oxidation states of apocytochrome *c*-b_{562} the were compared by measuring the combined chemical shift ($\Delta\delta(HN,N) = ((\Delta\delta^{1}H)^2 + 0.1(\Delta\delta^{15}N)^2)^{1/2}$)

2.7.4.3 pK_a values determination

pK_a values were determined from ^{1}H, ^{13}C or ^{15}N chemical shifts measured as a function of pH. The titration data were fitted to either one- or two-pK_a curves (Shrager et al. 1972) using in-house software. For titrations described by a single pK_a value, the chemical shift at each pH is defined as:

$$\delta = \delta_{HA} - [(\delta_{HA} - \delta_{A}-) / (1 + 10^{(pKa - pH)})].$$

δ stands for the observed chemical shift of a specific residue at any titration point, δ_{HA} for the chemical shift of the fully-protonated form and $\delta_{A}-$ for the chemical shift of the fully-deprotonated form.

For titrations described by two pK_a values the chemical shift at each pH is defined as:

$$\delta = ((\delta_{HAH})[H^+]^2 + (\delta_{HA}-)K_1[H^+] + (\delta_{A2}-) K_1K_2) / ([H^+]^2 + K_1[H^+] + K_1K_2).$$

δ stands for the observed chemical shift of a specific residue at any titration point, δ_{HAH} for the chemical shift of the doubly-protonated form, $\delta_{HA}-$ for the chemical shift of the first

deprotonated form and δ_{A2}- for the chemical shift of the second deprotonated form. K_1 and K_2 are the dissociation constants for the first and second deprotonation.

CHAPTER 3

3.1 Introduction

DsbD has been shown to transfer reducing power from the cytoplasm to the periplasm of Gram-negative bacteria via sequential thiol-disulfide exchange reactions between pairs of conserved cysteines in its three distinct domains (Stewart et al. 1999). This reducing power is then used for the further reduction of disulfide bonds of cysteine residues in the proteins DsbC, DsbG, CcmG and TrbB (see section 1.4.4). The phenotypes of a DsbD deletion strain lead to lack of activity of downstream proteins due to the necessity of reductant provision. In a DsbD deletion strain the levels of mature *c*-type cytochrome drop because the disulfide bond between the cysteines in the CXXCH heme binding motif cannot be reduced (Crooke and Cole 1995). Also the strain shows high sensitivity to copper (Fong et al. 1995). This can be explained because in the presence of copper the occurrence of non-native disulfide bonds is increased so there is a higher requirement for active reduced DsbC/DsbG. When there is no DsbD present or if it is not functional, DsbC and DsbG cannot be maintained in their reduced and active form, which leads to misfolding of periplasmic proteins.

Several studies conducted previously aimed to identify and characterise the role of conserved amino acid residues in the function of DsbD. Early studies (Stewart et al. 1999) focused on the evaluation of the seven cysteine residues present in DsbD and further studies revealed the importance of conserved proline and glycine residues in the transmembrane domain of the protein (Cho and Beckwith 2006), (Hiniker et al. 2006). Most of these studies exploited the phenotypes of a DsbD deletion strain to develop methods to assess the activity of DsbD variants.

For the characterisation of the cysteine variants of DsbD, the function of the protein was linked to the reduction of DsbC and DsbG (Stewart et al. 1999). Variants of DsbD were expressed in a DsbD deletion strain in a 5 ml culture and the oxidation state of DsbC (or DsbG) was analysed after trichloroacetic acid (TCA) precipitation of whole cells followed by

alkylation of thiols of cysteine residues with 4-acetamido-40-maleimidylstilbene-2,20-disulphonic acid (AMS). A single AMS addition at a reduced cysteine residue leads to a ~0.5 kDa increase to the molecular weight of the protein and this shift is monitored via SDS-PAGE. Western blotting was finally performed against DsbC and DsbD. This method was also used in studies of the importance of residues in the transmembrane domain of DsbD (Cho and Beckwith 2006). In additional experiments, the importance of the cysteine residues for the function of DsbD was also assessed by complementing a DsbD deletion strain with a plasmid expressing DsbD variants while the Ccm system and cytochromes NapB and NapC were overexpressed under aerobic conditions in 1 ml cultures (Stewart et al. 1999). The mature *c*-type cytochromes produced were analysed by SDS-PAGE and were stained for covalently bound heme. Both studies revealed that cysteine Cys103, Cys109, Cys163, Cys285, Cys461, Cys464 were absolutely essential for function.

Another method exploits the copper sensitive phenotype of DsbD deletion mutants. Variants of DsbD expressed from a plasmid in a DsbD deletion strain rescue the copper sensitive phenotype if the mutation does not affect the functionality of the protein; if function of the protein is impaired cells fail to grow on solid medium containing copper. This way the contribution of the residue to the activity of DsbD can be monitored (Hiniker et al. 2006). This method however, is not quantitative or sensitive enough for variants that do not affect the activity of the protein significantly.

These methods have not been able to generate quantitative data showing the extent to which the activity of DsbD is affected by each mutation. Also, in some of the cases the experiments were conducted in very small volumes of cultures (1 ml) (Stewart et al. 1999), they were not repeated more than once and protein expression was induced for four hours only. For the assessment of the contribution of specific residues to the activity of the protein a new method was developed.

3.2. Methodology

This method aims to assess the function of DsbD by linking the transfer of reducing power from this protein to the Ccm system. The reducing power provided is needed to maintain the *c*-type apocytochrome in its reduced form (cysteine residues in thiol form), so that the heme can be covalently attached (Figure 3.1). When there is no reductant provided, it is believed that a disulfide bond is inserted between the cysteines of the CXXCH heme binding motif; the bond cannot then be reduced so heme cannot be attached.

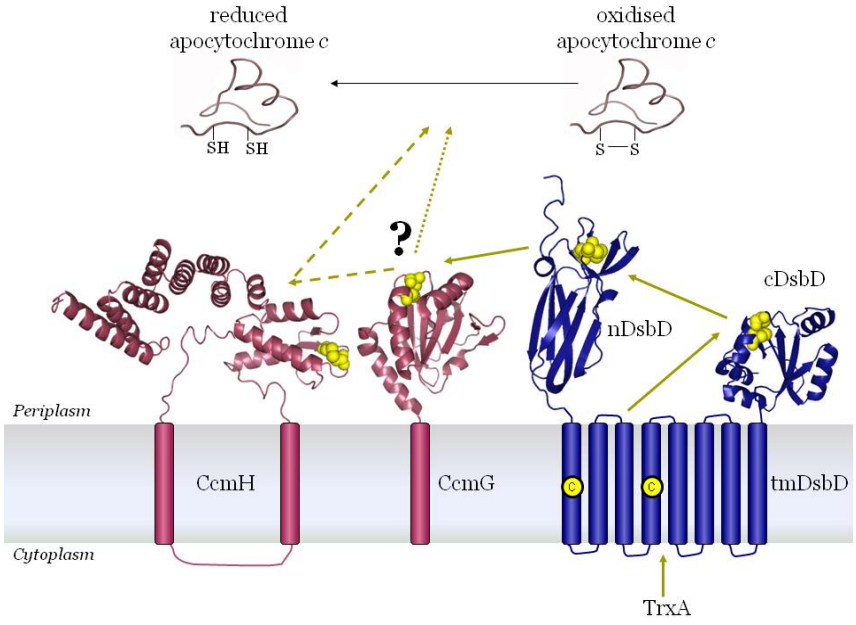

Figure 3. 1: Schematic representation of the transfer of reducing power from DsbD to the Ccm system for the reduction of the *c*-type apocytochrome. The yellow arrows represent transfer of reductant. The dotted yellow arrow depicts potential transfer of reductant from CcmG directly to the *c*-type apocytochrome. The dashed arrows represent potential transfer of reductant from CcmG indirectly to the *c*-type apocytochrome. N-CcmH (2HL7) (Di Matteo et al. 2007), for C-CcmH the structure used is of its analogue NrfG (2E2E) (Han et al. 2008), CcmG (2B1K) (Ouyang et al. 2006), N-DsbD (Goulding et al. 2002), C-DsbD (Stirnimann et al. 2006)

For this method, a DsbD deletion strain is complemented with a plasmid expressing wild-type full-length DsbD. As a probe cytochrome cd_1 from *Paracoccus denitrificans* expressing from a plasmid is used. cd_1 is a cytochrome that has both heme covalently bound to it (in its *c*-type cytochrome domain) and also incorporates d_1 heme in its polypeptide chain. In *E. coli* the

addition of d_1 heme is not possible because there is not a biosynthetic pathway for it. However, the apoprotein is being processed by the Ccm system and heme is attached to its CXXCH heme binding motif. Autoinduction was used for expressing DsbD constructs and cytochrome cd_1. Growths were performed anaerobically, for the endogenous Ccm system to be expressed; 1 l cultures were carried out to increase the reliability of results. The experimental procedure of this method is described thoroughly in section 2.6.

As a positive control the parental strain expressing cytochrome cd_1 from the same plasmid was used. As a negative control the DsbD deletion strain was complemented with a plasmid expressing C464A DsbD, a variant of DsbD where one of the conserved cysteine residues in the C-terminal domain of DsbD is mutated into an alanine and it has been shown previously that it is not able to transfer reducing power (Stewart et al. 1999). After 24 h of growth, the cultures were harvested and their periplasmic extracts were analysed by a SDS-PAGE. Staining of proteins that have heme covalently bound to them was performed with the method of Goodhew (Goodhew et al. 1986)(Figure 3.2). The intensity of the heme stained bands was measured using densitometry.

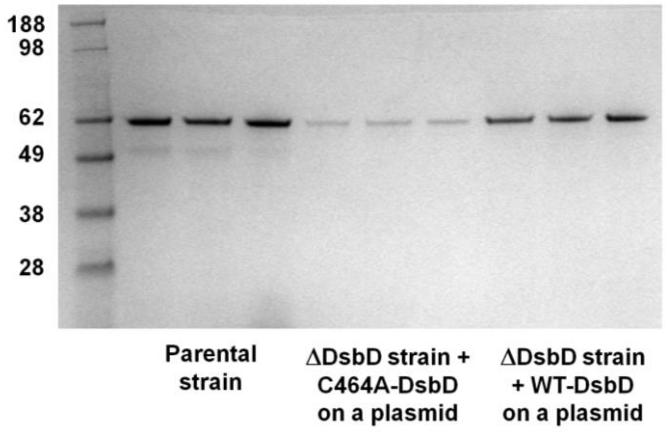

Figure 3. 2: SDS-PAGE analysis of normalised for wet cell pellet weight periplasmic extracts stained for covalently-bound heme. The extracts are from anaerobically grown cultures from the parental strain expressing cytochrome cd_1 from a plasmid, a DsbD deletion strain transformed with plasmids expressing C464A-DsbD and cytochrome cd_1, a DsbD deletion strain transformed with plasmids expressing wild-type DsbD and cytochrome cd_1.Triplicates from each growth condition are presented.

The levels of mature cd_1 produced by a DsbD deletion strain complemented by wild-type full-length DsbD are almost identical to those with the positive control. The low levels of cytochrome cd_1 produced when the DsbD deletion strain was complemented by the inactive C464A-DsbD variant reflect the amount of cytochrome matured by the Ccm system upon delivery of the apoprotein to the periplasm and before DsbA has a chance to oxidize the cysteines of the CXXCH heme-binding motif (Stevens et al. 2004). The levels of cd_1 produced by a DsbD deletion strain complemented with wild-type full-length DsbD provided the 100 % activity level against which the activity of DsbD variants will be tested. Variants in both the C-terminal and the transmembrane domain of DsbD were examined using this method.

3.3.1 Variants in the C-terminal domain of DsbD

This method was used to characterise variants of the C-terminal domain of DsbD (cDsbD) that have been shown in biophysical studies to be important for the function of the protein.

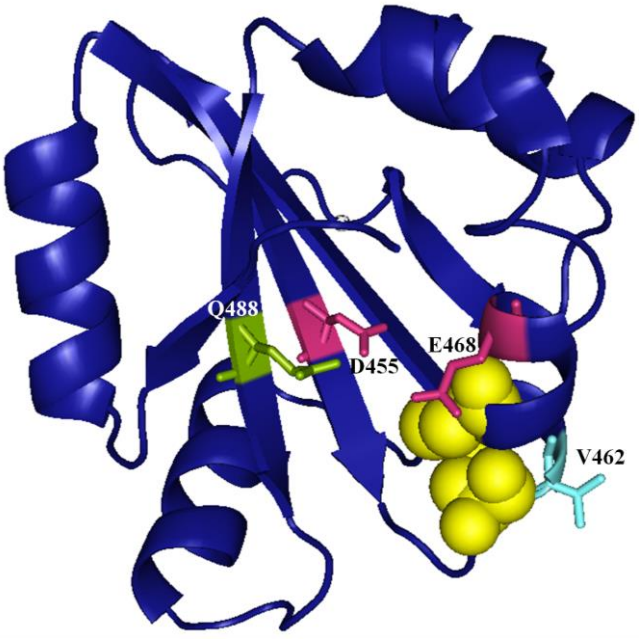

Figure 3. 3: Structural representation of the C-terminal domain of DsbD (2FWH) (Stirnimann et al. 2006). Variants that were examined as part of this thesis are residues Q488 (green), D455 and E468 (purple), V462 (cyan). The cysteine residues C461 and C464 are depicted as yellow spheres.

As has been shown in previous studies, Cys461 of cDsbD, which is the N-terminal cysteine of the CXXC motif and the reactive cysteine of the two, has a pK_a value of 10.5 (Mavridou et al. 2007). In order to understand why this cysteine has an unusually high pK_a value, residues around the active site of the protein were studied *in vitro*. From the crystal structure of the protein it can be seen that residues Asp455 and Glu468 are in close proximity to the cysteine (< 8 Å) (Figure 3.3). Using NMR spectroscopy, it was shown that a variant of DsbD with the Asp455N and Glu468Q mutations, has a significantly lower pK_a value of 8.6 for Cys461. This is the expected value for a random coil cysteine (Figure 3.4) (Mavridou et al. 2007). I was interested to determine the activity of this variant in the full-length protein *in vivo*. This variant produced almost comparable levels of cytochrome cd_1 to wild-type DsbD. 96 % activity was observed compared to the wild-type full-length DsbD expressed from a plasmid (Figure 3.5).

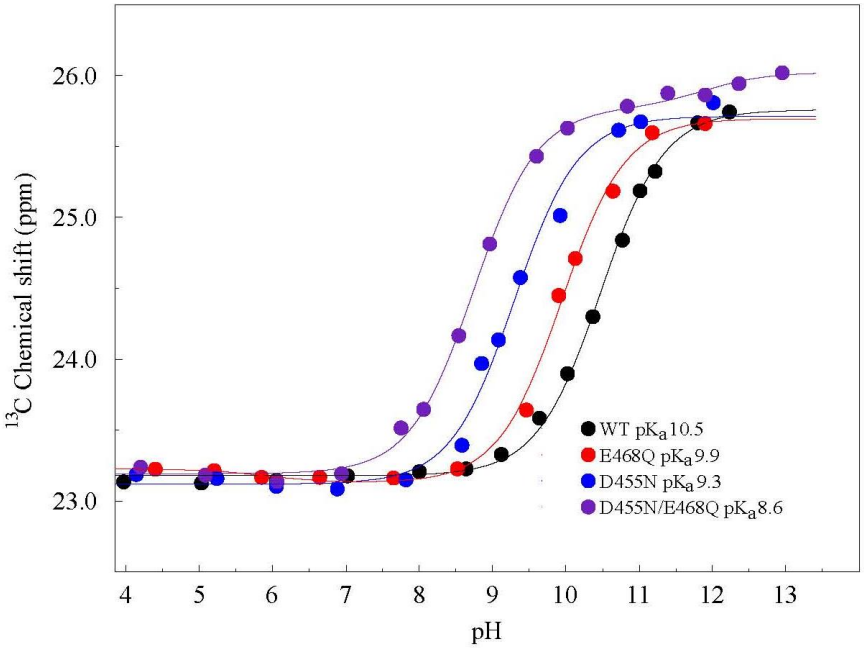

Figure 3. 4: pH dependence of the ^{13}Cβ chemical shift of Cys461 in reduced wild-type cDsbD (black), E468Q-cDsbD (red), D455N-cDsbD (blue), and D455N/E468Q-cDsbD (purple). pK_a values of 10.5, 9.9, 9.3 and 8.6 are obtained for these proteins, respectively (Mavridou et al. 2007).

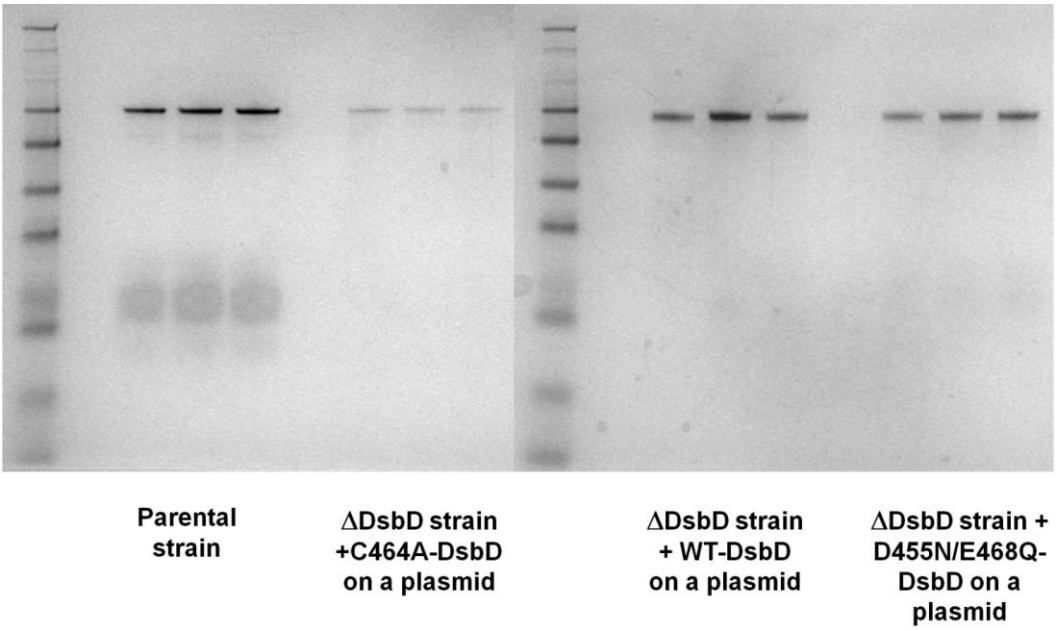

Figure 3. 5: SDS-PAGE analysis of normalised periplasmic extracts stained for covalently-bound heme. The extracts are from anaerobically grown cultures from the parental strain expressing cytochrome cd_1 from a plasmid, a DsbD deletion strain transformed with plasmids expressing C464A-DsbD and cytochrome cd_1, a DsbD deletion strain transformed with plasmids expressing wild-type DsbD and cytochrome cd_1, a DsbD deletion strain transformed with plasmids expressing D455N/E468Q-DsbD and cytochrome cd_1. Triplicates from each growth condition are presented.

Another residue of interest in cDsbD is Gln488. This residue is in a hydrogen bond network with the acidic residues Asp455 and Glu468. When this residue is mutated to an alanine, the phenomenon of microscopic pK_as is observed between Cys461 and Asp455. This means that Cys461 shares pK_a values with Asp455. If Asp455 ionises with a pK_a value of 7.5, then Cys461 has a pK_a value of 10.5 and *vice versa* (Figure 3.6). We were interested to see how this variant behaves *in vivo*. Analysis of the intensity of the cytochrome cd_1 band revealed a loss of function of the activity of the Q488A-DsbD variant. 74 % activity compared to the wild type was measured (Figure 3.7).

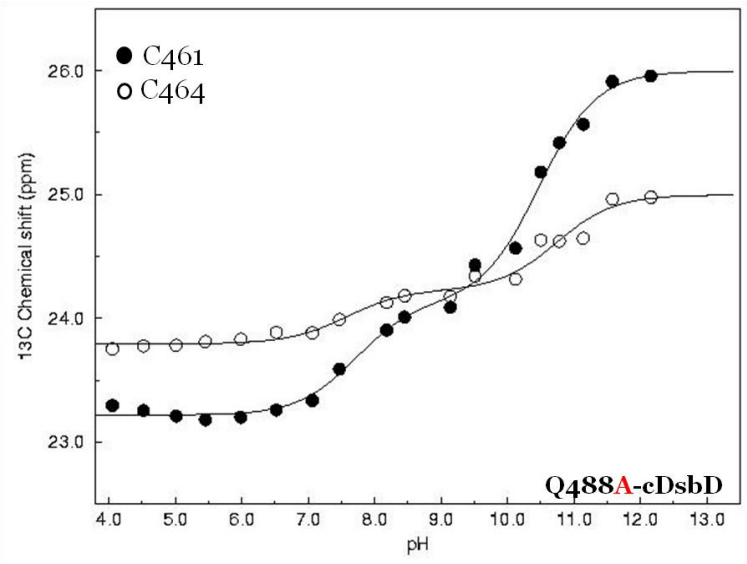

Figure 3. 6: pH dependence of the $^{13}C\beta$ chemical shift of Cys461 (black circles) and Cys464 (white circles) in reduced Q488A-cDsbD. Both curves could be fitted with pK_a values of 7.5 and 10.5. Figure was kindly provided by Erin Mosley.

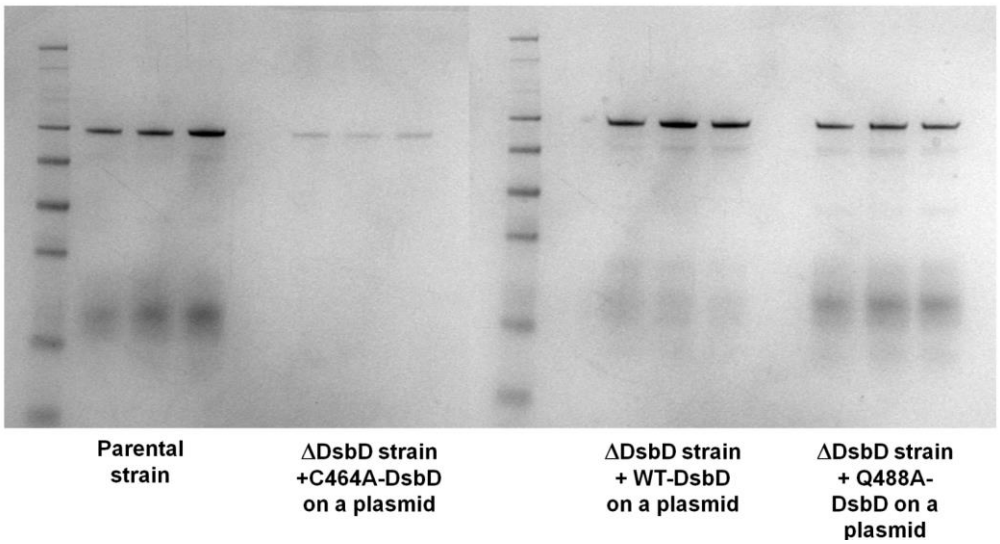

Figure 3. 7: SDS-PAGE analysis of normalised periplasmic extracts stained for covalently-bound heme. The extracts are from anaerobically grown cultures from the parental strain expressing cytochrome cd_1 from a plasmid, a DsbD deletion strain transformed with plasmids expressing C464A-DsbD and cytochrome cd_1, a DsbD deletion strain transformed with plasmids expressing wild-type DsbD and cytochrome cd_1, a DsbD deletion strain transformed with plasmids expressing Q488A-DsbD and cytochrome cd_1. Triplicates from each growth condition are presented.

In some Gram-negative bacteria Gln488 is replaced by other residues. In 15 % of all species it is replaced by a lysine and in 3 % by an arginine. C461 in Q488K-cDsbD was shown by

NMR spectroscopy to have a pK_a value of 10.5 (Figure 3.8), which is the same as the wild-type. I wanted to confirm that this variant behaves like wild-type DsbD *in vivo*. Analysis of the intensity of cytochrome cd_1 band revealed that the Q488K-DsbD variant is restored to greater levels than wild-type DsbD (138 % activity compare to the wild type full-length DsbD).

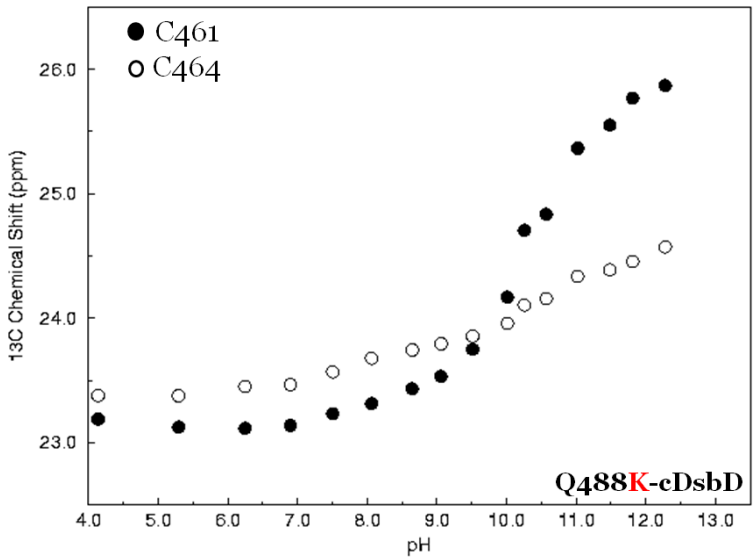

Figure 3. 8: pH dependence of the $^{13}C\beta$ chemical shift of Cys461 (black circles) and Cys464 (white circles) in Q488K-cDsbD. Both curves could be fitted with a single pK_a value of 10.5. Figure was kindly provided by Erin Mosley

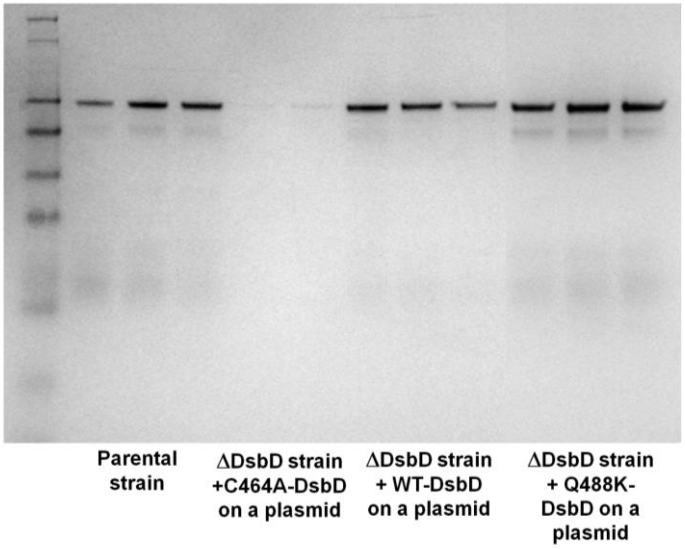

Figure 3. 9: SDS-PAGE analysis of normalised periplasmic extracts stained for covalently-bound heme. The extracts are from anaerobically grown cultures from the parental strain expressing cytochrome cd_1 from a plasmid, a DsbD deletion strain transformed with plasmids expressing C464A-DsbD and cytochrome cd_1, a DsbD deletion strain transformed with plasmids expressing wild-type DsbD and cytochrome cd_1, a DsbD deletion strain transformed with plasmids expressing Q488K-DsbD and cytochrome cd_1. Triplicates from each growth condition are presented apart from C464A-DsbD where a duplicate is presented.

Val462 is located between the two cysteines of the CXXC motif (CVAC in cDsbD) (Figure 3.3). In cDsbD it has been shown to participate in the interaction of the two periplasmic domains of DsbD (Mavridou et al. 2011). Using NMR spectroscopy it was shown that nDsbD interacts more weakly with a V462A-cDsbD variant than with wild-type cDsbD. To support this observation a Val462A variant in full-length protein was characterised *in vivo*. Analysis of the intensity of the cytochrome cd_1 band supported the proposed important role of this residue in the interaction of the two domains. The variant was 72 % active compared to wild-type DsbD (Figure 3.10).

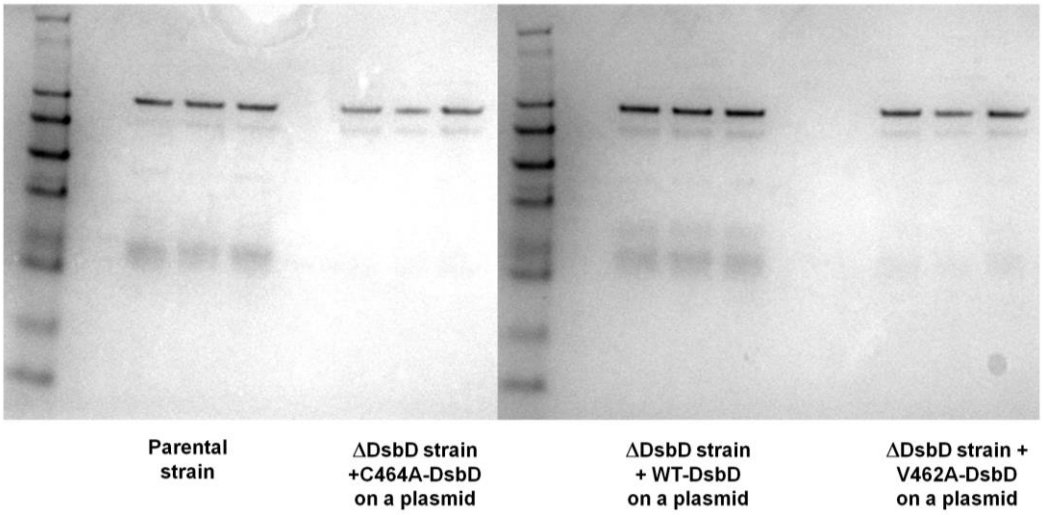

Figure 3. 10: SDS-PAGE analysis of normalised periplasmic extracts stained for covalently-bound heme. The extracts are from anaerobically grown cultures from the parental strain expressing cytochrome cd_1 from a plasmid, a DsbD deletion strain transformed with plasmids expressing C464A-DsbD and cytochrome cd_1, a DsbD deletion strain transformed with plasmids expressing wild-type DsbD and cytochrome cd_1, a DsbD deletion strain transformed with plasmids expressing V462A-DsbD and cytochrome cd_1. Triplicates from each growth condition are presented.

To assess the reliability of the periplasmic extraction and the effectiveness of the normalization process western blotting analysis was performed against DsbA (Figure 3.11). To verify that expression of DsbD variants from a plasmid was comparable to the expression of wild-type DsbD western blotting analysis against DsbD was conducted (Figure 3.12).

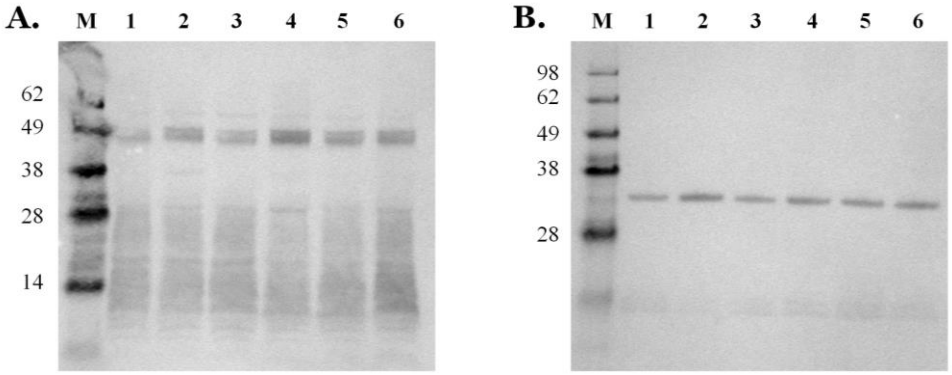

Figure 3. 11: Western blotting analysis of periplasmic extracts from the anaerobic growths against DsbD (A) or DsbA (B). (M) Prestained protein standard marker SeeBlue Plus 2 (Invitrogen), (1) parental strain transformed with a plasmid expressing cytochrome cd_1, (2) DsbD deletion strain transformed with plasmids expressing C464A-DsbD and cytochrome cd_1, (3) DsbD deletion strain transformed with plasmids expressing wild-type DsbD and cytochrome cd_1, (4) DsbD deletion strain transformed with plasmids expressing Q488A-DsbD and cytochrome cd_1, (5) DsbD deletion strain transformed with plasmids expressing Q488K-DsbD and cytochrome cd_1, (6) DsbD deletion strain with D455N/E468Q-DsbD and cytochrome cd_1.

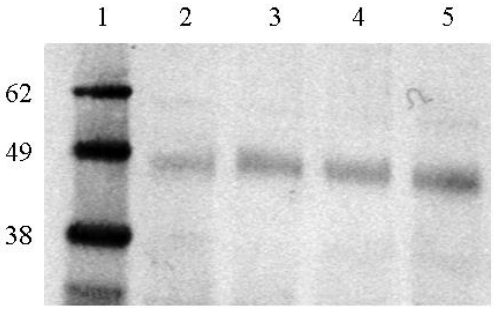

Figure 3. 12: Western blotting analysis of periplasmic extracts from the anaerobic growths against DsbD (1) Prestained protein standard marker SeeBlue Plus 2 (Invitrogen), (2) parental strain transformed with a plasmid expressing cytochrome cd_1, (3) DsbD deletion strain transformed with plasmids expressing C464A-DsbD and cytochrome cd_1, (4) DsbD deletion strain transformed with plasmids expressing wild-type DsbD and cytochrome cd_1, (5) DsbD deletion strain transformed with plasmids expressing V462A-DsbD and cytochrome cd_1

3.3.2 Discussion

A new method was developed to assess the function of DsbD variants and was used to examine *in vivo* specific residues in the C-terminal domain of the full-length protein that have been identified by NMR spectroscopy to have an important role. The results described in section 3.3.1 are summarised in Table 3.1.

Table 3. 1: Activity of DsbD variants compared to the wild-type as they result from densitometry analysis of the heme stained band for cytochrome cd_1.

DsbD form	Activity compared to wild-type
Endogenous (from MC1000)	89-105 (depending on the date of the growth)
C464A-DsbD	7-34 (depending on the date of the growth)
D455N/E468Q-DsbD	96
Q488A-DsbD	74
Q488K-DsbD	138
V462A-DsbD	72

The variation in the negative control has been previously reported. The low levels of mature cytochrome cd_1 observed when the deletion strain is complemented by C464A-DsbD are probably due to immediate processing of apocytochrome cd_1 by the Ccm system, before oxidation of the cysteines of the CXXCH heme binding motif can occur.

The activity of the D455N/E468Q-DsbD is understandable. The drop in the pK_a value of Cys461 from 10.5 to 8.6 might make it more prone to reoxidation but this effect might not be significant enough to be observed *in vivo.*

The profile for the activity of Q488A–DsbD *in vivo* is as expected. Cys461 can either have the wild-type pK_a value of 10.5 leading to normal activity, or a pK_a value of 7.5 which will make the protein more prone to reoxidation leading to a futile reoxidation cycle and failing to transfer reducing power to the N-terminal domain of DsbD.

In Q488K-cDsbD Cys461 has a pK_a of 10.5, the same for Cys461 in wild-type cDsbD. However, Q488K-DsbD *in vivo* achieves cytochrome *c* maturation levels even greater than the wild-type protein. The presence of a lysine instead of a glutamine residue can alter the properties of the active site of cDsbD without altering the pK_a value for Cys461 in a manner that would be favourable for the transfer of reductant further down the pathway.

Val462 seems to be important for the interaction of the two soluble domains of DsbD. Lack of this residue weakens the interaction of cDsbD with nDsbD which leads to decrease in the levels of *c*-type cytochrome maturation.

3.4.1 Variants in the transmembrane domain of DsbD

The structure of the transmembrane domain of DsbD has not yet been determined. There have been two previous studies with insights into the roles of conserved residues in this domain (Cho and Beckwith 2006; Hiniker et al. 2006).

In these studies the function of DsbD was assessed either by characterizing the oxidation state of the cysteine residues of DsbC (thus monitoring the transfer of reductant) using AMS labeling or by exploiting the copper sensitivity that occurs in DsbD deletion strains.

Conserved proline and glycine residues were identified to be important for the transfer of reductant and the function of the protein.

Using the method developed here the activity of some of these previously characterised variants has been quantified *in vivo* in large scale anaerobic cultures and also the role of other conserved residues that have not been studied previously has been characerised. The position of the residues on a predicted structure of DsbD is presented in Figure 3.13.

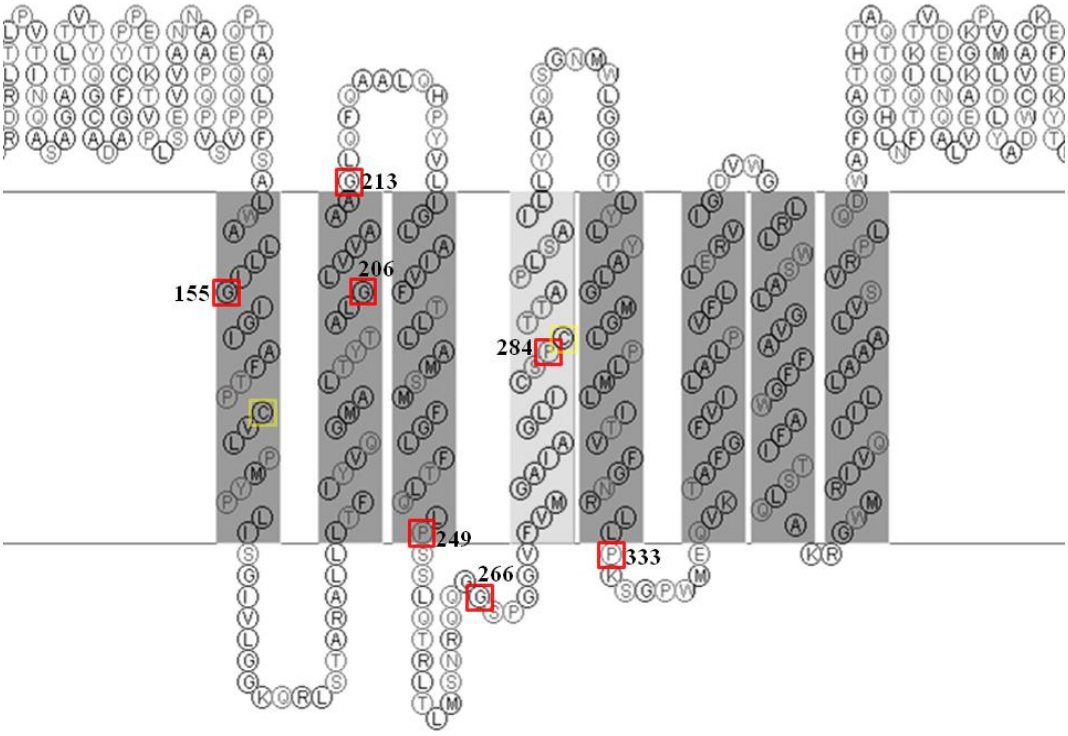

Figure 3. 13: Schematic representation of the position of variants of interest in the transmembrane helices of DsbD determined by bioinformatic analysis.

Three of the previously characterised variants (Cho and Beckwith 2006) (Hiniker et al. 2006) were monitored. G206A–DsbD was shown not to have an effect on the transfer of reductant, G155A–DsbD was shown to affect the transfer of reductant because there is not a good interaction of tmDsbD and cytoplasmic Trx and P284A–DsbD was shown to affect the transfer of reductant because the interaction of tmDsbD with cDsbD was blocked. The activity of these variants was assessed *in vivo*.

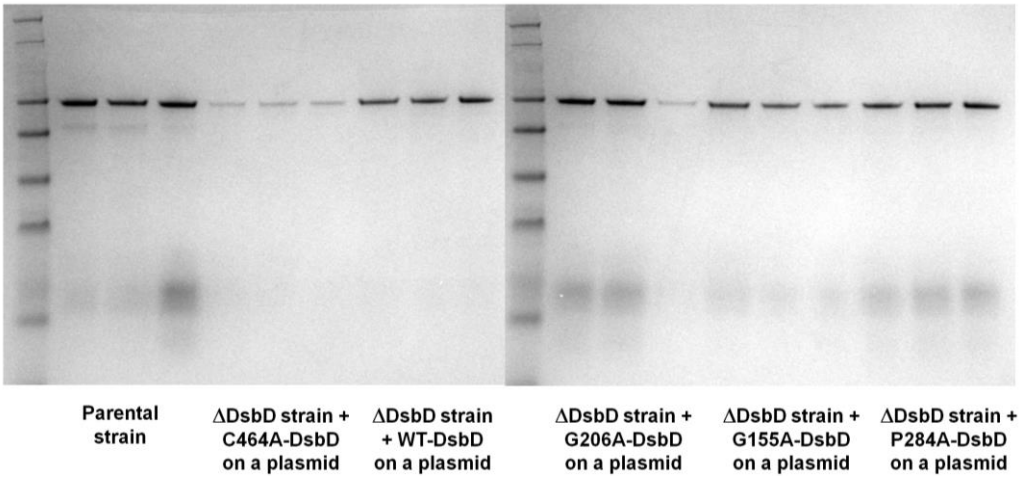

Figure 3. 14: SDS-PAGE analysis of normalised periplasmic extracts stained for covalently-bound heme. The extracts are from anaerobically grown cultures from the parental strain expressing cytochrome cd_1 from a plasmid, a DsbD deletion strain transformed with plasmids expressing C464A-DsbD and cytochrome cd_1, a DsbD deletion strain transformed with plasmids expressing wild-type DsbD and cytochrome cd_1, a DsbD deletion strain transformed with plasmids expressing G206A-DsbD and cytochrome cd_1, a DsbD deletion strain transformed with plasmids expressing G155A-DsbD and cytochrome cd_1, a DsbD deletion strain transformed with plasmids expressing P284A-DsbD and cytochrome cd_1. Triplicates from each growth condition are presented.

According to densitometry analysis of the cytochrome cd_1 heme-staining band variants G206A–DsbD, G155A–DsbD and P284A–DsbD are 96, 68 and 94 % active compared to the wild type, respectively.

Four new residues were characterised using this method. These are P249, G213, P333, G266. These residues were identified from sequence alignments of DsbD proteins from different Gram-negative bacteria and also from a pair wise sequence alignment of DsbD and CcdA, an analogue of DsbD from Gram-positive bacteria.

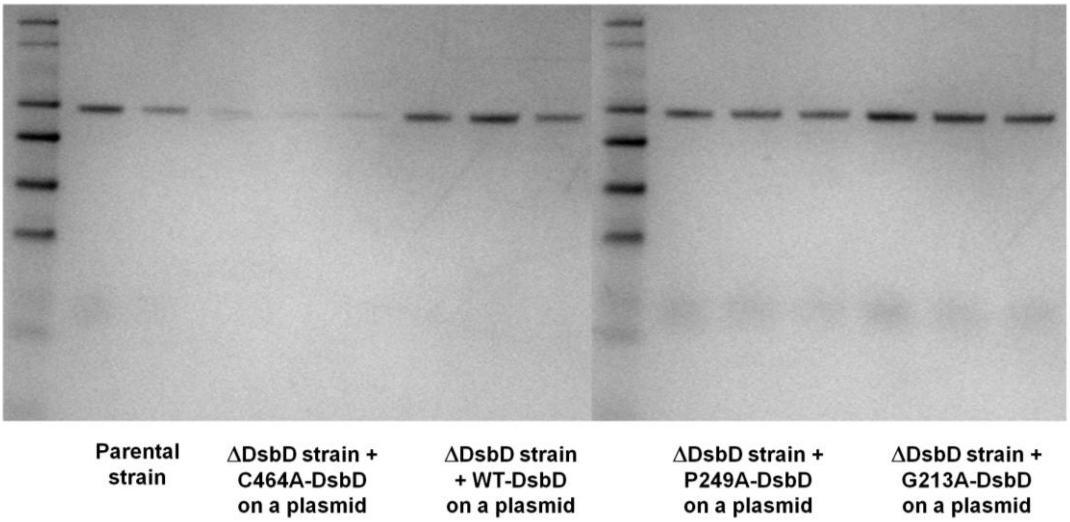

Figure 3. 15: SDS-PAGE analysis of normalised periplasmic extracts stained for covalently-bound heme. The extracts are from anaerobically grown cultures from the parental strain expressing cytochrome cd_1 from a plasmid, a DsbD deletion strain transformed with plasmids expressing C464A-DsbD and cytochrome cd_1, a DsbD deletion strain transformed with plasmids expressing wild-type DsbD and cytochrome cd_1, a DsbD deletion strain transformed with plasmids expressing P249A-DsbD and cytochrome cd_1, a DsbD deletion strain transformed with plasmids expressing G213A-DsbD and cytochrome cd_1 Triplicates from each growth condition are presented, apart from parental condition where duplicates are presented.

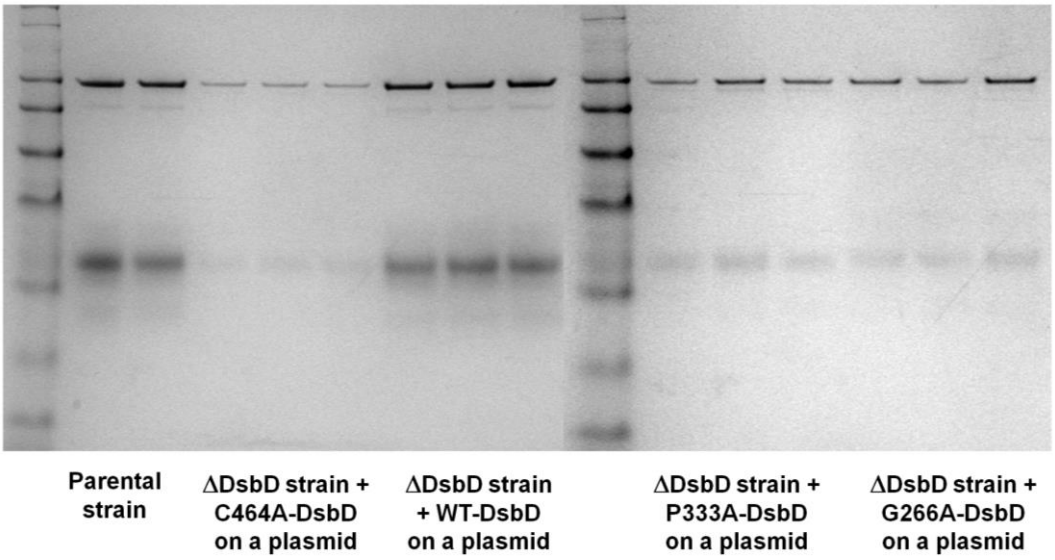

Figure 3. 16: SDS-PAGE analysis of normalised periplasmic extracts stained for covalently-bound heme. The extracts are from anaerobically grown cultures from the parental strain expressing cytochrome cd_1 from a plasmid, a DsbD deletion strain transformed with plasmids expressing C464A-DsbD and cytochrome cd_1, a DsbD deletion strain transformed with plasmids expressing wild-type DsbD and cytochrome cd_1, a DsbD deletion strain transformed with plasmids expressing P333A-DsbD and cytochrome cd_1, a DsbD deletion strain transformed with plasmids expressing G266A-DsbD and cytochrome cd_1 Triplicates from each growth condition are presented, apart from the parental condition where duplicates are presented.

Variants P249A–DsbD and G213A–DsbD are more active than the wild-type DsbD (147 and 141 % activity, respectively) whereas variants P333A–DsbD and G266A–DsbD appear to have a loss of function (36 and 40 % activity, respectively).Western blotting analysis against DsbD revealed that the protein expression levels for the P333A–DsbD and G266A–DsbD are very low (Figure 3.17 (A), lanes 9 and 10). Western blotting analysis against DsbA revealed that the loadings of the normalised periplasm are comparable through all the studies (Figure 3.17 (B))

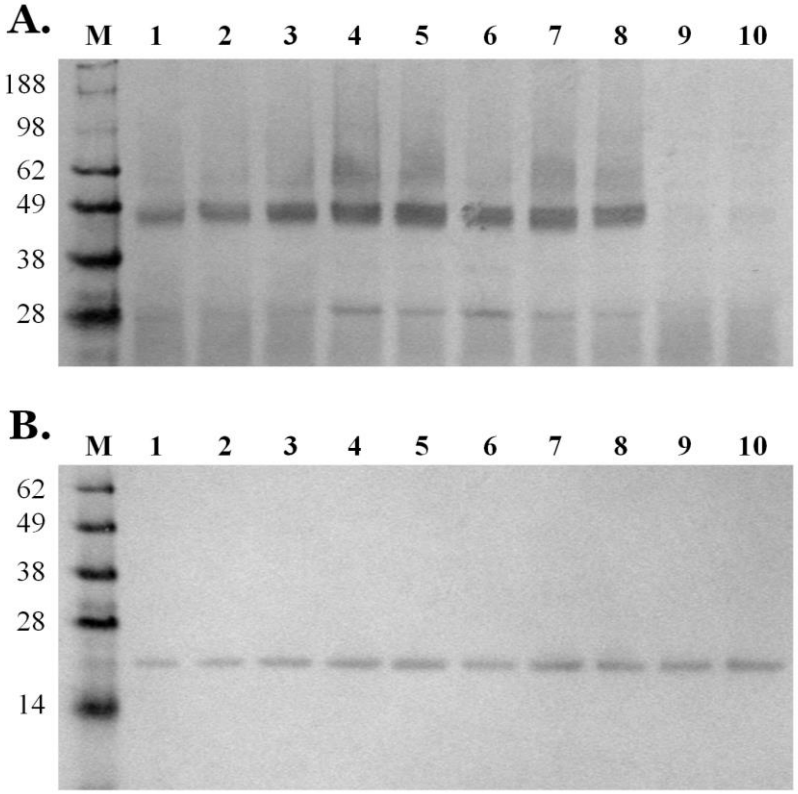

Figure 3. 17: Western blotting analysis of periplasmic extracts from the anaerobic growths against DsbD (A) or DsbA (B) (M) Prestained protein standard marker SeeBlue Plus 2 (Invitrogen), (1) parental strain transformed with plasmid expressing cytochrome cd_1, (2) DsbD deletion strain transformed with plasmids expressing wild-type DsbD and cytochrome cd_1, (3) DsbD deletion strain transformed with plasmids expressing C464A-DsbD and cytochrome cd_1, (4) DsbD deletion strain transformed with plasmids expressing G206A-DsbD and cytochrome cd_1, (5) ΔDsbD strain with G155A-DsbD and cytochrome cd_1, (6) DsbD deletion strain transformed with plasmids expressing P284A-DsbD and cytochrome cd_1, (7) DsbD deletion strain transformed with plasmids expressing P249A-DsbD and cytochrome cd_1 (8) DsbD deletion strain transformed with plasmids expressing G213A-DsbD and cytochrome cd_1 (9) DsbD deletion strain transformed with plasmids expressing P333A-DsbD and cytochrome cd_1 (10) DsbD deletion strain transformed with plasmids expressing G266A-DsbD and cytochrome cd_1

3.4.2 Discusion

The method was used to assess the role of conserved glycine and proline residues of the transmembrane domain of DsbD in the function of the protein *in vivo*. The results are summarised in Table 3. 2.

Table 3. 2: Activity of DsbD variants compared to the wild type complementation as they result from densitometry analysis of heme stained band for cytochrome cd_1.

DsbD form	Activity compared to wild type
Endogenous (MC1000 strain)	103-117 (depending on the date of the growth)
C464A-DsbD	19-32 (depending on the date of the growth)
G206A-DsbD	96
G155A-DsbD	68
P284A-DsbD	94
P249A-DsbD	147
G213A-DsbD	141
P333A-DsbD	36
G266A-DsbD	41

Analysis of previously characterised residues Gly206, Gly155 and Pro284 (Figure 3.14) revealed that *in vivo* the behaviour of P284A-DsbD is not as expected based on previous observations. This variant appears to be functional, it is almost as active as wild-type DsbD. The inconsistency with the previous report observed here can be explained by differences of the two methods in the volumes of the cultures (in this study 1 l of culture was used instead of 1 ml) and the expression time (24 h instead of 4 h). We are confident of the validity of our result and we are basing this on the consistent behaviour of the positive and negative control on the day of each growth. G206A-DsbD was identified to be as functional as the wild-type protein (Cho and Beckwith 2006), which is supported by our data (96 % activity compared to wild-type full-length DsbD). G155A-DsbD appears to have a loss of function; it is 68 %

active compared to the wild type. The expression levels of G155A-DsbD are higher than those of the wild-type DsbD, possibly suggesting an even greater effect.

Variants P249A-DsbD and G213A-DsbD (Figure 3.15) seem to be more active *in vivo* compared to the wild-type, however they also express at higher levels than the wild-type DsbD (Figure 3.17). It can be proposed that these residues are not essential for the function of the protein, and P249A-DsbD and G213A-DsbD have wild-type activity.

Variants P333A-DsbD and G266A-DsbD (Figure 3.16) are nearly inactive. However, they express very poorly or fail to incorporate in the membrane which can possibly lead to degradation of DsbD. This suggests that these residues are crucial for the folding of the protein and its insertion in the membrane.

To summarise, a novel method was developed to assess the importance of specific residues for the functionality of variants of DsbD *in vivo*. This method was used to examine variants of DsbD that had been characterised previously by NMR spectroscopy or that were identified by bioinformatic analysis. This method can be used for further studies. The N-terminal domain of DsbD has not been tackled. It is known that nDsbD has several protein partners, however the residues that contribute to this interaction have not been yet identified. This method could be used to examine the behaviour of variants of specific residues of interest *in vivo.*

CHAPTER 4

4.1 Introduction

Cytochrome b_{562} is a ~12 (11.8) kDa soluble protein that is classified as an electron-transfer protein. However, its biological role and/or its partner remains unknown even though it was first described many years ago (Itagaki and Hager 1968). It is located in the periplasm of *E. coli* and binds one heme *b* molecule to its polypeptide chain (Xavier et al. 1978).

The crystal structure of heme-bound (holo) b_{562} has been determined and revealed a four-helix bundle structure (Lederer et al. 1981) (Figure 4.1 (A)). The four helices are located between residues 3-20, 22-43, 61-78 and 87-106. The heme is located in the cavity formed by the four helices and the iron is coordinated by residues from the N- and C- terminal helices; Met7 and His102 are the axial ligands of the heme.

Like most apoproteins that incorporate heme *b*, the apo form of b_{562} is relatively stable (Gao and O'Brian 2007). Apocytochrome b_{562} has 60% helicity whereas the holo form has 80% (Feng and Sligar 1991). NMR studies revealed the structure of apo-b_{562} (Feng et al. 1994; Feng et al. 1991) (Figure 4.1 (B)) showing differences in the packing of the helices between the two forms of the protein. In apo-b_{562} the first helix is parallel to helix two and not aligned at the classical 20^{o} packing angle resulting in extremely poor packing at the inter-helical interface, whereas helices two and three are packed as in the holo form of the protein. The C-terminus of the protein, located on helix four, has been shown to be more unstructured than in the holo-form, with distortion at the last four turns of the helix. Consequently, there is poor packing also between helixes three and four which results in a longer distance between helices one and four. Thus, there is exposure of the heme binding cavity to the solvent, with 25% more accessible surface area than in holo-b_{562}.

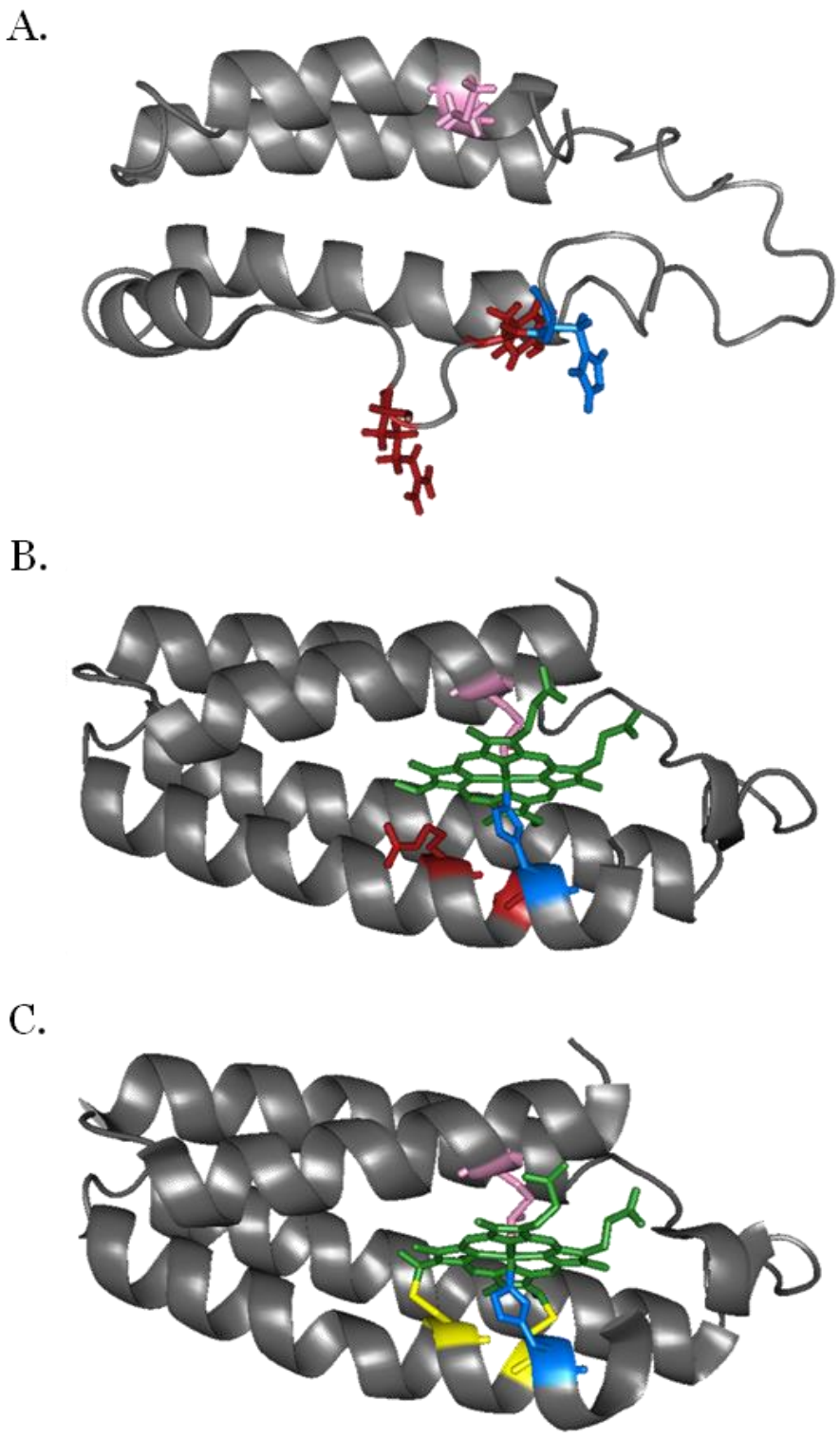

Figure 4. 1: A. Solution structure of apocytochrome b_{562} (PDB entry: 1APC) (Feng et al. 1994) B. Crystal structure of holocytochrome b_{562} (PDB entry: 256B) (Lederer et al. 1981) C. Crystal structure of holocytochrome *c*-b_{562} (PDB entry: 2BC5) (Faraone-Mennella et al. 2006). The axial ligands of the heme, Met7 and His102, are coloured in pink and blue, respectively. The heme moiety is coloured in green. The residues R98 and Y101 are coloured in red; when they are mutated to cysteines they are shown in yellow.

The structure of b_{562} is unique amongst *b*-type cytochromes. There are other cytochromes with a four-helix bundle structure, but all of them are *c*-type cytochromes. Therefore, it is considered to represent an evolutionary intermediate between *b*- and *c*-type cytochromes. This led to studies where residues in the sequence of b_{562} were mutated and the characteristic CXXCH heme binding motif for *c*-type cytochromes was introduced. The engineered CXXCH motif on b_{562} used the existent His102 which is one of the axial ligands of the heme in the wild-type protein (Barker et al. 1995). *c*-b_{562} was further characterised in its holoform by NMR spectroscopy and crystallography (Figure 4.1 (C)), confirming the presence of thioether linkage between the cysteine residues and the heme molecule. (Arnesano et al. 2000) (Faraone-Mennella et al. 2006). *c*-b_{562} has been identified to be more stable than wild-type b_{562} but structurally is almost identical to b_{562} apart from minor differences at the C-terminus (Faraone-Mennella et al. 2006). The structure of the apoform of *c*-b_{562} has not yet been characterised; however, it has been a very useful tool for folding studies of four helix bundles, where the protein was denatured in the presence of heme and its refolding was monitored. (Kimura et al. 2009).

The biosynthesis of holo *c*-b_{562} *in vivo* was of significant interest. Is the heme attached because it can be spontaneously incorporated in b_{562} or is the apoform processed by the Ccm system? In 2003 (Allen et al. 2003) it was shown that apo *c*-b_{562} interacts with the Ccm system in *E. coli* for covalent heme attachment to its polypeptide chain.

Apocytochrome *c*-b_{562} is an ideal probe for interaction studies with proteins of the Ccm system; it is a very stable *c*-type apocytochrome that in the presence of the Ccm system matures in a *bonafide* holo-form. In the studies that were conducted as part of this thesis the biophysical properties of apocytochrome *c*-b_{562} were examined by NMR spectroscopy with special focus on the CXXCH motif and the C-terminus of the protein.

4.2 Results

4.2.1 1D spectra of the two oxidation states

1D ^{1}H-NMR spectra were collected for apocytochrome *c*-b_{562} using unlabelled protein, to verify differences between the two oxidation states in order to identify characteristic markers of each oxidation state.

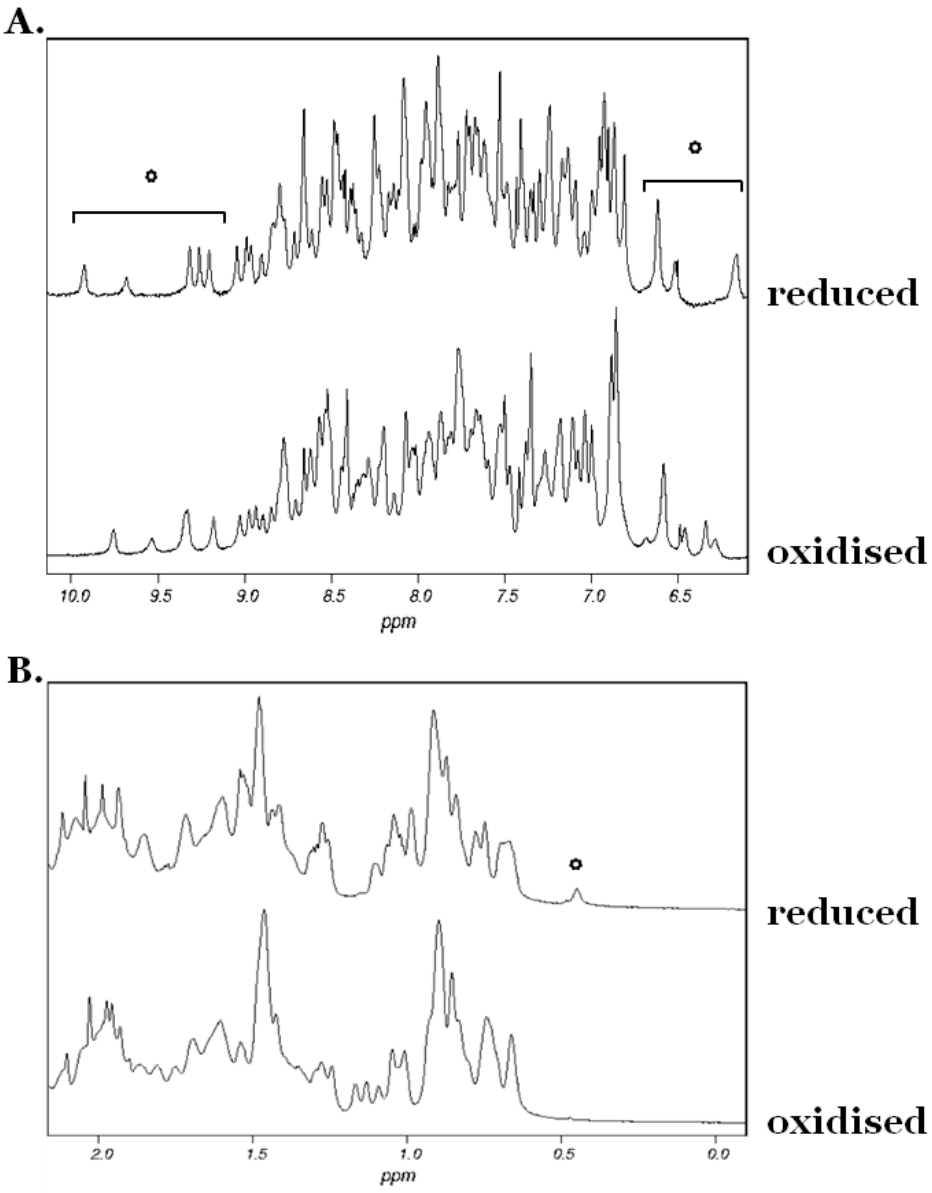

Figure 4. 2: Downfield (A) and upfield (B) 1D ^{1}H-NMR spectra collected using unlabelled apocytochrome *c*-b_{562} for both oxidation states at 500 MHz, pH 5.2 and 293 K. Distinct peaks, representative for each oxidation state, can be observed and are marked with an asterisk.

The spectra were different between the two oxidation states of the protein. Easily identified differences in peaks were found upfield and downfield in the spectra. There is a characteristic peak that appears in the reduced form at about 0.4 ppm (Figure 4.2 (B)) and does not exist in the oxidised form. There are also differences in the numbers and distribution of the peaks between 9-10 ppm. In addition there are differences at the spectra around 6.5 ppm.(Figure 4.2 (A)).

4.2.2. pH titrations monitored using 1D ^{1}H NMR spectra

To check the stability and folding of the apocytochrome through a range of pHs 1D spectra were collected for both oxidation states. Oxidised apocytochrome was monitored from pH 3.1- 10.2 (Figure 4.3), whereas reduced apocytochrome was monitored from pH 4.2-9.2 (Figure 4.4).

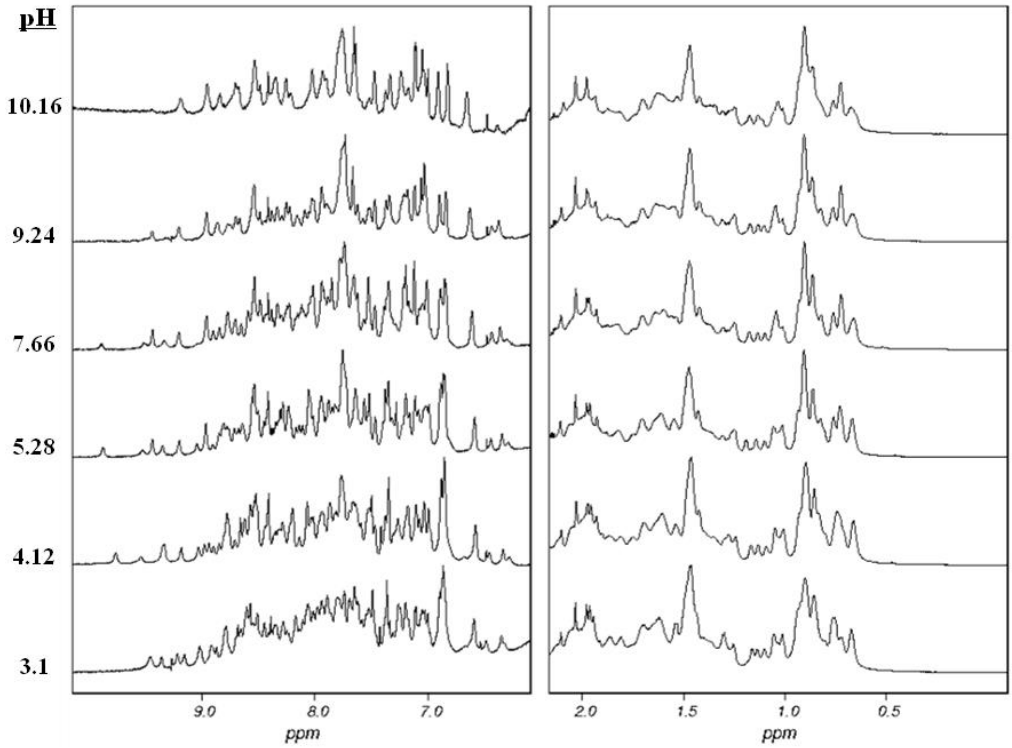

Figure 4. 3: 1D ^{1}H NMR spectra collected at different pHs for oxidised *c*-b_{562} at 500 MHz and 293 K. The protein remains folded through the whole pH value range.

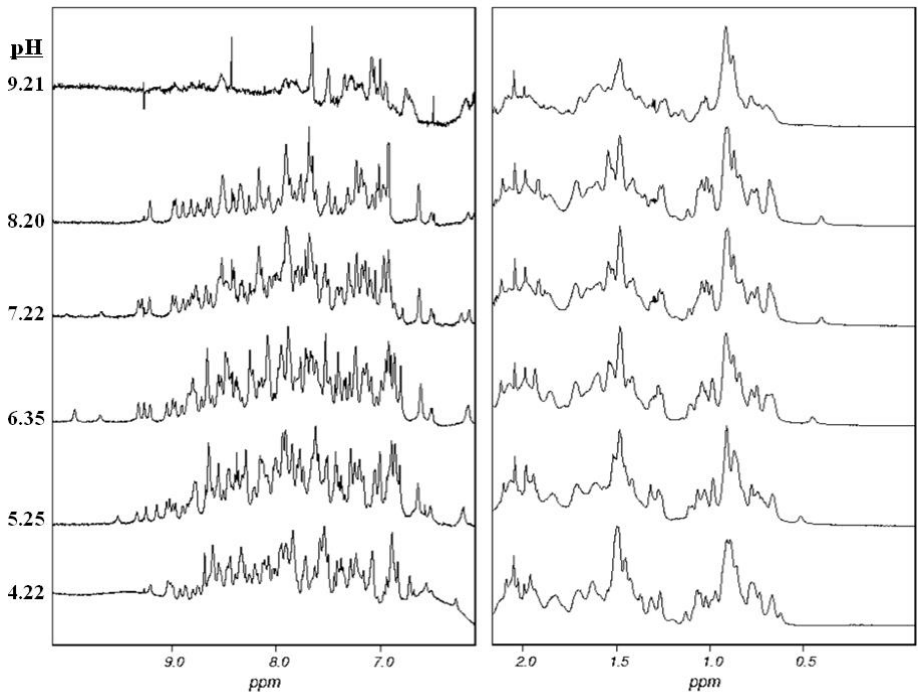

Figure 4. 4: 1D ^{1}H NMR spectra collected at different pHs for reduced *c*-b_{562} at 500 MHz and 293 K. The reduced protein remains folded up to pH 9.2.

4.2.3. Assignments of apocytochrome *c*-b_{562}

4.2.3.1 Introduction to sequential assignment procedure

After verifying that the protein is stable and folded at different pH values and that there are spectral differences between the two oxidation states, backbone assignments of *c*-b_{562} were done. To do this, 2D ^{1}H-^{15}N HSQC, 3D ^{15}N-edited TOCSY-HSQC, NOESY-HSQC and HSQC-NOESY-HSQC experiments were performed. The previously published ^{15}N ^{1}HN backbone assignments of wild-type apocytochrome b_{562} (Feng and Sligar 1991) were also considered.

The ^{1}H-^{15}N HSQC spectrum contains correlations of ^{1}H and ^{15}N chemical shifts. A single ^{15}N-^{1}H peak is observed for each residue except proline. The 3D ^{15}N-edited TOCSY-HSQC experiment provides information for determination of the spin system type of each ^{1}HN and the αCH and βCH chemical shifts. The ^{15}N NOESY-HSQC experiment provides information about sequential ^{1}HN -^{1}HN and ^{1}HN -αCH NOE connections.

4.2.3.1.1 ^{15}N-^{1}H HSQC experiment

Prior to collection of 3D ^{15}N-edited TOCSY-HSQC and NOESY-HSQC, a 2D ^{1}H-^{15}N HSQC was collected (Figures 4.5 and 4.6). In this experiment, a peak for each proton covalently attached to ^{15}N can been detected when the exchange of the proton with the solvent is slow. The peaks that can be observed are from most backbone amides and from the side chains of arginine, tryptophan, glutamine and asparagine residues. The position of each peak gives the $^{1}H^{N}$ chemical shift and the chemical shift of the ^{15}N to which the proton is attached. The Asn/Gln side-chain amide protons are easily differentiated from the other amides by their chemical shifts, which place them as pairs of peaks at the top right in the HSQC spectrum. The number of backbone amide HSQC peaks expected for apo *c*-b_{562} is 101. The protein after the cleavage of the N-terminal periplasmic sequence has 106 residues, 4 of which are prolines. Prolines do not have HN due to the cyclic nature of their backbones and they do not appear in ^{1}H-^{15}N HSQC spectra. In addition, the N-terminal residue (Ala1) exchanges very fast with the water and cannot be monitored in an HSQC spectrum. 122 peaks were counted for the oxidised and 120 for the reduced form which means that the majority of the peaks had unique chemical shifts and the good resolution of the spectra suggests that the apoprotein was folded as also expected from the 1D ^{1}H spectra.

4.2.3.1.2 ^{15}N edited TOCSY-HSQC

In a 2D TOCSY NMR experiment the cross peaks correspond to through bond correlations within the same spin system. In the 3D ^{15}N-edited TOCSY-HSQC experiment the protons are separated according to their ^{15}N chemical shift. After processing of the collected spectra, strips corresponding to a peak from each amide proton (^{1}HN) are generated (Figure 4.7). In each strip, peaks from the protons of the same spin systems are displayed. Therefore, an ^{15}N-edited TOCSY-HSQC experiment provides information about the side chain protons associated with each ^{1}HN-^{15}N.

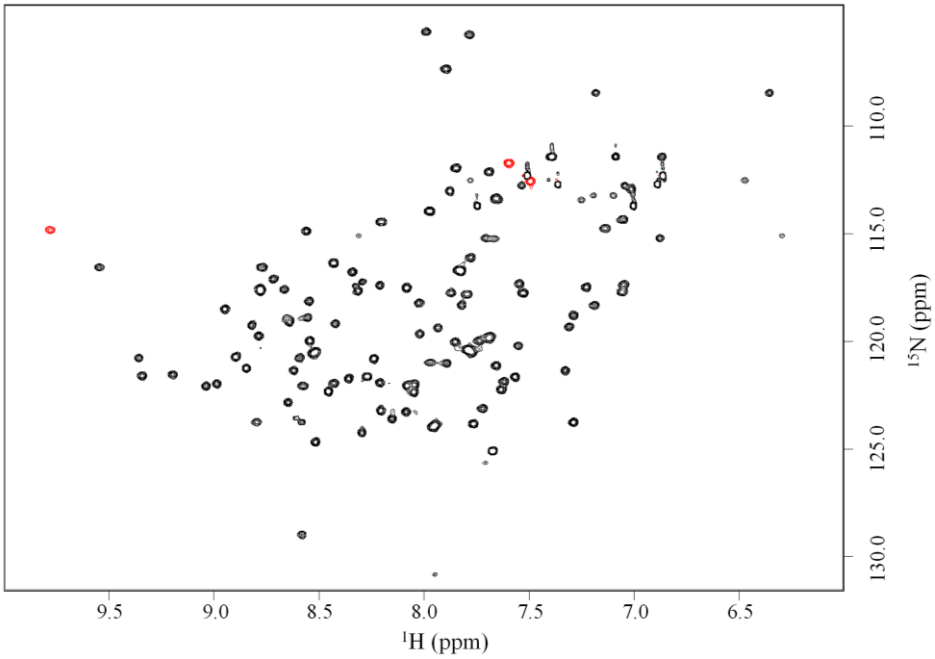

Figure 4. 5: ^{1}H-^{15}N HSQC spectra collected using oxidised apocytochrome *c*-b_{562} at 500 MHz, pH 5.2 and 293K. The red peaks are the folded side chain of arginine residues.

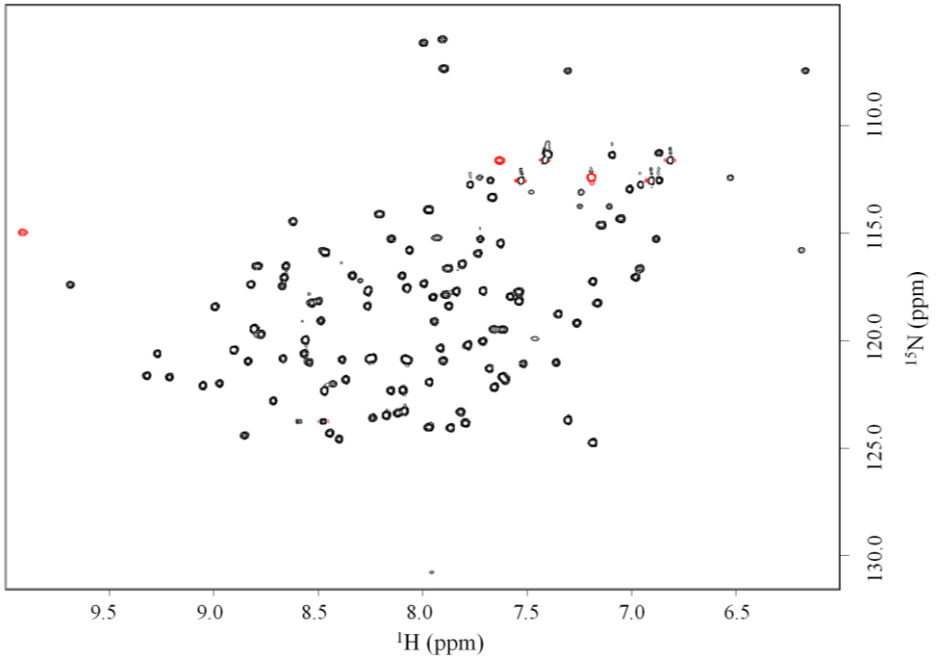

Figure 4. 6: ^{1}H-^{15}N HSQC spectra collected using reduced apocytochrome *c*-b_{562} at 500 MHz , pH 5.2 and 293K. The red peaks are the folded side chain of arginine residues.

Although information provided from ^{15}N-edited TOCSY-HSQC experiments is sufficient to identify the spin system type of each residue, it is not enough to identify particular amino acids.

The majority of spin systems fall into two main categories, J- or U-type. J-type spin system residues have no H$^{\gamma}$s (Asp, Asn, Tyr, Phe, His, Trp, Cys, Ser) and their two H$^{\beta}$s can be found downfield of ~2.5 ppm. U-type amino acids have H$^{\gamma}$s (Glu, Gln, Met, Arg, Lys, Ile, Leu, Val) and their H$^{\beta}$s can usually be found upfield of ~2.5 ppm. There are four exceptions: Ala residues do not have H$^{\gamma}$ but the methyl-proton resonance can be found upfield of ~1.7 ppm, Gly residues have two strong H$^{\alpha}$s peaks and no H$^{\beta}$s , Thr and Ser residues have chemical shifts around 3.5-6 ppm for their H$^{\beta}$s due to the O$^{\gamma}$. As an example, the strips of the ^{15}N-edited TOCSY-HSQC spectra of the residues of the CXXCH motif in the oxidised form are presented in Figure 4.7.

The cysteine residues C99 and C101, N99 and His102 are of the J-type spin systems so the peaks of their H$^{\beta}$s can be identified between 2.5-3.5 ppm. A100 has the unique alanine spin system profile where the H$^{\beta}$ is located around 1.5 ppm; this strip can be unambiguously assigned to an alanine. The remaining residues can only be classified to the J-type spin system. Extra information is needed to be able to verify connections between these residues. Such connections are generated using the ^{15}N-edited NOESY HSQC experiment. (Figure 4.8)

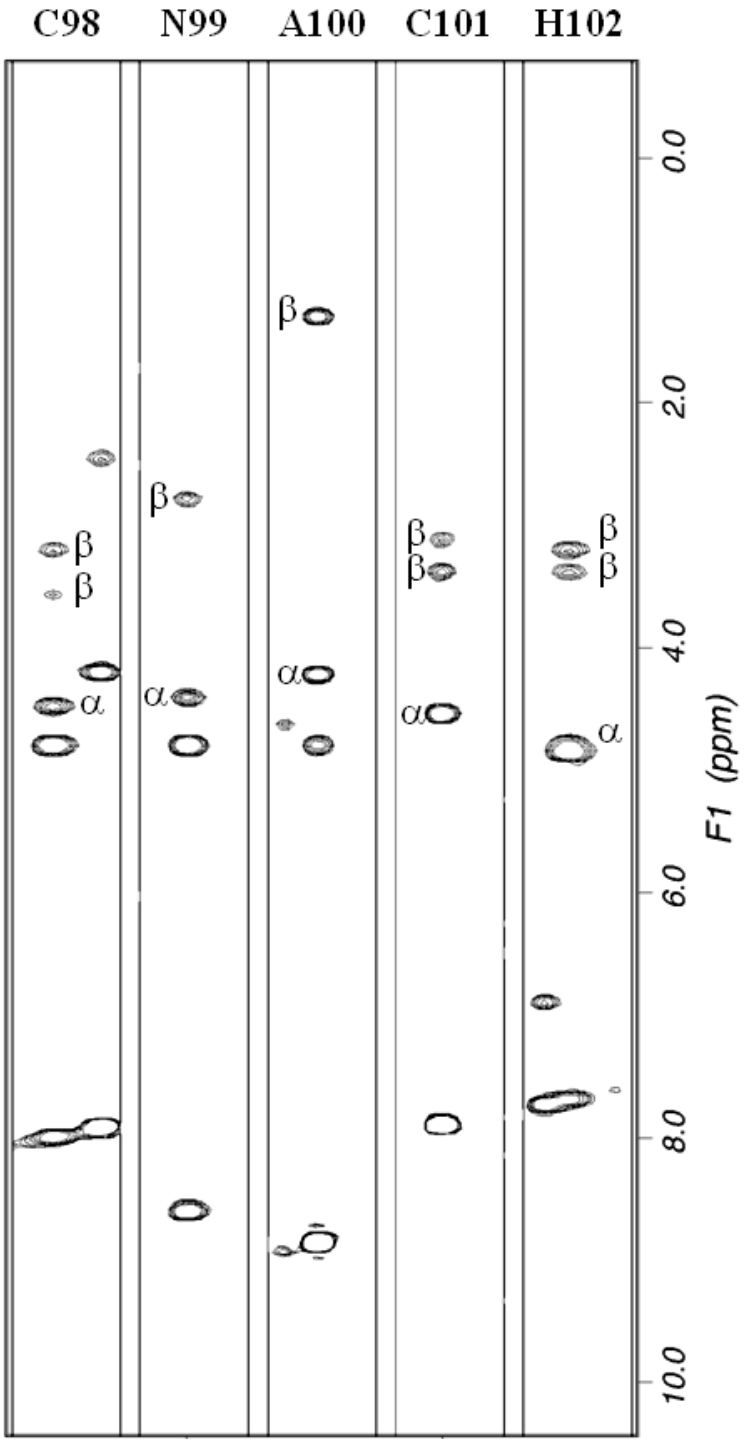

Figure 4. 7: Strips generated from a ^{15}N-edited TOCSY-HSQC NMR experiment for the residues of the CXXCH motif collected using oxidised apocytochrome *c*-b_{562} at 500 MHz, pH 5.2 and 293 K.. The α and β protons have been labeled for each residue's side chain. C98, N99, C101 and H102 have J-type spin systems. The unique spin system for alanine residues can be clearly seen at the strip of A100, where the β proton can be found at around 1.5 ppm.

4.2.3.1.3 ^{15}N-edited NOESY-HSQC and HSQC-NOESY-HSQC experiments

The NOESY experiment exploits the nuclear Overhauser enhancement effect that provides information about the through-space proximity of protons to other protons. This type of NMR experiment complements the through bond data provided by a TOCSY.

In the ^{15}N NOESY-HSQC experiment, the cross peaks of protons attached to the ^{15}N nuclei can be observed and strips for each peak can be generated for each NH proton. In these strips cross peaks from the NH to the protons of its own side chain but also to protons of nearby residues can be observed.

The ^{15}N-edited TOCSY-HSQC experiment allows the assignment of the ^{1}HN and α, β and γ protons for each residue. Then, connections between the different ^{1}HNs can be generated using the ^{15}N-edited NOESY-HSQC data, because extra peaks appear on the strip of each residue as a result of nearby protons. Using this information, residues can be linked in short chains. The type of the spin system of the residues can help assign those chains to parts of the protein sequence. In Figure 4.8 strips from the ^{15}N-edited NOESY HSQC experiment are presented for the residues of the CXXCH motif in the oxidised form.

Sometimes, the NH peaks of the diagonal are very close to each other or overlapping, so connections between residues might be ambiguous. The HSQC-NOESY-HSQC experiment shows only connections between the cross peaks of the NH groups with better resolution than the ^{15}N NOESY-HSQC experiment. Thus, it can be very helpful in cases of overlapping NH peaks. Strips from this experiment can be seen in Figure 4.9, where connections between the NH groups have been marked.

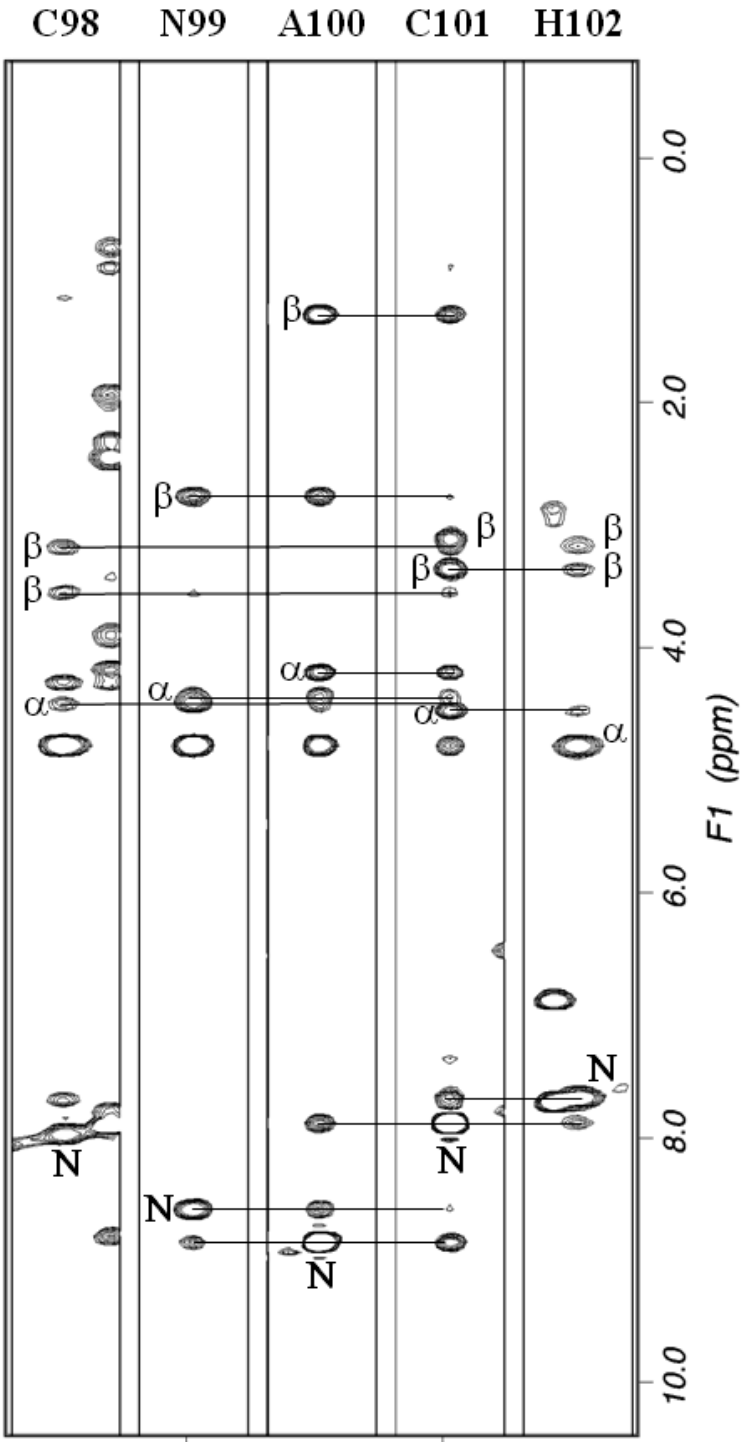

Figure 4. 8: Strips generated from an ^{15}N-edited NOESY-HSQC NMR experiment for the residues of the CXXCH motif collected using oxidised apocytochrome *c*-b_{562} at 500 MHz at pH 5.2 and 293K. The NH, $H^{\alpha}$and H^{β} are displayed. Connections between crosspeaks of different residues are shown via horizontal lines. C98 does not appear to be connected with N99. However, crosspeaks of the H^{β}s of C98 appear in the strip of C101 and are quite intense. This is due to the disulfide bond between the cysteines in the oxidised form.

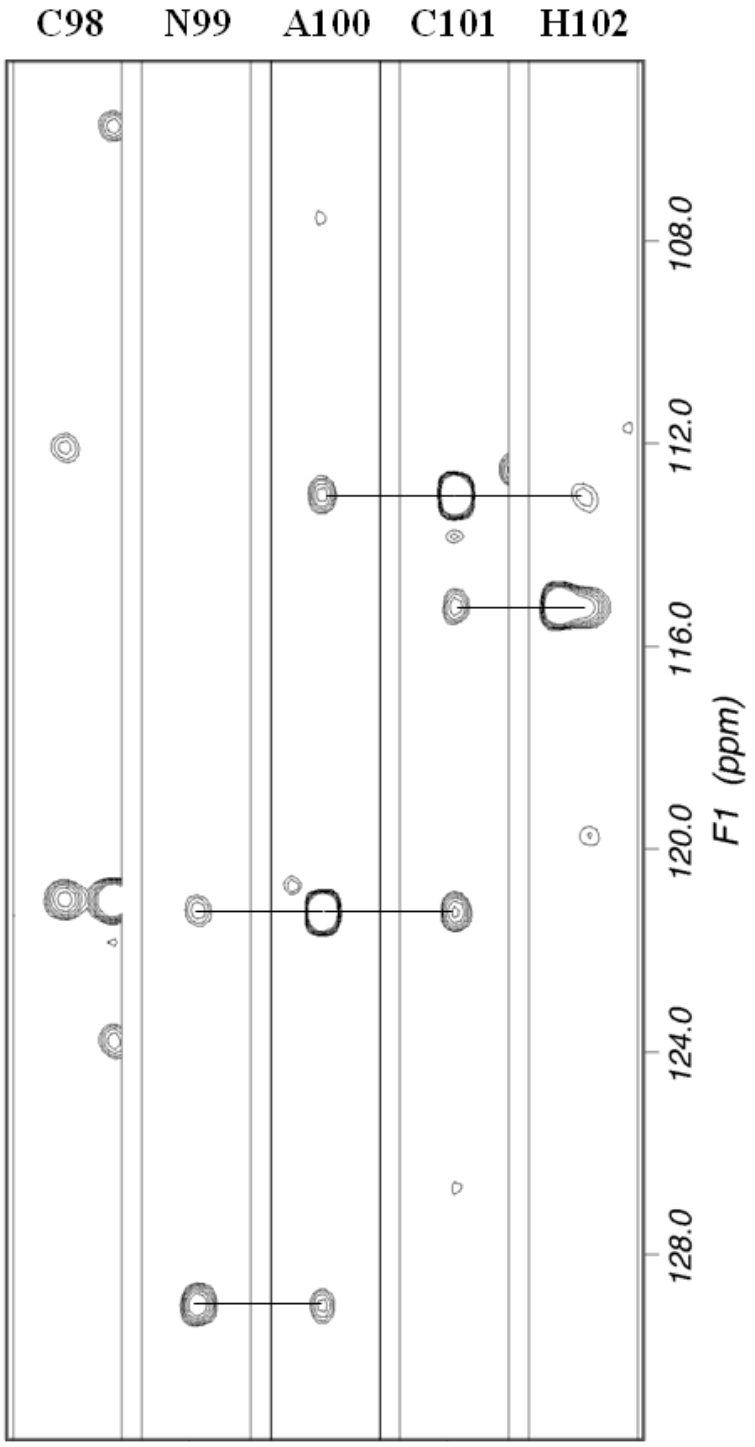

Figure 4. 9: Strips generated from an ^{15}N edited HSQC-NOESY-HSQC NMR experiment for the residues of the CXXCH motif collected using oxidised apoctochrome *c*-b_{562} at 500 MHz at pH 5.2 and 293K. Connections between the NH crosspeaks of different residues are shown using horizontal lines.

Assignments of wild-type apocytochrome b_{562} already existed. These assignments were used as a starting point for the assignment of *c*-b_{562}. Small differences were expected between the chemical shifts of the two forms in the main body of the protein. Clearly, differences were expected for the C-terminus of the protein, because two residues R98 and Y101 were replaced with cysteines as mentioned earlier.

4.2.3.2 Backbone assignments

Combining the information from the 2D ^{1}H-^{15}N HSQC, 3D ^{15}N-edited TOCSY-HSQC, NOESY-HSQC and HSQC-NOESY-HSQC experiments, the backbone assignments of apocytochrome *c*-b_{562} were completed for both oxidation states and are presented in Figures 4.10 and 4.11 for the oxidised and the reduced form, respectively.

When the two spectra are overlaid (Figure 4.12), it can be seen that there are important differences in the chemical shifts between the two states, especially in the area of the C-terminus of the protein.

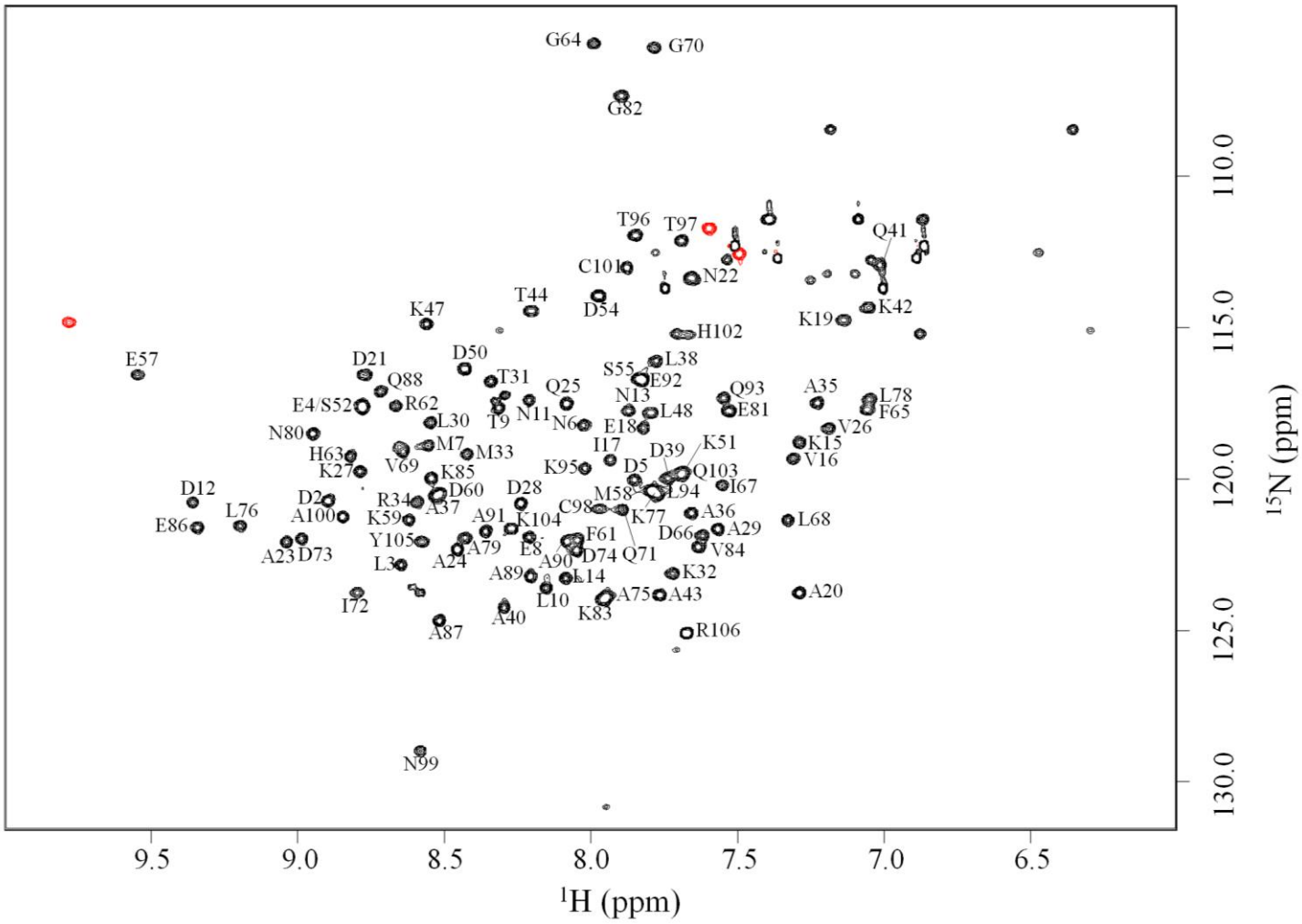

Figure 4. 10: ^{1}H-^{15}N HSQC assigned spectrum collected at 500 MHz, pH 5.2 and 293K using oxidised apocytochrome *c*-b_{562}

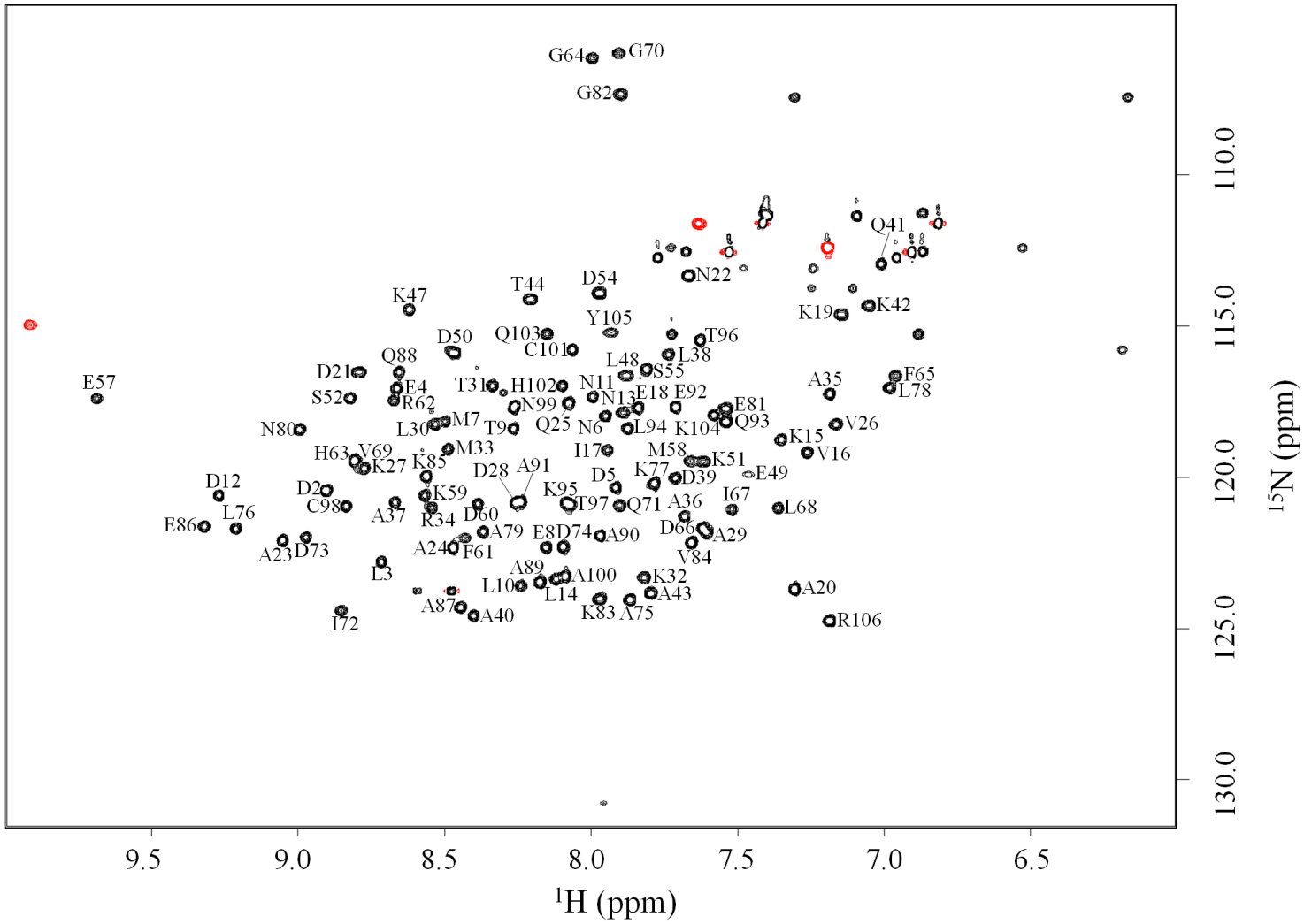

Figure 4. 11: ^{1}H-^{15}N HSQC assigned spectrum collected at 500 MHz, pH 5.2 and 293K using reduced apocytochrome *c*-b_{562}

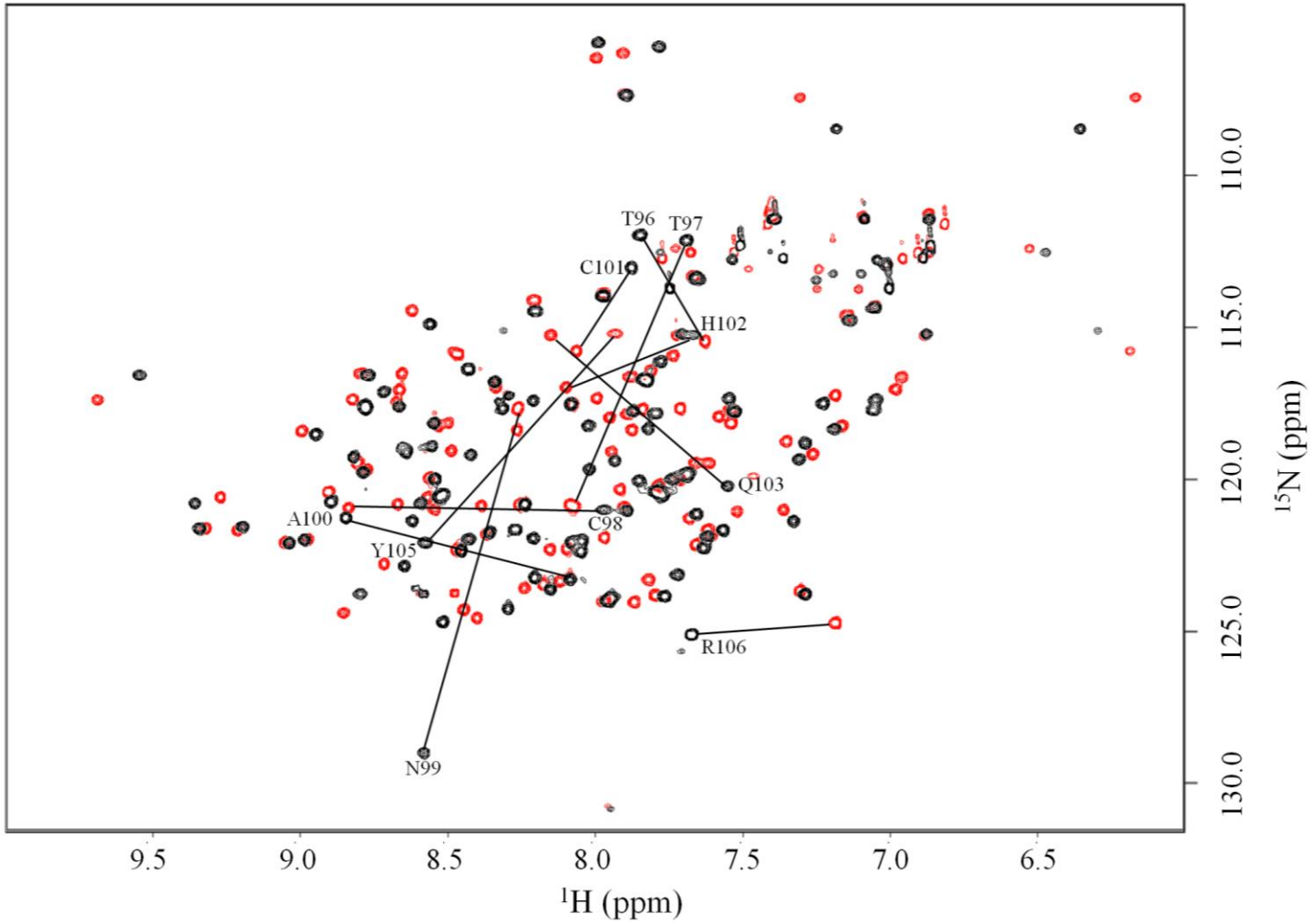

Figure 4. 12: Overlay of the ^{1}H-^{15}N HSQC spectra of both oxidation states of apocytochrome *c*-b_{562}. The spectrum of the oxidised form is shown in black and the spectrum from the reduced form is shown in red. Residues close to the CXXCH heme binding motif with large changes in chemical shift have been marked with a black line connecting their position in the oxidised with the one in the reduced spectrum.

4.2.4.1 Chemical shift analysis between the two oxidation states

The backbone assignments for all the cytochrome *c*-b_{562} residues in both oxidation states were completed. The chemical shift differences between the two oxidation states can be analysed (Figures 4.13, 4.14). Differences can be observed mainly for residues located at the C-terminus of the protein, from T96 onwards which undergo large chemical shift changes. According to combined chemical shift changes (Figure 4.14), both C98 and C101 appear to have changes of 0.87 and 0.90, respectively and H102 has a change of 0.69. The residues that appear to have the largest chemical shift changes are the ones before and after C98 and C101; T96 and T97 show changes of 1.13 and 2.80, respectively, and N99 shows the largest change of 3.59 with a shift of more 11 ppm in the ^{15}N. A100 showed a change of 1.00, and residues Q103, K104 and Y105 changes of 1.48, 1.36 and 2.24, respectively. The C-terminal residue R106 has a chemical shift difference of 0.50 between the oxidised and the reduced state of the protein. A full list of chemical shift differences is given in the appendix (Tables ST1 and ST2).

4.2.4.2 Discussion

The complete backbone assignments for both oxidation states of the apoprotein will be used for further protein-protein interaction studies between a *c*-type apocytochrome and proteins of the Ccm system by NMR spectroscopy. Using the apocytochrome *c*-b_{562} for these studies is ideal as this protein is small and gives well resolved NMR spectra.

Assignments of apocytochrome *c*-b_{562} can also be used as a starting point to study the biophysical properties of the characteristic CXXCH motif. The pK_a values of cysteines in a CXXC motif are representative of their reactivity. Thus, measuring the pK_a values of the *c*-b_{562} cysteines could provide, for the first time, insights into the reactivity of the cysteines of a

c-type apocytochrome towards heme but also on the reductant provision process via the Ccm system.

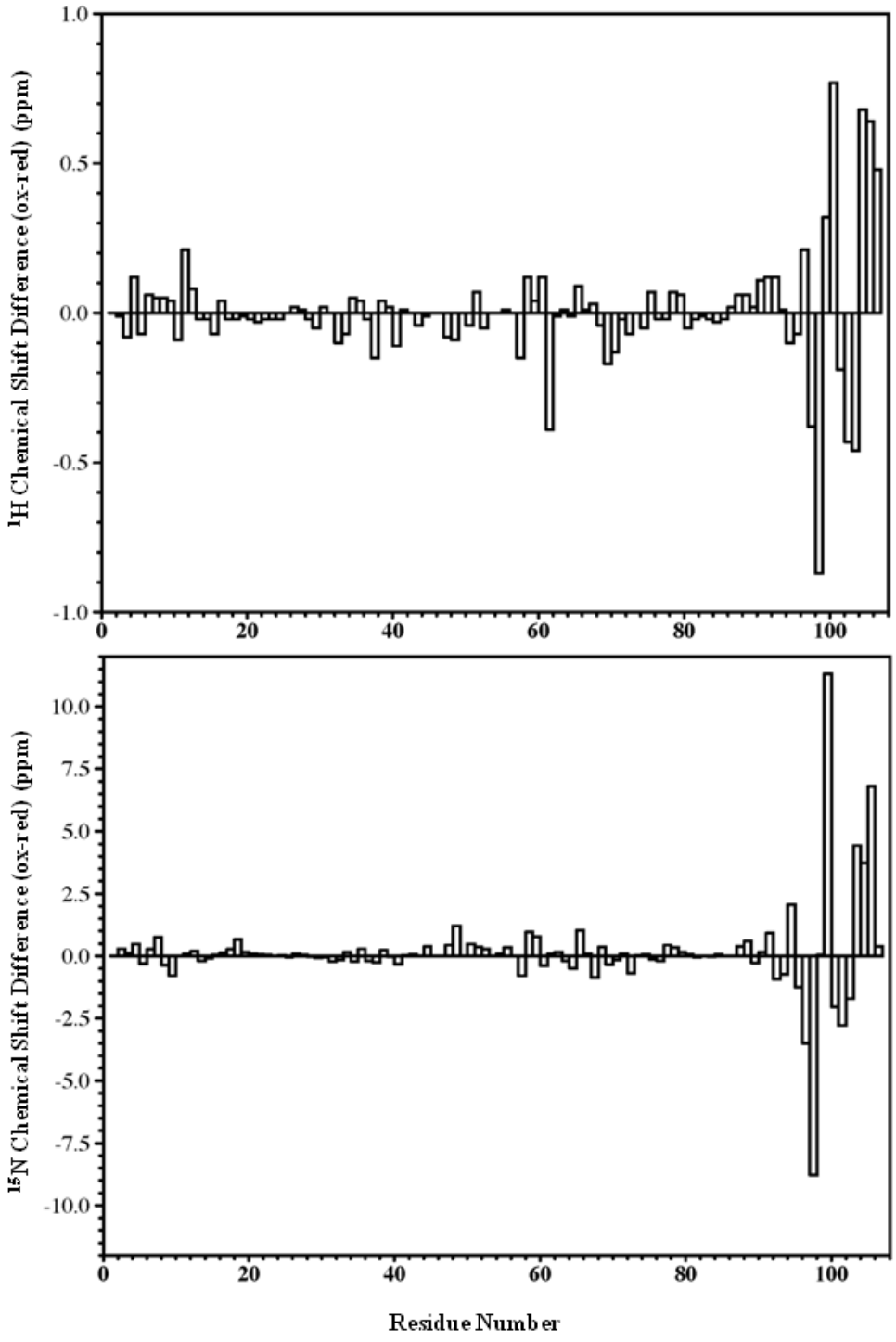

Figure 4. 13: Chemical shift differences between the two oxidation states (oxidised-reduced). In the top panel differences in the proton dimension are monitored and in the bottom panel differences in the nitrogen dimension are monitored.

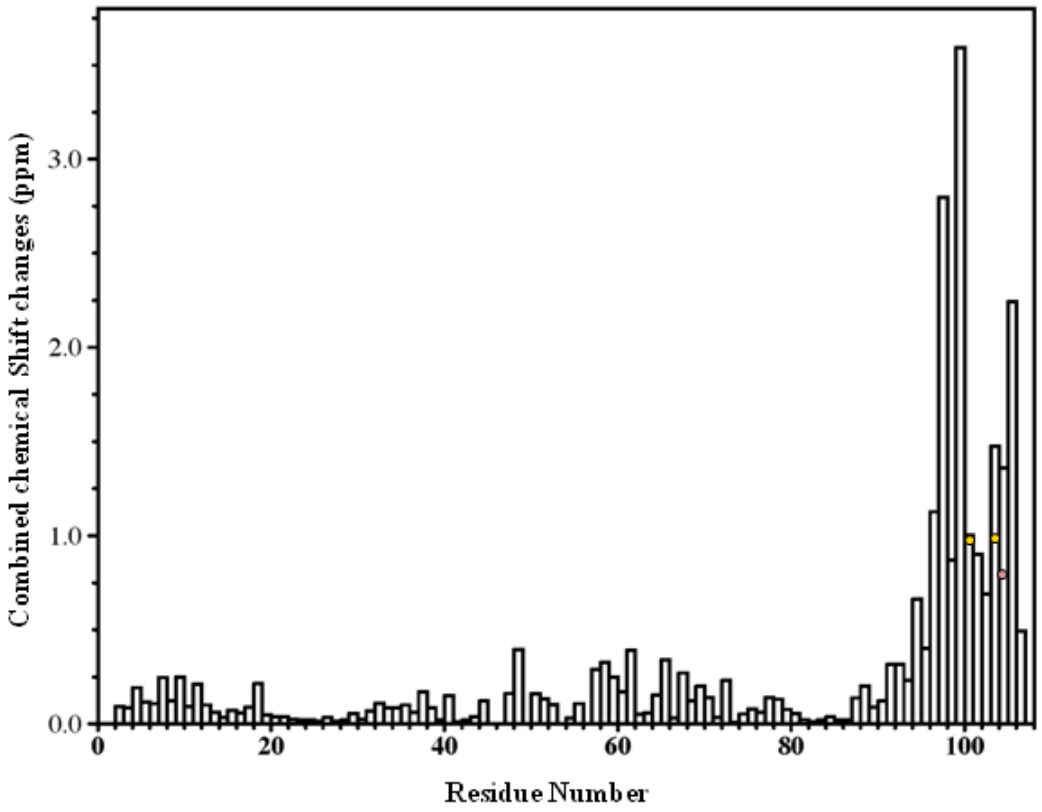

Figure 4. 14: Combined chemical shift changes, between the two oxidation states. The formula $(\Delta\delta(HN,N) = ((\Delta\delta^{1}H)^{2} + 0.1(\Delta\delta^{15}N)^{2})^{1/2v}$ was used.

4.2.5 Cysteine specific NMR studies

Apocytochrome *c*-b_{562} was expressed in the presence of 3-^{13}C L-cysteine and ^{1}H-^{13}C HSQC spectra were collected. The peaks from the CH_2 group of the side chain of the cysteine residues were assigned using the 3D ^{15}N-TOCSY-HSQC data. In this experiment, the chemical shifts of the H^{β}s had been identified for the cysteines in both oxidation states. The presence of other peaks in the ^{1}H-^{13}C HSQC spectra can be explained by the fact that the 3-^{13}C L-cysteine is metabolised and ^{13}C is incorporated in other amino acids. The full spectra collected at 750 MHz, pH 5.2 and 293K, can be seen in Figures 4.15 and 4.16 for the oxidised and the reduced state, respectively.

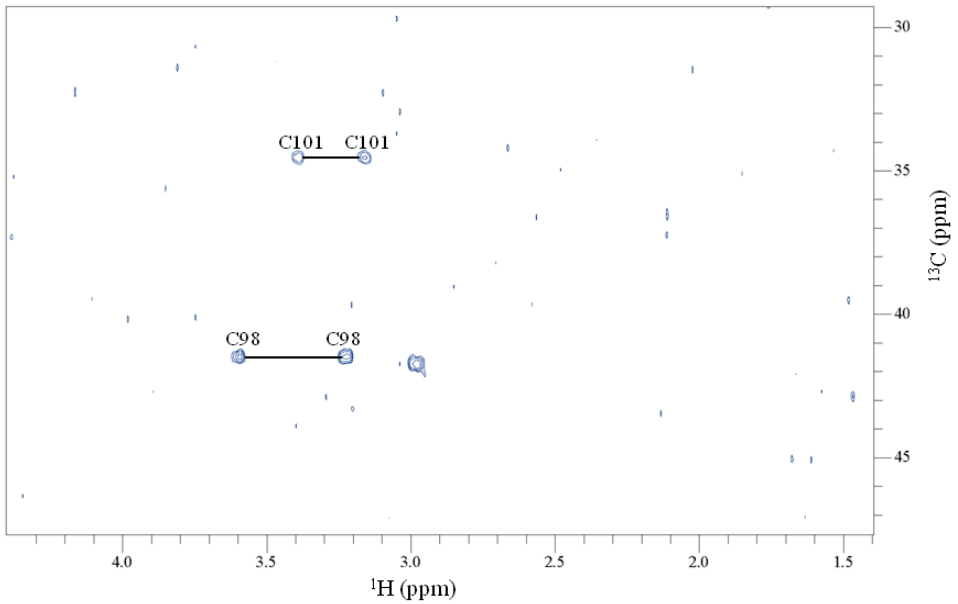

Figure 4. 15: ^{1}H-^{13}C HSQC NMR spectra collected at 750 MHz, pH 5.2 and 293 K using oxidised 3-^{13}C L-cysteine labeled apocytochrome *c*-b_{562}.

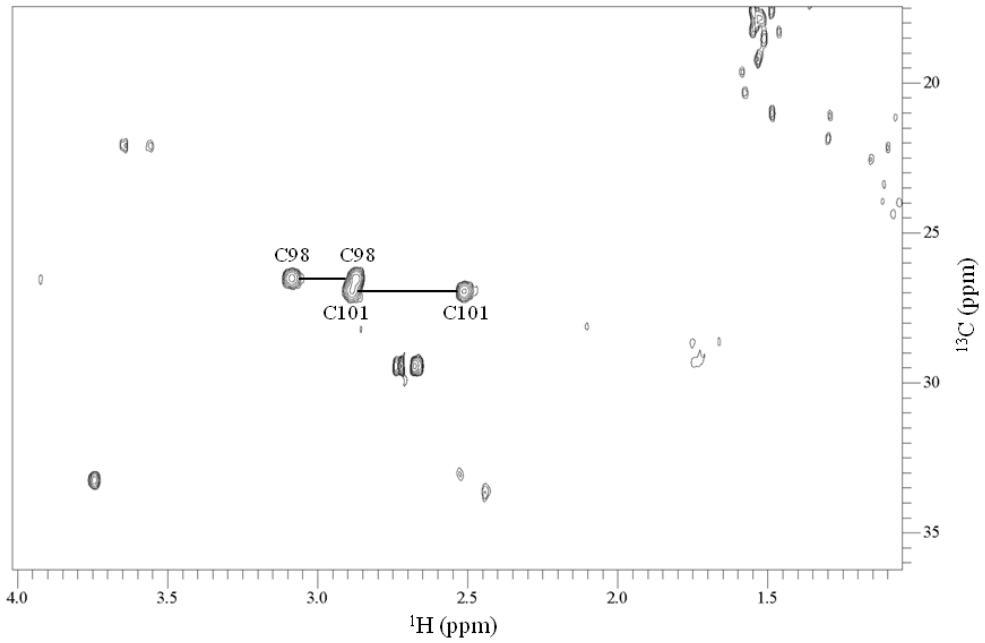

Figure 4. 16: ^{1}H-^{13}C HSQC NMR spectra collected at 750 MHz, pH 5.2 and 293 K using reduced 3-^{13}C L-cysteine labeled apocytochrome *c*-b_{562}.

pH titrations were conducted for both oxidation states of the protein by collecting ^{1}H-^{13}C HSQC spectra at different pH values. A shift of 2-3 ppm is expected in the ^{13}C dimension for the crosspeak of the CH2 group of the side chain of the titrating cysteine, reflecting the

change of the protonated (SH) to the deprotonated (S^-) form. The titration of the oxidised 3-^{13}C L-cysteine labeled protein is shown in Figure 4.17. The peaks from C101 seem to shift in both the ^{1}H and ^{13}C dimension. The peaks from C98 shift as well, but not as much as the C101 peaks. The cysteines are disulfide bonded, so any pH dependence of the chemical shifts of the cross peaks must be due to titration of other residues in close proximity to the cysteines. During the titration of the reduced 3-^{13}C L-cysteine-labeled apocytochrome *c*-b_{562} peak-shifting was observed for C101 in the ^{1}H dimension (Figure 4.19). Plotting these chemical shifts against pH resulted into two pK_as of 3.9 and 6.0 (Figure 4.18). Surprisingly, no shifts were observed in the ^{13}C dimension for either cysteine, suggesting that the cysteines either have a very high or a very low pK_a value.

In order to evaluate whether this result is due to the structure of the C-terminus of the protein or an intrinsic feature of the CXXCH motif, the protein was denatured with 8M urea. ^{15}N-HSQC NMR spectra were firstly obtained for both oxidation states (Figure 4.20).Reduction was carried out with the addition of 10mM DTT. In this case, the protein is denatured, so residues that appear to have different chemical shifts between the two oxidation states are only these located at the C-terminus of the protein and in close proximity to the cysteines of the CXXCH motif. In addition, 3D ^{15}N-edited TOCSY-HSQC and NOESY-HSQC experiments were collected for the reduced form of the protein and backbone assignments were done for the C-terminus of the protein, in order to identify the cysteines and obtain the the chemical shifts of the Hβs.

The CH2 chemical shifts were assigned through the H^β shifts (Figure 4.21) and pH dependent titrations were conducted using the reduced protein. The cysteine residues titrate in the ^{13}C dimension (Figure 4.22). Following the analysis of the chemical shift changes as a function of pH, titration curves for both cysteine residues were plotted and a single pK_a value can be

assigned for each residue. C98 has a pK_a value of 9.1 and C101 has a pK_a value of 8.8 when the protein is denatured (Figure 4.23).

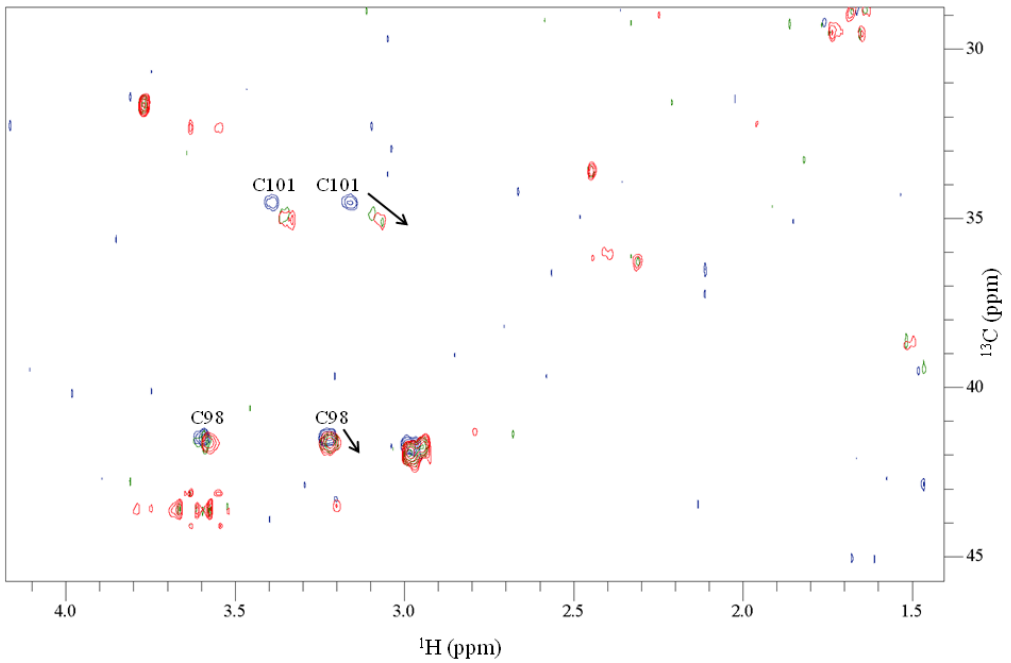

Figure 4. 17: Overlay of ^{1}H-^{13}C HSQC NMR spectra of oxidised 3-^{13}C L-cysteine labeled apocytochrome *c*-b_{562} collected at 750 MHz, 293 K and a range of pH values. The C^{β} of both cysteine residues shifts with pH. The spectra presented are at pH 4.65 (blue), pH 7.17 (green), pH 8.34 (red).

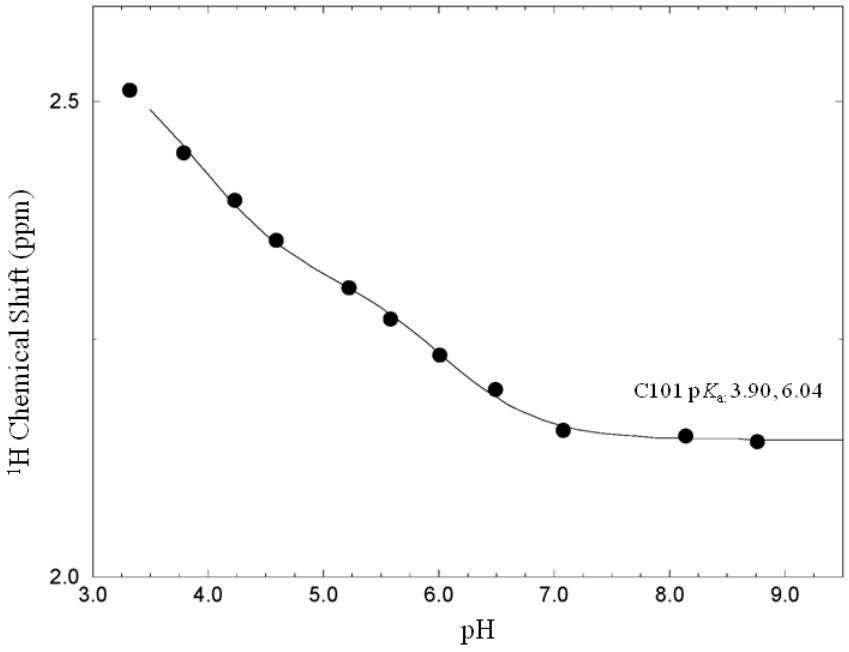

Figure 4. 18: pH dependence of one of the 1H chemical shifts of the side chain CH2 group of C101 for reduced 3-^{13}C L-cysteine labeled apocytochrome *c*-b_{562}. Fitting of the data results in two pK_a values of 3.9 and 6 .

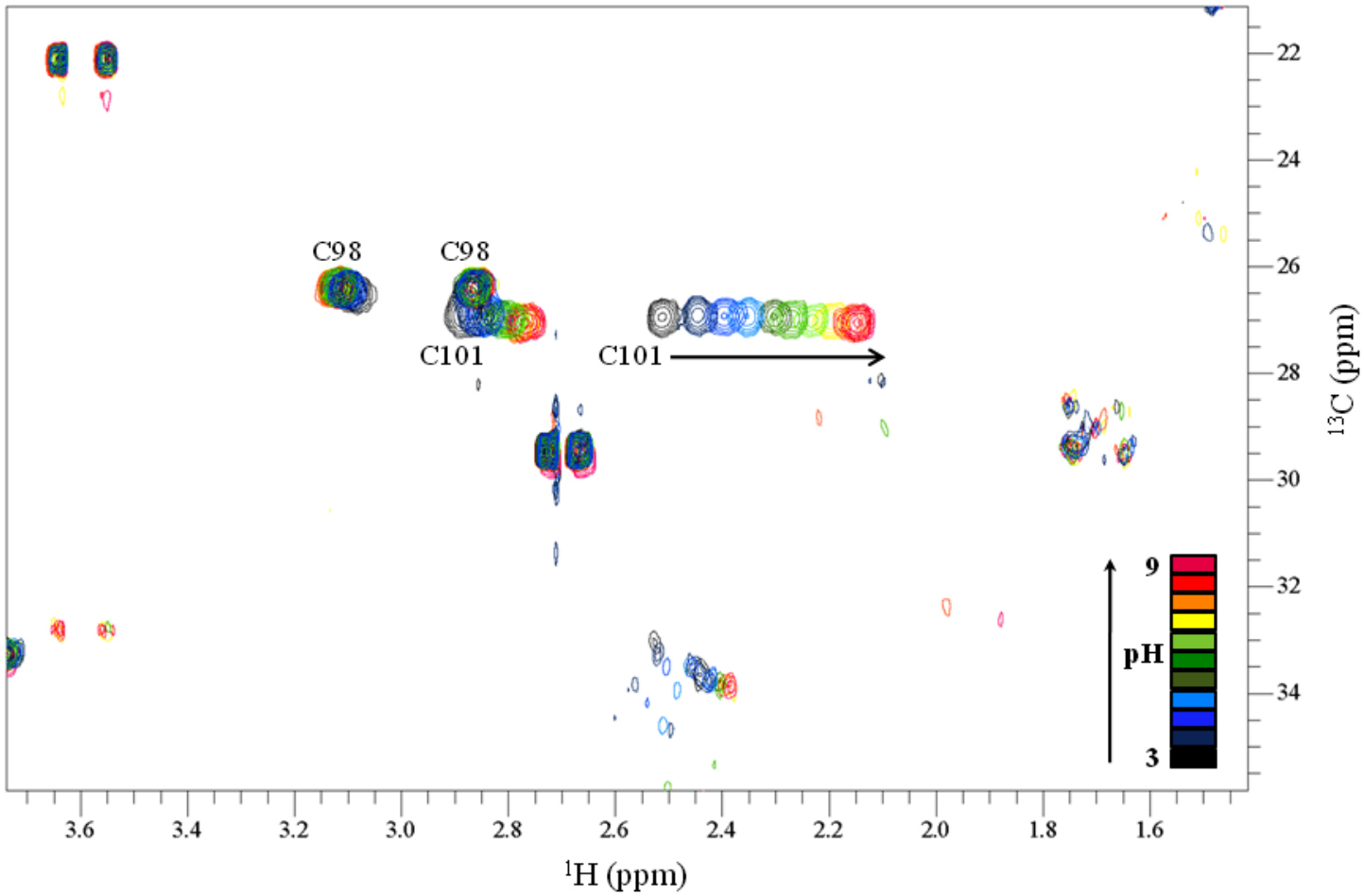

Figure 4. 19: Overlay of ^{1}H-^{13}C HSQC NMR spectra of reduced 3-^{13}C L-cysteine labeled apocytochrome *c*-b_{562}.collected at 750 MHz, 293 K and a range of pH values. The spectra presented are at pH 3.32 (black), pH 3.79 (dark blue), pH 4.23 (blue), pH 4.59 (light blue), pH 5.22 (dark green), pH 5.58 (light green), pH 6.01 (lime), pH 6.49 (yellow), pH 7.09 (orange), pH 8.14 (red) pH, 8.79 (pink).

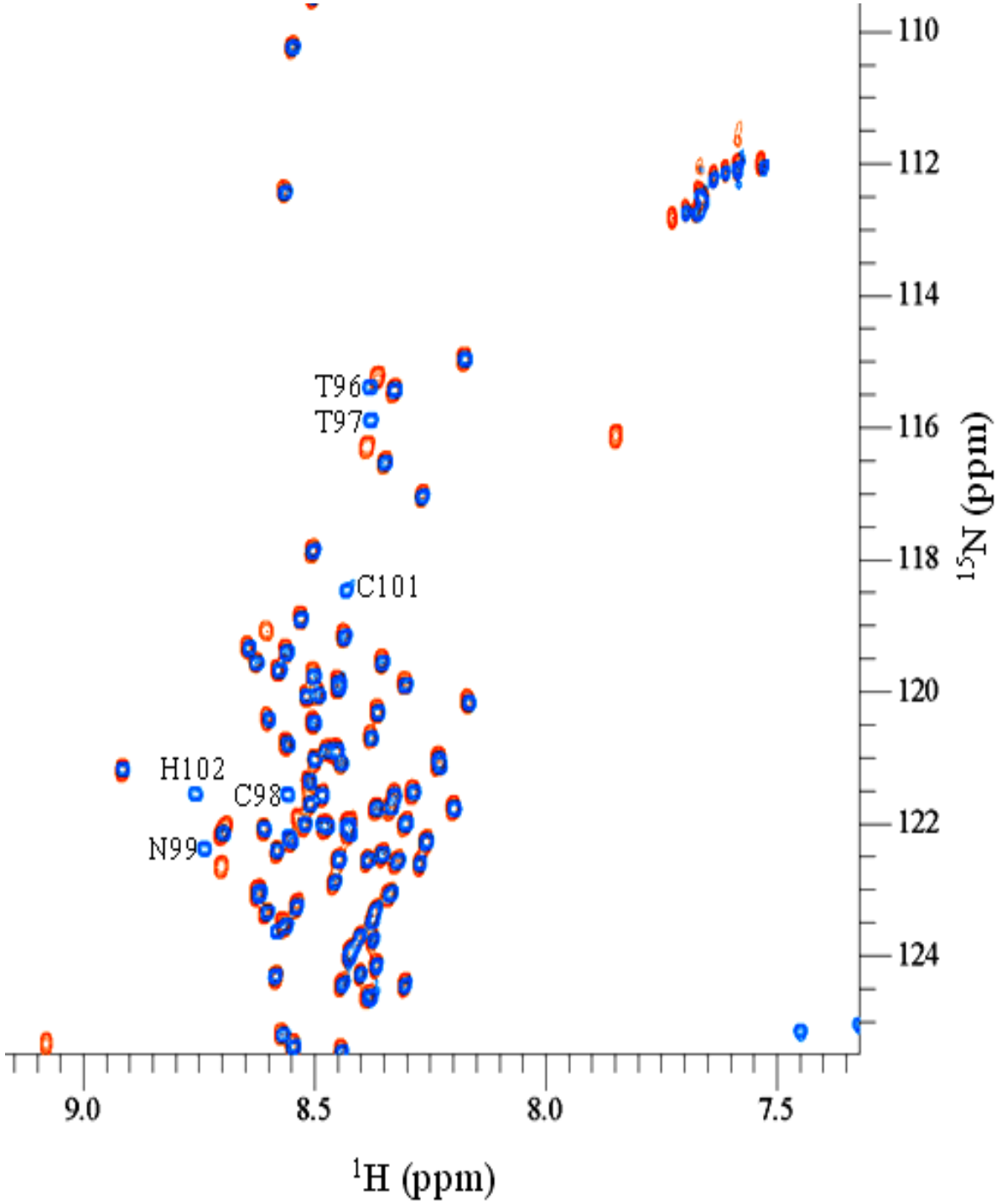

Figure 4. 20: Overlay of ^{1}H-^{15}N HSQC NMR spectra of the two oxidation states of ^{15}N labeled apocytochrome *c*-b_{562} in the presence of 8M urea collected at 600 MHz, 293 K, pH 5.2. The spectrum of the oxidised state of *c*-b_{562} is shown in orange and the spectrum of the reduced in blue. Non overlapping peaks arise from residues in close proximity to the CXXCH motif. Using 3D ^{15}N-edited TOCSY-HSQC and NOESY-HSQC NMR experiments most of the residues close to the cysteines were unambiguously assigned.

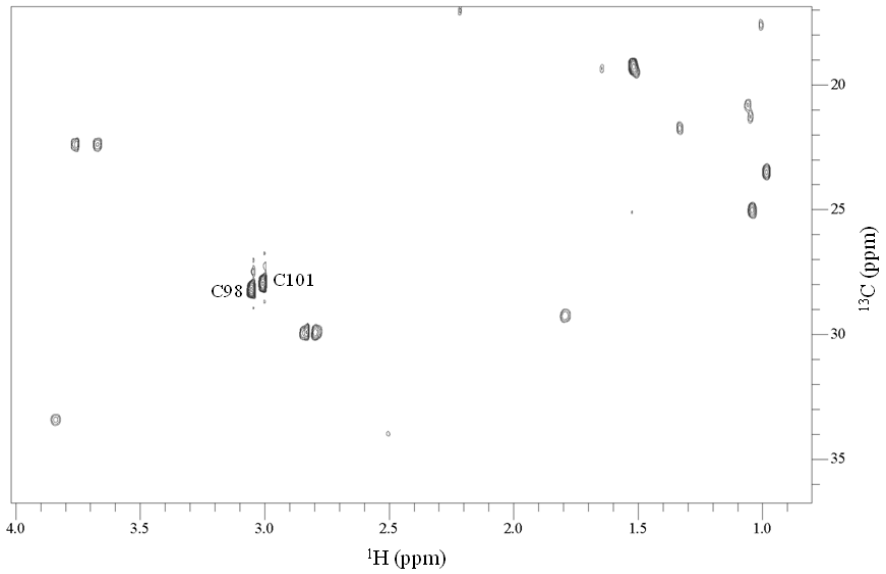

Figure 4. 21: ^{1}H-^{13}C HSQC NMR spectra of reduced 3-^{13}C L-cysteine labeled apocytochrome *c*-b_{562} collected at 750 MHz, 293 K and pH 3.2. The C$^{\beta}$s of the cysteines as identified from the ^{15}N-edited TOCSY-HSQC experiments were at 3.05(ppm) for C98 and 3.00 (ppm) for C101.

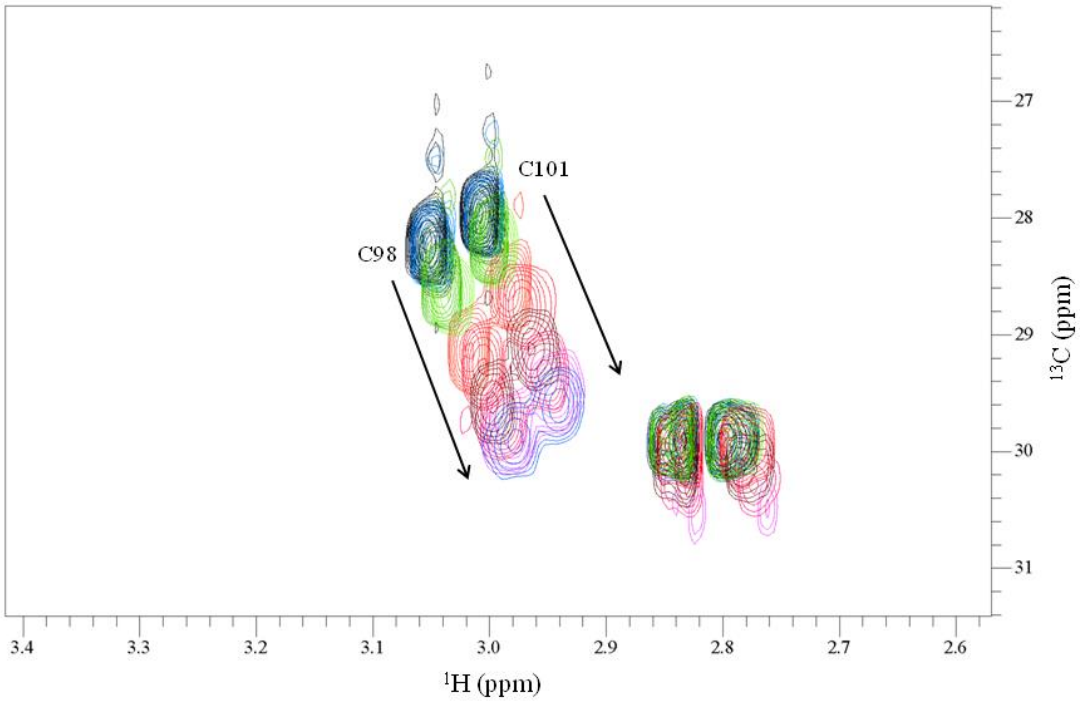

Figure 4. 22: Overlay of ^{1}H-^{13}C HSQC NMR spectra of reduced 3-^{13}C L-cysteine labeled apocytochrome *c*-b_{562} in 8M urea collected at 750 MHz, 293 K and different pH values. The spectra presented are at pH 5.34 (black) 6.51(dark blue), pH 7.22 (blue) ,pH 7.42 (dark green), pH 7.62 (green), pH 8.26(lime), pH 8.48 (orange), pH 8.78 (red), pH 9.04 (brown), pH 9.42 (pink), pH 9.70 (magenta), pH 10.04(light blue)

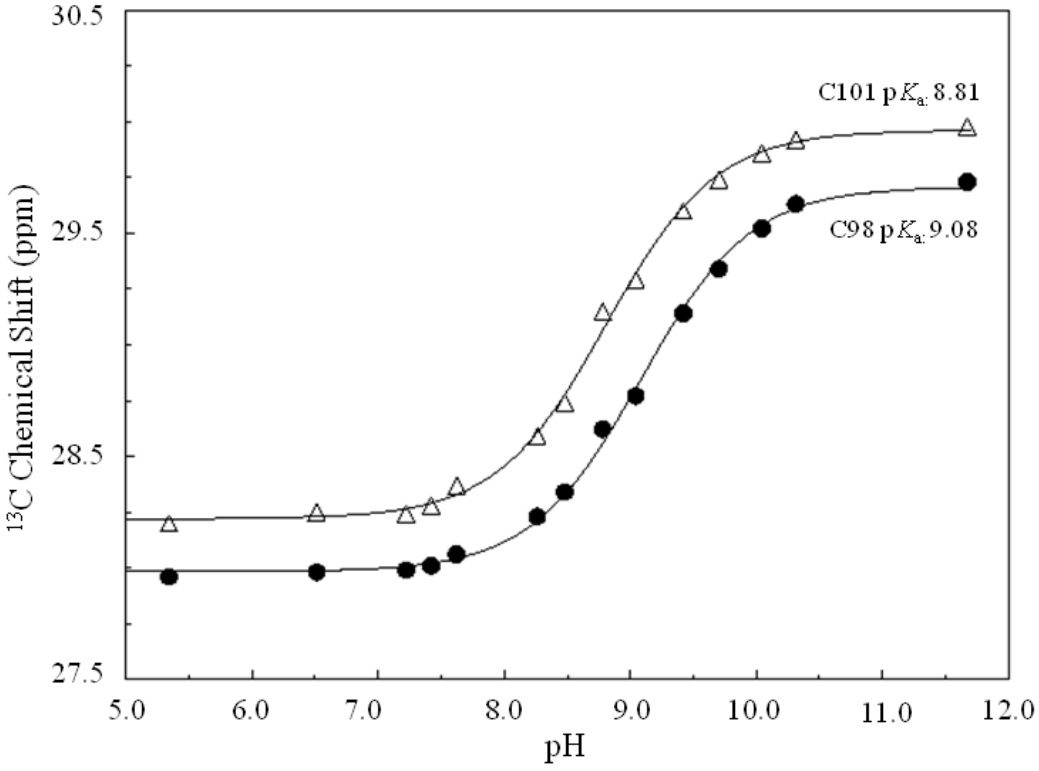

Figure 4. 23: pH dependence of the ^{13}C chemical shift of side chain CH2 group of cysteines C98 and C101 in reduced and denatured 3-^{13}C L-cysteine labeled apocytochrome *c*-b_{562}. pK_a values of 8.8 and 9.1 were obtained for C101 and C98, respectively.

4.2.6 Histidine-specific studies

From the cysteine-specific experiments it was not feasible to determine the pK_a values of the cysteine residues in native apocytochrome *c*-b_{562}. However, it was still interesting to examine if the presence of the histidine residue (H102) in proximity to the cysteines of the CXXCH was affecting them. Histidine specific experiments were done in order to measure the pK_a value of H102. In the protein sequence there is only one other histidine, H63, which is expected to have the same pK_a value in both the oxidised and the reduced state of the protein.

To measure only the pK_a values of the histidine residues, pH titrations were done collecting ^{1}H-^{15}N HMQC NMR spectra for both oxidation states. In this experiment, four peaks arise from the $H^{\delta 2}$ and $H^{\varepsilon 1}$ non exchangeable protons of the histidine ring for each histidine residue. These crosspeaks can be detected around 170-230 ppm in the ^{15}N dimension. Monitoring the shifting of the peaks with pH can generate information about the pK_a value of

the residue. In experiments for ^{15}N-labelled *c*-b_{562}, the peaks of both histidines disappeared for pH values above 6.5, so it was not feasible to record a full titration curve. However, from the points collected between pH 3.5-6.5 it could be observed that H102 has a different pK_a value between the two oxidation states, with the value of the reduced form being lower (Figure 4.24)

Further experiments were needed to determine the exact pK_a values of H102. Using the 3-^{13}C L-cysteine labeled apocytochrome *c*-b_{562} in 99% D_2O 1D spectra were collected at different pH values. In these spectra the characteristic peaks of the $H^{\delta 2}$ and $H^{\varepsilon 1}$ could be monitored. The peaks became very broad for the oxidised form of the protein and pK_a values could not be measured. However, for the reduced form of the protein pK_a values of 7.4 and 6.5 were measured for H63 and H102, respectively (Figure 4.25).

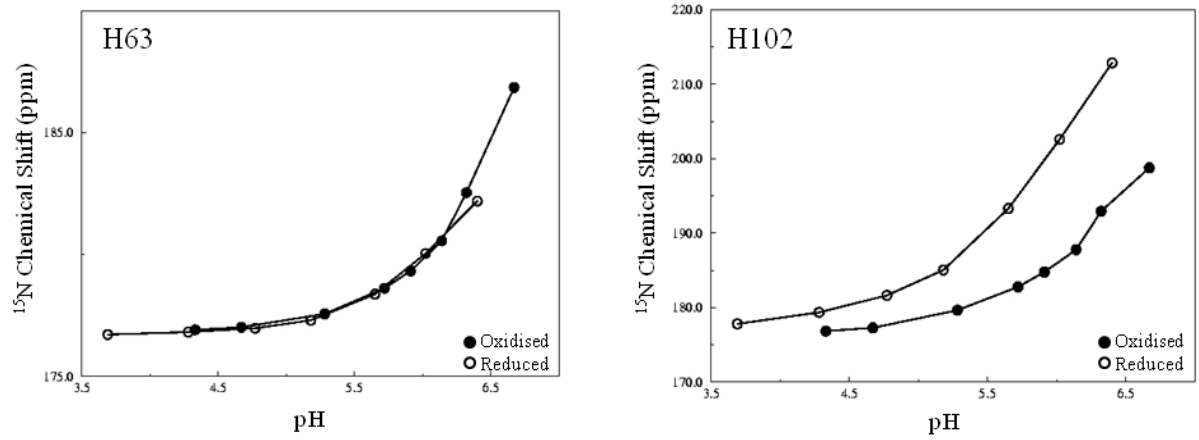

Figure 4. 24: pH dependence of the 15N chemical shift for histidine residues H63 (left) and H102 (right) in oxidised and reduced apocytochrome *c*-b_{562}. Only the beginning of the titration curves is depicted as peaks for both histidine residues disappear above pH 6.5. White circles are the titration points for the reduced form and black for the oxidised form of the protein. It can be extrapolated that H63 has almost the same pK_a in both oxidation states, whereas H102 has different pK_a values between the two oxidation states of *c*-b_{562}.

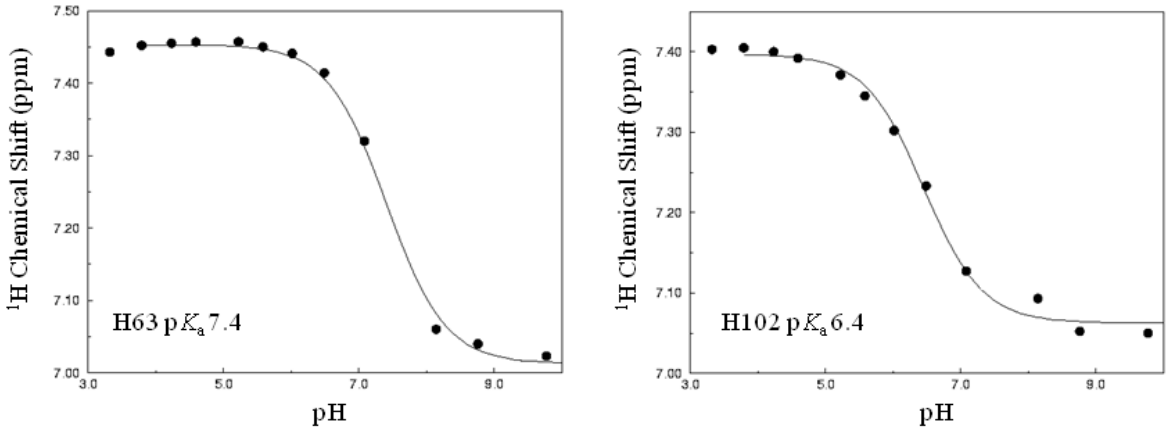

Figure 4. 25: pH dependence of the 1H chemical shift of H63 and H102 for reduced apocytochrome *c*-b_{562}. H63 has a pK_a value of 7.4 and H102 a pK_a value of 6.4, as identified by 1D experiments performed in 99 % D_2O.

In order to determine the pK_a values of the histidines for the oxidised state of the protein, ^{1}H-^{15}N HSQC spectra were collected at different pH values for both oxidation states. Backbone assignments were completed so the shifting of peaks of several residues could be monitored simultaneously. The peak of His102 becomes very broad in oxidised apocytochrome *c*-b_{562} and can not be monitored. However, the peak of C101 is shifting although it is disulfide bonded to C98 (the peak of which also becomes broad). Therefore the observed shifting for C101 reflects the titration of a neighbouring residue; H102 is likely to be affecting C101. Plotting of C101 chemical shift against pH results in a pK_a of 6.6 (Figure 4.26 (B)). As a comparison, H63 is titrating with a pK_a of 6.8 (Figure 4.26(A))

For the reduced form of the protein the 2D titrations show a very complicated profile. His102 appears to have a complicated V shaped titration curve which could arise by two pK_as of 6.0 and 5.9 (Figure 4.26 (C)). C101 is shifting slightly, however this shift compared to the shift of the oxidised form is less obvious (Figure 4.26 (B)). C98 cannot be monitored because it overlaps with residue D2. H63 appears to have a pK_a of 7 (Figure 4.26 (A)).

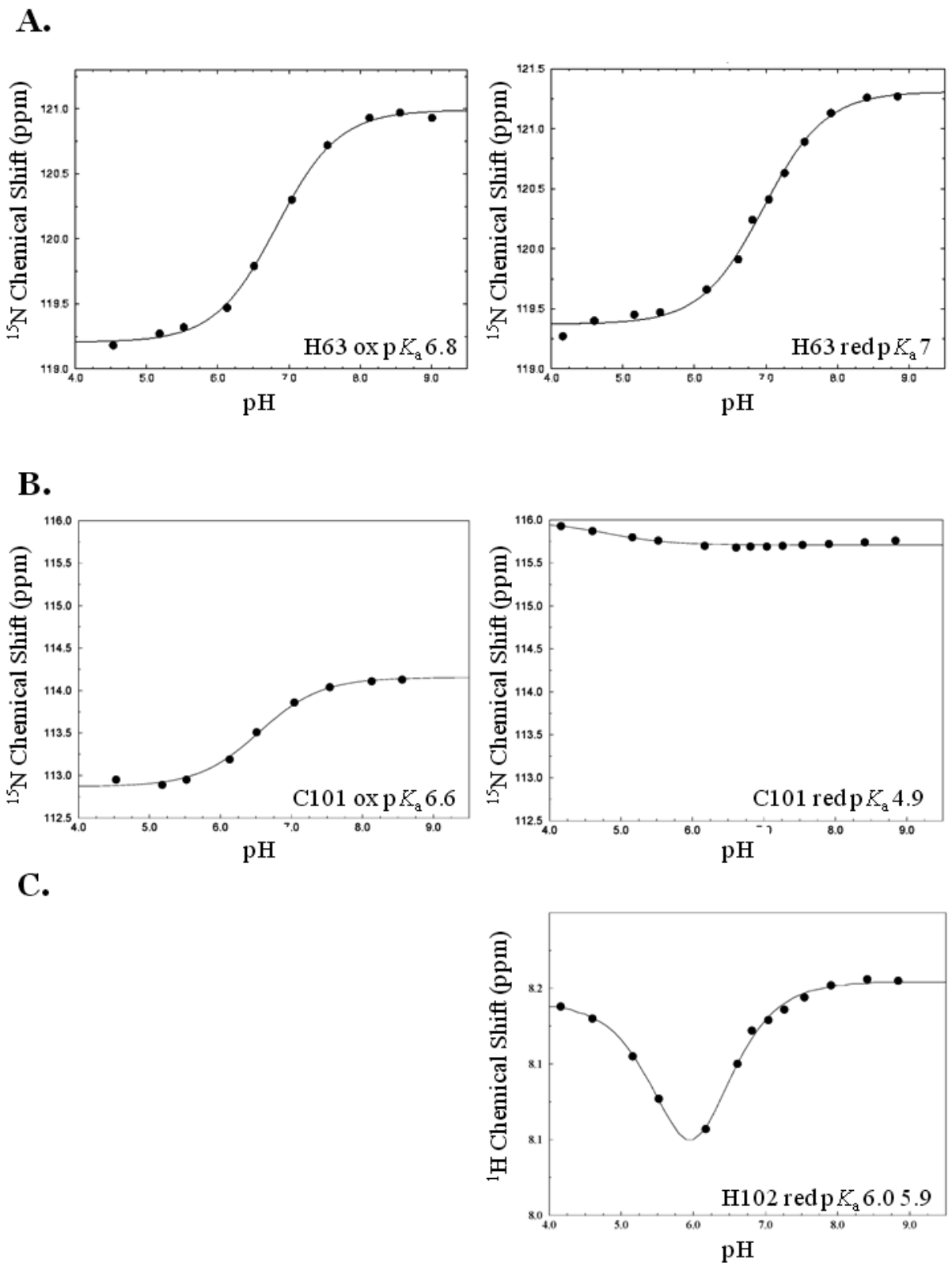

Figure 4. 26: pH dependence of 15N or 1H chemical shifts for H63 (A), C101 (B) and H102 (C) from ^{1}H-^{15}N HSQC NMR spectra collected at 500 MHz and 293 K. Complicated behavior is observed for H102.

4.3 Discussion

In this chapter, biophysical studies on a *c*-type apocytochrome were conducted using NMR spectroscopy. The main goal was to assign the ^{1}H-^{15}N HSQC spectrum for both oxidation states of the protein in order to be able to use it as a probe for future protein-protein interaction studies using NMR spectroscopy between a *c*-type apocytochrome and proteins of the Ccm system. As well, another aim was to determine the pK_a values of the cysteines and the histidine residue of the conserved CXXCH heme binding motif of this protein.

The backbone assignments of apocytochrome *c*-b_{562} were conducted for both oxidation states using ^{15}N-labeled apoprotein. Comparison of the oxidised and reduced spectra showed that there are differences in the chemical shifts of several residues between the two oxidation states. Analysis of these chemical shift changes revealed that the largest differences can be observed for residues located at the C-terminus of the protein, from T96 onwards. C98, C101 and H102 appear to have chemical shift differences. However, residues located prior, between and after the cysteines have larger chemical shift differences, with N99 showing the largest effect.

In order to determine the pK_a values of the cysteine residues 3-^{13}C L-cysteine-labeled apocytochrome *c*-b_{562} was produced. pH titrations were performed for both oxidation states by collecting ^{1}H-^{13}C HSQC NMR spectra. The peaks from the oxidised protein shifted slightly in both ^{1}H and ^{13}C. A shift of 2-3 ppm of the crosspeaks at the ^{13}C dimension for the C^{β}s of the cysteine residues was expected for the reduced form of the apocytochrome. This shift was not observed. The one C^{β} of C101 shifted only in the ^{1}H dimension, giving two pK_a values of 3.1 and 6. The fact that the cysteines do not titrate in the reduced state in the ^{13}C dimension suggest an atypical behavior; the cysteine residues can either have a very high or a

very low pK_a value compared to the pK_a value of a cysteine residue in a random coil (pK_a 8.5-9.1). In order to establish if this unusual behavior was related to the structure of the apoprotein denatured and reduced apocytochrome *c*-b_{562} was used. Assignments of the residues around at the C-terminus were conducted in order to identify the position of the C^{β} in the denatured reduced form of the protein. When ^{1}H-^{13}C HSQC spectra were collected at different pH values, pK_a values of 8.8 and 9.1 were determined for C101 and C98, respectively.

The pK_a values measured for the denatured protein are normal for a typical cysteine residue in a random coil (Harris and Turner 2002; Thurlkill et al. 2006). This suggests that since the cysteines did not appear to titrate when the protein is folded in its reduced form, it is highly likely that the atypical pK_a values of the cysteines are due to the structural conformation of the C-terminus of the apoprotein. The role of the conserved His residue located next to C101 was subsequently examined.

Several experiments were performed aiming to measure the pK_a value of H102. For these studies H63 was also monitored, however the profile for H102 was more complicated than the profile of H63. From the 1D experiments in 99 % D_2O for the reduced apocytochrome, H63 had a pK_a of 7.4 and H102 had a pK_a value of 6.4. From the 2D ^{1}H-^{15}N HSQC experiments for the reduced apocytochrome H63 appears to have a pK_a of 7 and H102 two pK_as of 5.9 and 6 resulting from a fitting of a V-shaped titration curve (Figure 4.26 (C)). The differences between the pK_a values observed in these two different experiments can be explained by the differences in the behavior of the protein when it is in D_2O or H_2O (correction by a factor of 0.4). For H_2O experiments we can conclude that His102 is likely to have one pK_a value of about 6.0, but from the complicated V-shaped titration curve it can be suggested that the histidine is affected by two ionisable groups in reduced apocytochrome *c*-

b_{562}. From the data generated from the ^{1}H-^{15}N HMQC experiment it can be suggested that if the pK_a value of H102 is 6 in the reduced state of the protein, then for the oxidised state it is going to be higher. The shifting of C101 in the ^{1}H-^{15}N HSQC experiment in the oxidised form can reflect the titration of H102 that cannot be monitored directly. That gives a pK_a value of 6.5. It cannot be explained based on the current data why the peak of the histidine becomes broad and disappears in the oxidised form. It could also be suggested that the shift of the C$^{\beta}$ of C101 observed in the ^{1}H dimension could be partially due to the ionization of H102. Two pK_a values were observed at 3.9 and 6.0 for C101 but none is due to ionisation of the –SH group as this should lead to a shift of 2-3 ppm in the ^{13}C dimension. The pK_a value of 6.0 could be attributed to H102.

The complicated pK_a value profile for the residues of the CXXCH can be probably explained from the ionization profile of other residues, such as the C-terminal residue R106 and residues at the N-terminus of the protein, D2, E4, D5, which could be in close proximity to the CXXCH motif and thus could contribute to the electrostatics of the protein. For acidic residues like these, pK_a values around 4 or less are expected. However, when the protein is folded more complicated behavior can be observed.

In summary, the cysteine residues of the CXXCH motif, either have very high or very low pK_a values that were not able to be identified from these experiments. Other experiments can be done using NMR spectroscopy to monitor if at one specific pH point the cysteines are protonated or deprotonated. For this experiment a ^{1}H-^{13}C HSQC spectrum of the 3-^{13}C L-cysteine-labeled protein in a specific pH is collected when the protein is in 95 % H_2O and when it is in 99 % D_2O. If the cysteines are ionised the crosspeaks of the C$^{\beta}$s are going to be at the same position for both spectra. However, if the cysteines at this pH are

protonated/deuterated a small difference between the crosspeaks will be observed because of the presence of a ^{1}H or ^{2}H on the exchangeable –SH group.

CHAPTER 5

Conclusion

The first part of this thesis focuses on the periplasmic membrane protein DsbD. It describes the development of a new and more quantitative method to assess the contribution of specific conserved residues to the functionality of DsbD *in vivo*. This method exploits one of the phenotypes of the DsbD deletion strain. When DsbD is not active, there is no transfer of reductant to its protein partners, such as CcmG. CcmG is a protein of the Ccm system that either directly or indirectly is able to reduce the disulfide bond formed between the cysteines of the CXXCH-heme binding motif in *c*-type apocytochromes. The necessary reducing power for CcmG is provided by DsbD. Hence, when DsbD is not active the levels of mature *c*-type cytochrome are very low.

In this method, *E. coli* strains (either wild-type or with a deletion of the gene that encodes DsbD) were grown under anaerobic conditions for the endogenous Ccm system to be expressed. An exogenous cytochrome, cytochrome cd_1 from *Paracoccus denitrificans*, was used as a probe to monitor the activity of DsbD. Full-length DsbD and variants of it were expressed from a plasmid in a DsbD deletion strain. The production of mature cd_1 was monitored by SDS-PAGE analysis and staining for heme covalently-bound to polypeptides.

Variants of DsbD in both the C-terminal and the transmembrane domains were assessed using this method. The variants of the C-terminal domain that were assessed, had been identified by NMR spectroscopy to be important, however their *in vivo* behaviour had not been tested. The variants of the transmembrane domain of DsbD had been poorly characterized previously or they have never been characterised before.

This newly developed method can be used in the future for assessment of the role of other important residues of DsbD. One such example would be residues of the N-terminal domain of DsbD. This domain of DsbD has multiple periplasmic partners (DsbC, DsbG, CcmG and TrbB) so it is believed that it functions as a "hub" for reductant transfer. Are there specific residues at the N-terminus responsible for these interactions?

The second part of this thesis focuses on biophysical studies of a *c*-type apocytochrome, *c*-b_{562}, using NMR spectroscopy. Backbone assignments of both oxidation states of apocytochrome *c*-b_{562} were completed. Then, studies on the biophysical properties of the CXXCH heme binding motif were conducted. The aim was to determine the pK_a value of the cysteines; with this information interaction and reaction of the *c*-type apocytochome with the heme and proteins of the Ccm system could be elucidated. It was not feasible to measure the pK_a values of the cysteine residues. This means that they either have a very high or a very low pK_a value. In denatured conditions in the reduced state of the protein Cys101 and Cys98 have pK_a values of 8.9 and 9.1, respectively.

The role of the histidine residue (His102) of the CXXCH heme binding motif was also investigated. The histidine residue has different pK_a values between the oxidized and the reduced state of the protein (6.0 in the reduced and probably 6.5 in the oxidized).

Further work can be done to determine the pK_a values of the cysteines and to investigate the contribution of the histidine residue to their properties. In addition, the backbone assignments can be used in protein-protein interaction studies by NMR spectroscopy between apocytochrome *c*-b_{562} and proteins of the Ccm system.

Bibliography

Ahuja, U. and L. Thony-Meyer (2003). "Dynamic features of a heme delivery system for cytochrome *c* maturation." J Biol Chem **278**(52): 52061-70.

Ahuja, U. and L. Thony-Meyer (2005). "CcmD is involved in complex formation between CcmC and the heme chaperone CcmE during cytochrome *c* maturation." J Biol Chem **280**(1): 236-43.

Allen, J. W., P. D. Barker and S. J. Ferguson (2003). "A cytochrome b_{562} variant with a *c*-type cytochrome CXXCH heme-binding motif as a probe of the *Escherichia coli* cytochrome *c* maturation system." J Biol Chem **278**(52): 52075-83.

Aragao, D., C. Frazao, L. Sieker, G. M. Sheldrick, J. LeGall and M. A. Carrondo (2003). "Structure of dimeric cytochrome c_3 from *Desulfovibrio gigas* at 1.2 A resolution." Acta Crystallogr D Biol Crystallogr **59**(Pt 4): 644-53.

Arnesano, F., L. Banci, P. D. Barker, I. Bertini, A. Rosato, X. C. Su and M. S. Viezzoli (2002). "Solution structure and characterization of the heme chaperone CcmE." Biochemistry **41**(46): 13587-94.

Arnesano, F., L. Banci, I. Bertini, S. Ciofi-Baffoni, T. L. Woodyear, C. M. Johnson and P. D. Barker (2000). "Structural consequences of *b*- to *c*-type heme conversion in oxidized *Escherichia coli* cytochrome b_{562}." Biochemistry **39**(6): 1499-514.

Arslan, E., H. Schulz, R. Zufferey, P. Kunzler and L. Thony-Meyer (1998). "Overproduction of the *Bradyrhizobium japonicum* c-type cytochrome subunits of the cbb_3 oxidase in *Escherichia coli*." Biochem Biophys Res Commun **251**(3): 744-7.

Bader, M., W. Muse, D. P. Ballou, C. Gassner and J. C. Bardwell (1999). "Oxidative protein folding is driven by the electron transport system." Cell **98**(2): 217-27.

Bardwell, J. C., J. O. Lee, G. Jander, N. Martin, D. Belin and J. Beckwith (1993). "A pathway for disulfide bond formation *in vivo*." Proc Natl Acad Sci U S A **90**(3): 1038-42.

Bardwell, J. C., K. McGovern and J. Beckwith (1991). "Identification of a protein required for disulfide bond formation *in vivo*." Cell **67**(3): 581-9.

Barker, P. D. and S. J. Ferguson (1999). "Still a puzzle: why is haem covalently attached in *c*-type cytochromes?" Structure **7**(12): R281-90.

Barker, P. D., E. P. Nerou, S. M. Freund and I. M. Fearnley (1995). "Conversion of cytochrome b_{562} to *c*-type cytochromes." Biochemistry **34**(46): 15191-203.

Bertini, I., G. Cavallaro and A. Rosato (2007). "Evolution of mitochondrial-type cytochrome *c* domains and of the protein machinery for their assembly." J Inorg Biochem **101**(11-12): 1798-811.

Caroppi, P., F. Sinibaldi, L. Fiorucci and R. Santucci (2009). "Apoptosis and human diseases: mitochondrion damage and lethal role of released cytochrome *c* as proapoptotic protein." Curr Med Chem **16**(31): 4058-65.

Casadaban, M. J. and S. N. Cohen (1980). "Analysis of gene control signals by DNA fusion and cloning in *Escherichia coli*." J Mol Biol **138**(2): 179-207.

Charbonnier, J. B., P. Belin, M. Moutiez, E. A. Stura and E. Quemeneur (1999). "On the role of the cis-proline residue in the active site of DsbA." Protein Sci **8**(1): 96-105.

Cho, S. H. and J. Beckwith (2006). "Mutations of the membrane-bound disulfide reductase DsbD that block electron transfer steps from cytoplasm to periplasm in *Escherichia coli*." J Bacteriol **188**(14): 5066-76.

Christensen, O., E. M. Harvat, L. Thony-Meyer, S. J. Ferguson and J. M. Stevens (2007). "Loss of ATP hydrolysis activity by CcmAB results in loss of *c*-type cytochrome synthesis and incomplete processing of CcmE." FEBS J **274**(9): 2322-32.

Cook, G. M. and R. K. Poole (2000). "Oxidase and periplasmic cytochrome assembly in *Escherichia coli* K-12: CydDC and CcmAB are not required for haem-membrane association." Microbiology **146 (Pt 2)**: 527-36.

Crooke, H. and J. Cole (1995). "The biogenesis of c-type cytochromes in *Escherichia coli* requires a membrane-bound protein, DipZ, with a protein disulphide isomerase-like domain." Mol Microbiol **15**(6): 1139-50.

Daltrop, O., J. W. Allen, A. C. Willis and S. J. Ferguson (2002). "*In vitro* formation of a *c*-type cytochrome." Proc Natl Acad Sci U S A **99**(12): 7872-6.

Daltrop, O., J. M. Stevens, C. W. Higham and S. J. Ferguson (2002). "The CcmE protein of the *c*-type cytochrome biogenesis system: unusual *in vitro* heme incorporation into

apo-CcmE and transfer from holo-CcmE to apocytochrome." Proc Natl Acad Sci U S A **99**(15): 9703-8.

Delaglio, F., S. Grzesiek, G. W. Vuister, G. Zhu, J. Pfeifer and A. Bax (1995). "NMRPipe: A multidimensional spectral processing system based on UNIX pipes." Journal of Biomolecular NMR **6**(3): 277-293.

Depuydt, M., S. E. Leonard, D. Vertommen, K. Denoncin, P. Morsomme, K. Wahni, J. Messens, K. S. Carroll and J. F. Collet (2009). "A periplasmic reducing system protects single cysteine residues from oxidation." Science **326**(5956): 1109-11.

Di Matteo, A., S. Gianni, M. E. Schinina, A. Giorgi, F. Altieri, N. Calosci, M. Brunori and C. Travaglini-Allocatelli (2007). "A strategic protein in cytochrome *c* maturation: three-dimensional structure of CcmH and binding to apocytochrome *c*." J Biol Chem **282**(37): 27012-9.

Einsle, O., A. Messerschmidt, P. Stach, G. P. Bourenkov, H. D. Bartunik, R. Huber and P. M. Kroneck (1999). "Structure of cytochrome *c* nitrite reductase." Nature **400**(6743): 476-80.

Fabianek, R. A., H. Hennecke and L. Thony-Meyer (1998). "The active-site cysteines of the periplasmic thioredoxin-like protein CcmG of *Escherichia coli* are important but not essential for cytochrome *c* maturation *in vivo*." J Bacteriol **180**(7): 1947-50.

Faraone-Mennella, J., F. A. Tezcan, H. B. Gray and J. R. Winkler (2006). "Stability and folding kinetics of structurally characterized cytochrome *c*-b_{562}." Biochemistry **45**(35): 10504-11.

Feissner, R. E., C. L. Richard-Fogal, E. R. Frawley and R. G. Kranz (2006). "ABC transporter-mediated release of a haem chaperone allows cytochrome *c* biogenesis." Mol Microbiol **61**(1): 219-31.

Feng, Y., S. G. Sligar and A. J. Wand (1994). "Solution structure of apocytochrome b_{562}." Nat Struct Biol **1**(1): 30-5.

Feng, Y. Q. and S. G. Sligar (1991). "Effect of heme binding on the structure and stability of *Escherichia coli* apocytochrome b_{562}." Biochemistry **30**(42): 10150-5.

Feng, Y. Q., A. J. Wand and S. G. Sligar (1991). "1H and 15N NMR resonance assignments and preliminary structural characterization of *Escherichia coli* apocytochrome b_{562}." Biochemistry **30**(31): 7711-7.

Fong, S. T., J. Camakaris and B. T. Lee (1995). "Molecular genetics of a chromosomal locus involved in copper tolerance in *Escherichia coli* K-12." Mol Microbiol **15**(6): 1127-37.

Fulop, V., K. A. Sam, S. J. Ferguson, M. L. Ginger and J. W. Allen (2009). "Structure of a trypanosomatid mitochondrial cytochrome *c* with heme attached via only one thioether bond and implications for the substrate recognition requirements of heme lyase." FEBS J **276**(10): 2822-32.

Gao, T. and M. R. O'Brian (2007). "Control of DegP-dependent degradation of c-type cytochromes by heme and the cytochrome *c* maturation system in *Escherichia coli*." J Bacteriol **189**(17): 6253-9.

Goddard, A. D., J. M. Stevens, F. Rao, D. A. Mavridou, W. Chan, D. J. Richardson, J. W. Allen and S. J. Ferguson (2010). "*c*-type cytochrome biogenesis can occur via a natural Ccm system lacking CcmH, CcmG, and the heme-binding histidine of CcmE." J Biol Chem **285**(30): 22882-9.

Goldman, B. S., D. L. Beckman, A. Bali, E. M. Monika, K. K. Gabbert and R. G. Kranz (1997). "Molecular and immunological analysis of an ABC transporter complex required for cytochrome *c* biogenesis." J Mol Biol **268**(4): 724-38.

Goodhew, C. F., K. R. Brown and G. W. Pettigrew (1986). "Haem staining in gels, a useful tool in the study of bacterial *c*-type cytochromes." Biochimica et Biophysica Acta (BBA) - Bioenergetics **852**(2-3): 288-294.

Goulding, C. W., M. R. Sawaya, A. Parseghian, V. Lim, D. Eisenberg and D. Missiakas (2002). "Thiol-disulfide exchange in an immunoglobulin-like fold: structure of the N-terminal domain of DsbD." Biochemistry **41**(22): 6920-7.

Guddat, L. W., J. C. Bardwell, R. Glockshuber, M. Huber-Wunderlich, T. Zander and J. L. Martin (1997). "Structural analysis of three His32 mutants of DsbA: support for an electrostatic role of His32 in DsbA stability." Protein Sci **6**(9): 1893-900.

Guddat, L. W., J. C. Bardwell and J. L. Martin (1998). "Crystal structures of reduced and oxidized DsbA: investigation of domain motion and thiolate stabilization." Structure **6**(6): 757-67.

Haebel, P. W., D. Goldstone, F. Katzen, J. Beckwith and P. Metcalf (2002). "The disulfide bond isomerase DsbC is activated by an immunoglobulin-fold thiol oxidoreductase: crystal structure of the DsbC-DsbDalpha complex." Embo J **21**(18): 4774-84.

Han, D., K. Kim, J. Oh, J. Park and Y. Kim (2008). "TPR domain of NrfG mediates complex formation between heme lyase and formate-dependent nitrite reductase in *Escherichia col*i O157:H7." Proteins **70**(3): 900-14.

Harris, T. K. and G. J. Turner (2002). "Structural basis of perturbed pK_a values of catalytic groups in enzyme active sites." IUBMB Life **53**(2): 85-98.

Hartshorne, R. S., M. Kern, B. Meyer, T. A. Clarke, M. Karas, D. J. Richardson and J. Simon (2007). "A dedicated haem lyase is required for the maturation of a novel bacterial cytochrome *c* with unconventional covalent haem binding." Mol Microbiol **64**(4): 1049-60.

Harvat, E. M., C. Redfield, J. M. Stevens and S. J. Ferguson (2009). "Probing the heme-binding site of the cytochrome *c* maturation protein CcmE." Biochemistry **48**(8): 1820-8.

Hemmis, C. W., M. Berkmen, M. Eser and J. F. Schildbach (2011). "TrbB from conjugative plasmid F is a structurally distinct disulfide isomerase that requires DsbD for redox state maintenance." J Bacteriol **193**(18): 4588-97.

Heras, B., M. A. Edeling, H. J. Schirra, S. Raina and J. L. Martin (2004). "Crystal structures of the DsbG disulfide isomerase reveal an unstable disulfide." Proc Natl Acad Sci U S A **101**(24): 8876-81.

Herbaud, M. L., C. Aubert, M. C. Durand, F. Guerlesquin, L. Thony-Meyer and A. Dolla (2000). "*Escherichia coli* is able to produce heterologous tetraheme cytochrome *c*(3) when the ccm genes are co-expressed." Biochim Biophys Acta **1481**(1): 18-24.

Hiniker, A., D. Vertommen, J. C. Bardwell and J. F. Collet (2006). "Evidence for conformational changes within DsbD: possible role for membrane-embedded proline residues." J Bacteriol **188**(20): 7317-20.

Hussain, H., J. Grove, L. Griffiths, S. Busby and J. Cole (1994). "A seven-gene operon essential for formate-dependent nitrite reduction to ammonia by enteric bacteria." Mol Microbiol **12**(1): 153-63.

Inaba, K., S. Murakami, A. Nakagawa, H. Iida, M. Kinjo, K. Ito and M. Suzuki (2009). "Dynamic nature of disulphide bond formation catalysts revealed by crystal structures of DsbB." Embo J **28**(6): 779-91.

Inaba, K., S. Murakami, M. Suzuki, A. Nakagawa, E. Yamashita, K. Okada and K. Ito (2006). "Crystal structure of the DsbB-DsbA complex reveals a mechanism of disulfide bond generation." Cell **127**(4): 789-801.

Inaba, K., Y. H. Takahashi, K. Ito and S. Hayashi (2006). "Critical role of a thiolate-quinone charge transfer complex and its adduct form in *de novo* disulfide bond generation by DsbB." Proc Natl Acad Sci U S A **103**(2): 287-92.

Iobbi-Nivol, C., H. Crooke, L. Griffiths, J. Grove, H. Hussain, J. Pommier, V. Mejean and J. A. Cole (1994). "A reassessment of the range of *c*-type cytochromes synthesized by *Escherichia coli* K-12." FEMS Microbiol Lett **119**(1-2): 89-94.

Itagaki, E. and L. P. Hager (1968). "The amino acid sequence of cytochrome b_{562} of *Escherichia coli*." Biochem Biophys Res Commun **32**(6): 1013-9.

Kadokura, H. and J. Beckwith (2002). "Four cysteines of the membrane protein DsbB act in concert to oxidize its substrate DsbA." EMBO J **21**(10): 2354-63.

Kadokura, H. and J. Beckwith (2010). "Mechanisms of oxidative protein folding in the bacterial cell envelope." Antioxid Redox Signal **13**(8): 1231-46.

Kadokura, H., F. Katzen and J. Beckwith (2003). "Protein disulfide bond formation in prokaryotes." Annu Rev Biochem **72**: 111-35.

Kimura, T., J. C. Lee, H. B. Gray and J. R. Winkler (2009). "Folding energy landscape of cytochrome cb_{562}." Proc Natl Acad Sci U S A **106**(19): 7834-9.

Kranz, R. G., C. Richard-Fogal, J. S. Taylor and E. R. Frawley (2009). "Cytochrome *c* biogenesis: mechanisms for covalent modifications and trafficking of heme and for heme-iron redox control." Microbiol Mol Biol Rev **73**(3): 510-28, Table of Contents.

Lederer, F., A. Glatigny, P. H. Bethge, H. D. Bellamy and F. S. Matthew (1981). "Improvement of the 2.5 A resolution model of cytochrome b_{562} by redetermining the primary structure and using molecular graphics." J Mol Biol **148**(4): 427-48.

Lee, D., K. Pervushin, D. Bischof, M. Braun and L. Thony-Meyer (2005). "Unusual heme-histidine bond in the active site of a chaperone." J Am Chem Soc **127**(11): 3716-7.

Mavridou, D. A., E. Saridakis, P. Kritsiligkou, A. D. Goddard, J. M. Stevens, S. J. Ferguson and C. Redfield (2011). "Oxidation state-dependent protein-protein interactions in disulfide cascades." J Biol Chem **286**(28): 24943-56.

Mavridou, D. A., J. M. Stevens, S. J. Ferguson and C. Redfield (2007). "Active-site properties of the oxidized and reduced C-terminal domain of DsbD obtained by NMR spectroscopy." J Mol Biol **370**(4): 643-58.

Mavridou, D. A., J. M. Stevens, A. D. Goddard, A. C. Willis, S. J. Ferguson and C. Redfield (2009). "Control of periplasmic interdomain thiol:disulfide exchange in the transmembrane oxidoreductase DsbD." J Biol Chem **284**(5): 3219-26.

McCarthy, A. A., P. W. Haebel, A. Torronen, V. Rybin, E. N. Baker and P. Metcalf (2000). "Crystal structure of the protein disulfide bond isomerase, DsbC, from *Escherichia coli*." Nat Struct Biol **7**(3): 196-9.

Missiakas, D., C. Georgopoulos and S. Raina (1994). "The *Escherichia coli* dsbC (xprA) gene encodes a periplasmic protein involved in disulfide bond formation." EMBO J **13**(8): 2013-20.

Missiakas, D., F. Schwager and S. Raina (1995). "Identification and characterization of a new disulfide isomerase-like protein (DsbD) in *Escherichia coli*." Embo J **14**(14): 3415-24.

Mogi, T., K. Saiki and Y. Anraku (1994). "Biosynthesis and functional role of haem O and haem A." Mol Microbiol **14**(3): 391-8.

Mowat, C. G. and S. K. Chapman (2005). "Multi-heme cytochromes--new structures, new chemistry." Dalton Trans(21): 3381-9.

Nelson, J. W. and T. E. Creighton (1994). "Reactivity and ionization of the active site cysteine residues of DsbA, a protein required for disulfide bond formation *in vivo*." Biochemistry **33**(19): 5974-83.

Ouyang, N., Y. G. Gao, H. Y. Hu and Z. X. Xia (2006). "Crystal structures of *E. coli* CcmG and its mutants reveal key roles of the N-terminal beta-sheet and the fingerprint region." Proteins **65**(4): 1021-31.

Reid, E., J. Cole and D. J. Eaves (2001). "The *Escherichia coli* CcmG protein fulfils a specific role in cytochrome *c* assembly." Biochem J **355**(Pt 1): 51-8.

Ren, Q., U. Ahuja and L. Thony-Meyer (2002). "A bacterial cytochrome *c* heme lyase. CcmF forms a complex with the heme chaperone CcmE and CcmH but not with apocytochrome *c*." J Biol Chem **277**(10): 7657-63.

Richard-Fogal, C. and R. G. Kranz (2010). "The CcmC:heme:CcmE complex in heme trafficking and cytochrome *c* biosynthesis." J Mol Biol **401**(3): 350-62.

Richard-Fogal, C. L., E. R. Frawley, E. R. Bonner, H. Zhu, B. San Francisco and R. G. Kranz (2009). "A conserved haem redox and trafficking pathway for cofactor attachment." EMBO J **28**(16): 2349-59.

Richard-Fogal, C. L., E. R. Frawley and R. G. Kranz (2008). "Topology and function of CcmD in cytochrome *c* maturation." J Bacteriol **190**(10): 3489-93.

Rietsch, A., P. Bessette, G. Georgiou and J. Beckwith (1997). "Reduction of the periplasmic disulfide bond isomerase, DsbC, occurs by passage of electrons from cytoplasmic thioredoxin." J Bacteriol **179**(21): 6602-8.

Rozhkova, A. and R. Glockshuber (2007). "Kinetics of the intramolecular disulfide exchange between the periplasmic domains of DsbD." J Mol Biol **367**(4): 1162-70.

Sanders, C., S. Turkarslan, D. W. Lee and F. Daldal (2010). "Cytochrome *c* biogenesis: the Ccm system." Trends Microbiol **18**(6): 266-74.

Schulz, H., R. A. Fabianek, E. C. Pellicioli, H. Hennecke and L. Thony-Meyer (1999). "Heme transfer to the heme chaperone CcmE during cytochrome *c* maturation requires the CcmC protein, which may function independently of the ABC-transporter CcmAB." Proc Natl Acad Sci U S A **96**(11): 6462-7.

Shrager, R. I., J. S. Cohen, S. R. Heller, D. H. Sachs and A. N. Schechter (1972). "Mathematical models for interacting groups in nuclear magnetic resonance titration curves." Biochemistry **11**(4): 541-7.

Stevens, J. M., E. H. Gordon and S. J. Ferguson (2004). "Overproduction of CcmABCDEFGH restores cytochrome *c* maturation in a DsbD deletion strain of *E. coli*: another route for reductant?" FEBS Lett **576**(1-2): 81-5.

Stewart, E. J., F. Katzen and J. Beckwith (1999). "Six conserved cysteines of the membrane protein DsbD are required for the transfer of electrons from the cytoplasm to the periplasm of Escherichia coli." EMBO J **18**(21): 5963-71.

Stirnimann, C. U., A. Rozhkova, U. Grauschopf, R. A. Bockmann, R. Glockshuber, G. Capitani and M. G. Grutter (2006). "High-resolution structures of *Escherichia coli* cDsbD in different redox states: A combined crystallographic, biochemical and computational study." J Mol Biol **358**(3): 829-45.

Thony-Meyer, L. (1997). "Biogenesis of respiratory cytochromes in bacteria." Microbiol Mol Biol Rev **61**(3): 337-76.

Thony-Meyer, L. and P. Kunzler (1997). "Translocation to the periplasm and signal sequence cleavage of preapocytochrome *c* depend on *sec* and *lep*, but not on the *ccm* gene products." Eur J Biochem **246**(3): 794-9.

Thurlkill, R. L., G. R. Grimsley, J. M. Scholtz and C. N. Pace (2006). "pK values of the ionizable groups of proteins." Protein Sci **15**(5): 1214-8.

Timkovich, R. and R. E. Dickerson (1976). "The structure of *Paracoccus denitrificans* cytochrome c_{550}." J Biol Chem **251**(13): 4033-46.

Van den Berg, J. J., F. A. Kuypers, J. H. Qju, D. Chiu, B. Lubin, B. Roelofsen and J. A. Op den Kamp (1988). "The use of cis-parinaric acid to determine lipid peroxidation in

human erythrocyte membranes. Comparison of normal and sickle erythrocyte membranes." Biochim Biophys Acta **944**(1): 29-39.

Vranken, W. F., W. Boucher, T. J. Stevens, R. H. Fogh, A. Pajon, M. Llinas, E. L. Ulrich, J. L. Markley, J. Ionides and E. D. Laue (2005). "The CCPN data model for NMR spectroscopy: development of a software pipeline." Proteins **59**(4): 687-96.

Xavier, A. V., E. W. Czerwinski, P. H. Bethge and F. S. Mathews (1978). "Identification of the haem ligands of cytochrome b_{562} by X-ray and NMR methods." Nature **275**(5677): 245-7.

Appendix

S1.

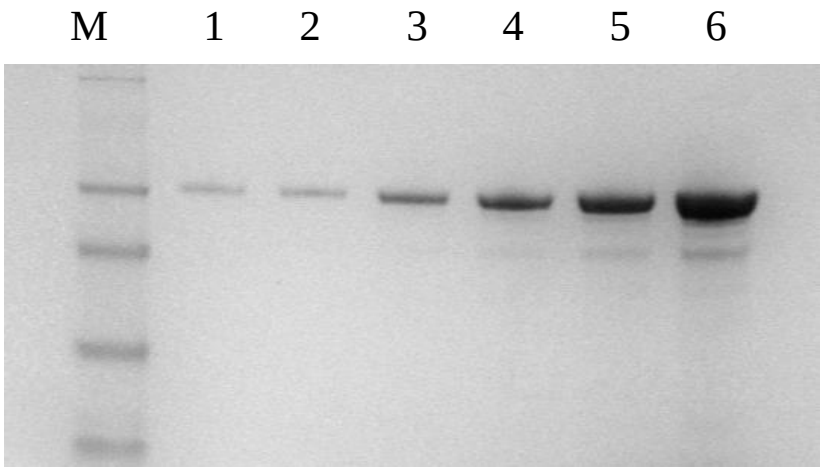

Figure S1: SDS-PAGE analysis of extracts stained for covalently-bound heme. The extracts are from anaerobically grown cultures from a DsbD deletion strain transformed with plasmids expressing wild-type DsbD. Loadings are (1) 0.3 ul, (2) 0.6 ul, (3) 1.15 ul, (4) 2.3 ul, (5) 4.6 ul, (6) 9.2 ul.

S2.

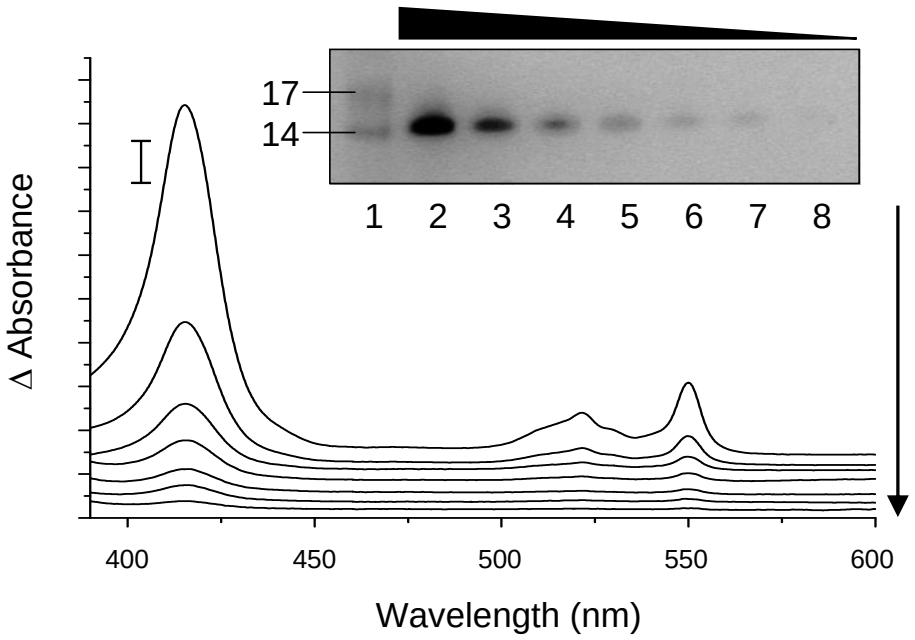

Fig. S2. Detection of *P. denitrificans* cytochrome c_{550}. The periplasmic fraction from *E. coli* EC06 cells containing pEC86 and pKPD1 was diluted to determine the lower limits of cytochrome detection. The absorbance spectra of dilutions of the periplasm, reduced with a few grains of sodium dithionite, are shown (determined using a 1 cm path-length cuvette). The baseline absorbance (650 nm) was subtracted from the magnitude of the Soret peak of cytochrome c_{550} (415 nm) and this value used to calculate the concentration of cytochrome using the extinction coefficient for reduced *P. denitrificans* cytochrome c_{550} at 415 nm, which is 140 mM^{-1} cm^{-1}. The spectra are offset for clarity and the concentrations of cytochrome (from top to bottom) are 1.14 μM, 0.47 μM, 0.22 μM, 0.12 μM, 0.08 μM, 0.05 μM and 0.03 μM. The scale bar is equivalent to 0.02 OD units. 20 μl samples of these solutions were analysed by SDS-PAGE followed by heme-staining (inset). The amount of cytochrome c_{550} loaded per lane was calculated from the appropriate absorption spectrum. The amount per lane is (2) 23 pmoles, (3) 9.4 pmoles, (4) 4.3 pmoles, (5) 2.5 pmoles, (6) 1.7 pmoles, (7) 1.1 pmoles and (8) 0.6 pmoles. The gel was stained until no further bands developed. Lane 1 shows molecular weight markers of the indicated masses (kDa). (Adapted from Goddard et al, 2009)

S3. Protein sequence of *c*-b_{562} The residues consisting of the signal peptide that gets cleaved for the mature heme-free form of the protein is highlighted.

```
        10         20         30         40         50         60
MRKSLLAILA VSSLVFSSAS FAADLEDNME TLNDNLKVIE KADNAAQVKD ALTKMRAAAL

        70         80         90        100        110        120
DAQKATPPKL EDKSPDSPEM KDFRHGFDIL VGQIDDALKL ANEGKVKEAQ AAAEQLKTTR

NAYHQKYR
```

ST1. Chemical shift differences ox-red states of the *c*-b_{562} apoprotein. Differences in both the proton and the nitrogen dimension are presented.

2	8.890	8.900	-0.010	120.750	120.460	0.290
3	8.640	8.720	-0.080	122.880	122.770	0.110
4	8.780	8.660	0.120	117.590	117.110	0.480
5	7.850	7.920	-0.070	120.080	120.380	-0.300
6	8.020	7.960	0.060	118.270	117.990	0.280
7	8.550	8.500	0.050	118.920	118.160	0.760
8	8.210	8.160	0.050	121.940	122.300	-0.360
9	8.310	8.270	0.040	117.630	118.410	-0.780
10	8.150	8.240	-0.090	123.590	123.590	0.000
11	8.210	8.000	0.210	117.430	117.340	0.090
12	9.350	9.270	0.080	120.790	120.600	0.190
13	7.870	7.890	-0.020	117.700	117.890	-0.190
14	8.090	8.110	-0.020	123.260	123.350	-0.090
15	7.290	7.360	-0.070	118.810	118.760	0.050
16	7.310	7.270	0.040	119.330	119.200	0.130
17	7.930	7.950	-0.020	119.390	119.120	0.270
18	7.820	7.840	-0.020	118.340	117.670	0.670
19	7.140	7.150	-0.010	114.790	114.640	0.150
20	7.290	7.310	-0.020	123.770	123.670	0.100
21	8.760	8.790	-0.030	116.630	116.570	0.060
22	7.650	7.670	-0.020	113.370	113.330	0.040
23	9.030	9.050	-0.020	122.130	122.130	0.000
24	8.450	8.470	-0.020	122.330	122.310	0.020
25	8.080	8.080	0.000	117.530	117.570	-0.040
26	7.190	7.170	0.020	118.360	118.270	0.090
27	8.780	8.770	0.010	119.750	119.710	0.040
28	8.240	8.260	-0.020	120.870	120.890	-0.020
29	7.570	7.620	-0.050	121.700	121.770	-0.070
30	8.540	8.520	0.020	118.160	118.210	-0.050
31	8.340	8.340	0.000	116.770	116.990	-0.220
32	7.720	7.820	-0.100	123.130	123.280	-0.150
33	8.420	8.490	-0.070	119.200	119.040	0.160
34	8.590	8.540	0.050	120.810	121.020	-0.210
35	7.230	7.190	0.040	117.540	117.250	0.290
36	7.660	7.680	-0.020	121.130	121.320	-0.190
37	8.520	8.670	-0.150	120.610	120.870	-0.260
38	7.780	7.740	0.040	116.180	115.950	0.230
39	7.740	7.720	0.020	120.040	120.060	-0.020
40	8.290	8.400	-0.110	124.210	124.530	-0.320
41	7.020	7.010	0.010	112.970	112.950	0.020
42	7.060	7.060	0.000	114.390	114.330	0.060
43	7.760	7.800	-0.040	123.870	123.860	0.010
44	8.200	8.210	-0.010	114.530	114.150	0.380
47	8.540	8.620	-0.080	114.960	114.520	0.440
48	7.790	7.880	-0.090	117.890	116.670	1.220
50	8.430	8.470	-0.040	116.400	115.910	0.490
51	7.690	7.620	0.070	119.880	119.520	0.360
52	8.770	8.820	-0.050	117.670	117.390	0.280
54	7.970	7.970	0.000	114.030	113.930	0.100
55	7.820	7.810	0.010	116.780	116.440	0.340
57	9.540	9.690	-0.150	116.640	117.420	-0.780
58	7.790	7.670	0.120	120.420	119.460	0.960
59	8.610	8.570	0.040	121.390	120.610	0.780
60	8.510	8.390	0.120	120.520	120.900	-0.380
61	8.040	8.430	-0.390	122.060	121.960	0.100
62	8.660	8.670	-0.010	117.620	117.460	0.160
63	8.820	8.810	0.010	119.260	119.440	-0.180
64	7.990	8.000	-0.010	105.650	106.140	-0.490
65	7.060	6.970	0.090	117.720	116.680	1.040
66	7.630	7.620	0.010	121.890	121.800	0.090
67	7.560	7.530	0.030	120.210	121.060	-0.850
68	7.330	7.370	-0.040	121.400	121.030	0.370
69	8.640	8.810	-0.170	119.120	119.450	-0.330

70	7.780	7.910	-0.130	105.840	106.000	-0.160
71	7.890	7.910	-0.020	121.040	120.950	0.090
72	8.790	8.860	-0.070	123.720	124.410	-0.690
73	8.980	8.980	0.000	122.020	122.000	0.020
74	8.050	8.100	-0.050	122.350	122.290	0.060
75	7.940	7.870	0.070	123.900	124.020	-0.120
76	9.190	9.210	-0.020	121.550	121.740	-0.190
77	7.770	7.790	-0.020	120.630	120.190	0.440
78	7.060	6.990	0.070	117.420	117.070	0.350
79	8.430	8.370	0.060	121.970	121.820	0.150
80	8.950	9.000	-0.050	118.500	118.430	0.070
81	7.530	7.550	-0.020	117.770	117.800	-0.030
82	7.890	7.900	-0.010	107.370	107.360	0.010
83	7.960	7.980	-0.020	123.990	124.010	-0.020
84	7.630	7.660	-0.030	122.240	122.180	0.060
85	8.540	8.560	-0.020	120.030	120.040	-0.010
86	9.340	9.320	0.020	121.630	121.620	0.010
87	8.510	8.450	0.060	124.700	124.310	0.390
88	8.710	8.650	0.060	117.140	116.530	0.610
89	8.200	8.180	0.020	123.200	123.470	-0.270
90	8.080	7.970	0.110	122.080	121.920	0.160
91	8.360	8.240	0.120	121.750	120.830	0.920
92	7.840	7.720	0.120	116.730	117.650	-0.920
93	7.550	7.540	0.010	117.370	118.100	-0.730
94	7.780	7.880	-0.100	120.490	118.420	2.070
95	8.010	8.080	-0.070	119.650	120.900	-1.250
96	7.840	7.630	0.210	111.970	115.470	-3.500
97	7.690	8.070	-0.380	112.180	120.950	-8.770
98	7.970	8.840	-0.870	121.010	120.980	0.030
99	8.580	8.260	0.320	129.000	117.680	11.320
100	8.840	8.070	0.770	121.290	123.320	-2.030
101	7.880	8.070	-0.190	113.040	115.820	-2.780
102	7.670	8.100	-0.430	115.310	117.020	-1.710
103	7.690	8.150	-0.460	119.780	115.340	4.440
104	8.270	7.590	0.680	121.670	117.940	3.730
105	8.570	7.930	0.640	122.080	115.280	6.800
106	7.670	7.190	0.480	125.140	124.750	0.390

ST2. The combined chemical shift differences for all the residues of the protein

1	0.0000	60	0.1698
2	0.0922	61	0.3913
3	0.0872	62	0.0516
4	0.1935	63	0.0578
5	0.1179	64	0.1553
6	0.1070	65	0.3410
7	0.2455	66	0.0302
8	0.1243	67	0.2705
9	0.2499	68	0.1237
10	0.0900	69	0.1995
11	0.2119	70	0.1395
12	0.1000	71	0.0348
13	0.0633	72	0.2292
14	0.0348	73	0.0063
15	0.0718	74	0.0535
16	0.0574	75	0.0796
17	0.0877	76	0.0633
18	0.2128	77	0.1406
19	0.0485	78	0.1310
20	0.0374	79	0.0765
21	0.0355	80	0.0547
22	0.0237	81	0.0221
23	0.0200	82	0.0105
24	0.0210	83	0.0210
25	0.0126	84	0.0355
26	0.0348	85	0.0202
27	0.0161	86	0.0202
28	0.0210	87	0.1371
29	0.0547	88	0.2020
30	0.0255	89	0.0877
31	0.0696	90	0.1211
32	0.1107	91	0.3147
33	0.0864	92	0.3147
34	0.0831	93	0.2311
35	0.1000	94	0.6622
36	0.0633	95	0.4014
37	0.1711	96	1.1265
38	0.0830	97	2.7992
39	0.0210	98	0.8701
40	0.1495	99	3.5940
41	0.0118	100	1.0025
42	0.0190	101	0.8994
43	0.0401	102	0.6909
44	0.1206	103	1.4775
45	0.0000	104	1.3615
46	0.0000	105	2.2436
47	0.1605	106	0.4956
48	0.3962	107	0.0000
49	0.0000		
50	0.1600		
51	0.1336		
52	0.1017		
53	0.0000		
54	0.0316		
55	0.1080		
56	0.0000		
57	0.2887		
58	0.3264		
59	0.2499		